Development of Modified Lignosulfonate Based Encapsulating Agent for Slow Release of Urea

Sirno Yonas Beyena

A Thesis Submitted to

The Department of Chemical Engineering

School of Mechanical, Chemical and Material Engineering

Presented in Partial Fulfillment of the Requirement for the Degree of Master's in Chemical Engineering (Specialization in Process Engineering)

Office of Graduate Studies

Adama Science and Technology University

June, 2023

Adama, Ethiopia

Development of Modified Lignosulfonate Based Encapsulating Agent for Slow Release of Urea

Sirno Yonas Beyena

Advisor: Zelalem Tumsa (Ph.D.)

Co- Advisor: P. Selvakumar (Ph.D.)

A Thesis Submitted to

The Department of Chemical Engineering

School of Mechanical, Chemical and Material Engineering

Presented in Partial Fulfillment of the Requirement for the Degree of Master's

In Chemical Engineering (Specialization in Process Engineering)

Office of Graduate Studies

Adama Science and Technology University

June, 2023

Adama, Ethiopia

DECLARATION

I hereby declare that this Master Thesis entitled "***Development of Modified Lignosulfonate Based Encapsulating Agent for Slow Release of Urea"*** is my original work. That is, it has not been submitted for the award of any academic degree, diploma, or certificate in any other university. All sources of materials that are used for this thesis have been duly acknowledged through citation.

Sirno Yonas Beyena _____ _____

Name of the student Signature Date

RECOMMENDATION

We, the advisors of this thesis, hereby certify that we have read the revised version of the thesis entitled "***Development of Modified Lignosulfonate Based Encapsulating Agent for Slow Release of Urea***" prepared under our guidance by ***Sirno Yonas Beyena*** submitted in partial fulfillment of the requirements for the degree of Masters of Science in Chemical Engineering. Therefore, we recommend the submission of the revised version of the thesis to the department following the applicable procedures.

Dr. Zelalem Tumsa	_____	_____
Major advisor	Signature	Date
Dr. P. Selvakumar	_____	_____
Co-advisor	Signature	Date

APPROVAL PAGE

We, the advisors of the thesis entitled **"*Development of Modified Lignosulfonate Based Encapsulating Agent for Slow Release of Urea"*** and developed by ***Sirno Yonas Beyena***; hereby certify that the recommendation and suggestions made by the board of examiners are appropriately incorporated in to the final version of the thesis.

Dr.Zelalem Tumsa		
Major Advisor	Signature	Date
Dr. P. Selvakumar		
Co-advisor	Signature	Date

We, the undersigned, members of the Board of Examiners of the thesis by **Sirno Yonas Beyena** have read and evaluated the thesis entitled **"*Development of Modified Lignosulfonate Based Encapsulating Agent for Slow Release of Urea*"** and examined the candidate during the open defense. This is, therefore, to certify that the thesis is accepted for partial fulfillment of the requirement of the degree of Master of Science in Chemical Engineering (Specialization in Process Engineering).

Chairperson	Signature	Date
Internal Examiner	Signature	Date
External Examiner	Signature	Date
Dr. Wondalem Misganaw		10-07-2023

Finally, approval and acceptance of the thesis is contingent upon submission of its final Copy to the Office of Postgraduate Studies (OPGS) through the Department Graduate Council (DGC) and School Graduate Committee (SGC).

Department Head	Signature	Date
School Dean	Signature	Date
Office of Postgraduate Studies, Dean	Signature	Date

ACKNOWLEDGEMENT

First of all, thanks to Almighty **God** for safeguarding and helping me throughout my ups and down to complete this thesis work successfully. Next, I am eager to express my heartfelt and deepest gratitude to my advisors, **Zelalem Tumsa (Ph.D.)** and **P. Selvakumar (Ph.D.),** for their deepest advisory and fruitful guidance, assistance, and unwary encouragement throughout this research work without showing me any sign of aggressiveness.

I would like to thank all my family members with the deepest gratitude because of their initiation, encouragement, prayer, acceptance, and un-measurable caring and help throughout my journey of Life. May Almighty **God** bless them all!

Last but not least, I am eager to thank all my friends and people who helped, encouraged, motivated, guided, and donated to me during my time of need throughout this research work.

TABLE OF CONTENTS

LIST OF TABLES

LIST OF FIGURES

LIST OF ACRONYMS AND ABBREVIATIONS

AA	Acetic Anhydride
A/Acid	Acetic Acid
Ac-Ls	Acetylated Lignosulfonate
AMO	Ammonia Monooxygenase
CRF	Controlled Release Fertilizer
CRU	Controlled Release Urea
CU	Coated Urea
DCM	Dichloromethane
FTIR	Fourier Transform Infrared spectroscopy
HAO	Hydroxylamine Oxido-reductase
NI	Nitrification Inhibitor
NF	Nano Fertilizer
N-Ls	Normal Lignosulfonate
NMR	Nuclear Magnetic Resonance
NUE	Nutrient Use Efficiency
S-CRF	Slow or Controlled Release Fertilizer
SRF	Slow Release Fertilizer
U-e-Ac-Ls	Urea encapsulated Acetylated Lignosulfonate
UI	Urease Inhibitor

ABSTRACT

The most well-known fertilizer in the world is urea, which provides plants with the greatest nitrogen. Although urea has favorable properties in terms of production cost, handling, storage, and transport, it has a restriction in terms of how much nitrogen it can give. Most plants require urea's vital component N throughout their entire life. The release of N from urea must be managed since various plants have varying life spans. In order to manage the rate at which urea dissolves in water and to enhance the rate at which it degrades in soil, urea was encapsulated in a biodegradable encapsulating agent that was synthesized through the acetylation reaction of Lignosulfonate (Ls). The acetylation reaction was carried out at various temperatures ranging from 60 °C to 100 °C, with different reaction durations of 6 to 24 hrs using a conventional heating system. The impact of those independent variables on the acetylation of lignosulfonate (Ac-Ls) was investigated. The results of solubility and hydrophobicity tests of Ac-Ls exhibits that as lignosulfonate acetylated, its solubility decreases in water, in contrary, its hydrophobicity increases. FTIR analysis confirmed the effect of acetylation time and temperature on the substitution of O-H group by C=O group on the structure of Lignosulfonate and the result showed as acetylation temperature and time icreases, the peak of O-H declines while the peak of C=O increases. The rate of N release from U-e-Ac-Ls was investigated using Kjeldhal method. Additionally, the effects of acetylation time and temperature on the nitrogen release rate was analyzed. The outcome shows that the nitrogen release rate and acetylation time and temperature were inversely related. As a result, it is possible to regulate the nitrogen release rate of U-e-Ac-Ls by simply adjusting the acetylation temperature and time of Ac-Ls. The nitrogen release rate was also affected by medium's temperature, urea concentration and pH. The formulated U-e-Ac-Ls (analyzed at pH-7) was able to extend nitrogen release rate to 22hrs (99.48%) while the commercial urea released 98.12% of its nitrogen in an hour. Of the four released kinetic model equations examined, the Korsmeyer-Peppas equation exhibits the best fit with correlation coefficients ($R^2 > 0.99$), and the release exponent (n) values for U-e-Ac-Ls were greater than 0.89, suggesting a combination of diffusion and erosion mechanisms were used to release N. The results of the soil degradation test confirmed that U-e-Ac-Ls almost completely degraded in the soil, and as the concentration of urea in formulated U-e-Ac-Ls rises, the degradation rate increases.

Keywords: *Acetylation reaction, Encapsulating Agent, Urea encapsulation, Controlled Release, Release kinetics.*

CHAPTER ONE

INTRODUCTUON

1.1 Background of the study

The most important task for achieving the tremendous challenge of feeding an estimated 9.5 billion people by 2050 is to continue working to increase agricultural production (Fertahi et al., 2021). Therefore, it is crucial to use fertilizers as a crop production input in order to meet the growing population's demand for food. Fertilizer, a crucial chemical in agriculture, has a crucial function in maintaining soil fertility, boosting crop yields, and improving the quality of the harvest (Shan et al., 2021). For their best growth and productivity, plants need more than 14 nutrients. The three macronutrients nitrogen, phosphorous, and potassium, which are present in the majority of packaged fertilizers used in agriculture, is the most crucial and necessary in the greatest quantity from these nutrients (Hasanuzzaman et al., 2018). However, out of all of these nutrients, nitrogen is the most critical and crucial for crop growth because it is a fundamental protein building block and because nearly every process required for a plant's growth depends on it (Dimkpa, Fugice, et al., 2020). As a result, N-fertilizer has long been a crucial component of agriculture and is expected to supply 48% of global demand (Galloway et al., 2008; Xia et al., 2022). It currently accounts for more than half of global food production (Dimkpa, Andrews, et al., 2020; X. Zhang et al., 2015), and it is possible to say that it will continue to do so in the future in order to meet the world's food needs. The most well-known fertilizer in the world is urea, which provides plants with the greatest nitrogen (Beig et al., 2020). Although urea has favorable properties in terms of production cost, handling, storage, and transport (Herrera et al., 2016), it has a restriction in terms of how much nitrogen it can give. Nitrogen is a highly important nutrient for plant growth. A significant drawback of urea is that it readily dissolves in water and nitrates quickly. Therefore, losses from nitrous emission, ammonia volatilization, leaching, and surface runoff threaten the vital nutrient nitrogen from urea (Azeem et al., 2020; Ma et al., 2019). As a result, numerous researchers have worked to develop fertilizers with gradual nutrient releases in an effort to improve plants' ability to absorb nitrogen (An et al., 2021; Beig et al., 2020; El Assimi et al., 2021; Lyu et al., 2021; Madzokere et al., 2020). S-CRFs, or slow or controlled-release fertilizers, contain plant nutrients in a way that postpones their availability for

Plants absorption. In addition to improving plants' capacity to absorb nutrients, S-CRFs lowers issues with human health and the environment brought on by leaching and volatilization as a result of the rapid nitrification and dissolution of commercial urea fertilizer (Lawrencia et al., 2021). These fertilizers have been developed by researchers utilizing the following mechanisms: 1) Coating fertilizer with semi-permeable or impermeable membranes such sulfur, gypsum, lignin, and polymers; 2) Urea super granules (USG); 3) Utilizing urease and nitrification inhibitors; and 4) Utilizing Nano technology, i.e., Nano fertilizers. Although using these mechanisms to create slow or controlled release fertilizers helps to reduce nutrient loss, these methods have their own drawbacks, including high processing costs, coating materials that are easily cracked and non-biodegradable, and a continued vulnerability to nutrient loss that can have negative effects on human health and the environment (Dimkpa, Fugice, et al., 2020).Utilizing urea super granules is labor- and time-intensive (L. Liu et al., 2018); applying urease and nitrification inhibitors delays urea hydrolysis and reduces osmotic shock (Abalos et al., 2014); and employing nano fertilizers has a high production cost and toxicity (Zulfiqar et al., 2019). In order to find a mechanism for the efficient delivery of nitrogen that is technically and financially feasible to allow the slow release of fertilizer to significantly reduce nutrient loss in the environment and to water bodies, work on improving the mechanisms of developing a slow or controlled released fertilizer has continued.

Since they are nontoxic, biodegradable, and have a low carbon footprint, bio-based polymers like cellulose, chitosan, and Lignin have attracted a lot of attention recently to develop slow or controlled release fertilizers (Abd El-Aziz et al., 2022; Mohammadbagheri et al., 2021; Zonatto et al., 2017). There are currently just a few practical uses for bio-based polymers because they are frequently hydrophilic in their native forms. If the polymers can be transformed into hydrophobic materials, their range of possible uses dramatically increases. The by-product of making paper pulp using the sulfite process is lignosulfonate (Ls), which is easily dissolved in water (Lora & Glasser, 2002). An estimated 1.8 billion tones of lignin and lignin sulfonate are produced globally each year, with an estimated value-added of $0.1 per kilogram of lignin (Areskogh et al., 2010; Kreetachat et al., 2007; J. Liu et al., 2013) from the process of turning it into new compounds. In its natural state, lignosulfonate (Ls) is a hydrophilic biopolymer due to the presence of sulfonate and hydroxyl group that increase its solubility in aqueous media; however, if specific structural alterations are made, it turns to hydrophobic and can be employed for nutrient encapsulation applications (Lamsen, 2019).Additionally, during the modification step, its hydrophobicity may be regulated, making it

appropriate for use in a slow nutrient delivery system. It is required to first acetylate lingo- sulfonate in order to minimize its solubility due to the high solubility of lignosulfonate in water or aqueous solutions (Sadeghi et al., 2017). In order to create a biodegradable and hydrophobic adhesive, Lignosulfonate (Ls) was modified with acetic anhydride using esterification procedure. In addition, urea was successfully encapsulated in the synthetic hydrophobic and biodegradable binder, resulting in the formulation of a controlled dissolution rate fertilizer with an improved soil degradation rate.

1.2 Statement of the problem

By providing the greatest amount of nitrogen to plants, urea is the most well-known and highly significant fertilizer utilized in agricultural production worldwide (Beig et al., 2020). It also has favorable properties in terms of manufacturing cost, handling, storage, and transport (Herrera et al., 2016). However, the delivery of nutrients by urea is constrained. Its significant drawbacks include its propensity to dissolve quickly in water and nitrify quickly. Due to ammonia volatilization, leaching, and surface runoff, its vital nutrient nitrogen is susceptible to losses (Azeem et al., 2020; Ma et al., 2019). As a result, between 40% and 70% of the nitrogen used by plants is lost (Ma et al., 2019), which causes a severe economic problem because it lowers the potential yield of crops and increases the cost of farmers' investments in agricultural inputs. Additionally, the nitrogen released into the water bodies and the atmosphere through leaching and volatilization causes human health issues like respiratory conditions, cardiac conditions, and cancer, as well as other environmental issues like the effects of greenhouse gases (Fertahi et al., 2021).To reduce the aforementioned urea fertilizer restrictions, it is crucial to develop a new kind of controlled release fertilizer by encapsulating urea in hydrophobic and biodegradable encapsulating agent. In this study, lignin particularly lignosulfonate lignin has been modified by acetylation reaction to improve the hydrophobicity and compatibility for successful urea encapsulation. Moreover, this Lignosulfonate used for urea encapsulation was the one considered as waste and underutilized biopolymer in pulp and paper industry. So valorizing this waste in to valuable encapsulating agent also increases the requirements of this waste and initiates other scholars to aware and to do and search more with it.

1.3 Objectives

1.3.1 General objective

The general objective of this study is to develop modified lignosulfonate as an encapsulating agent for the slow release of urea.

1.3.2 Specific Objectives

To achieve the above general objective, the following specific objectives are articulated as follows,

- To modify/ acetylize lignosulfonate structure by using acetic anhydride and studying the effect of acetylation temperature and time on the lignosulfonate acetylation
- To encapsulate urea using acetylated lignosulfonate to enable a slow release rate
- To characterize urea encapsulated acetylated lignosulfonate (U-e-Ac-Ls)
- To investigate the effects of acetylation time and temperature on nitrogen release rate
- To investigate Nitrogen release rate in water at various ranges of temperatures, urea concentrations, and pH
- To study the behaviors of release kinetics of the formulated U-e-Ac-Ls in water
- To evaluate encapsulated urea degradation rate test in the soil

1.4 Significance of the study

This work is extremely important for ensuring the creation of a biodegradable fertilizer with a controlled dissolving rate for effective nitrogen delivery to plants. Reduced nutrient volatilization, leaching, and runoff from urea fertilizer are the main benefit of this study. It plays a significant part in the government's objective of expanding food production and diversifying current farming to achieve long-term food security and reduce poverty. Additionally, it is important to use underutilized material, lignin, for its valorization. Using the slow release mechanism reduces environmental issues and human health by directly using commercial urea fertilizer.

1.5 Scope of the project

This research work is basically focused on the following articulated tasks:

- Modifiy/acetylyze lignosulfonate, to mitigate the solubility of lignosulfonate lignin.
- Study the parameters, namely acetylation temperature and time, that affect the acetylation of lignosulfonate.

- Study the effects of acetylation time and temperature on the nitrogen release rate in water.
- Investigate effect of temperature, urea concentration, and pH on the nitrogen release rate in water.
- Analyze the effects of urea concentration on urea degradation rate in the soil.
- Evaluate hydrophobicity of the acetylated Lignosulfonate.
- Aanalyze functional groups of acetylated Lignosulfonate using FTIR spectrums.
- Study the release kinetics of nitrogen of encapsulated urea using different kinetic models.
- Investigate soil degradation rate of urea encapsulated by acetylated Lignosulfonate and compare it with conventional commercial urea.

CHAPTER TWO

LITERATURE REVIEW

2.1 Fertilizer

An organic or inorganic chemical material used to promote plant growth and fertility is known as a fertilizer. Additionally, it can increase water retention and filter any surplus liquid, increasing the efficiency of the soil. Organic fertilizers, such as sheep manure, chicken litter, green manures, sewage sludge, press mud, compost, or other animal and plant products, are made from natural materials (Hammad et al., 2020). They typically take their time and work slowly and continuously (Singh, 2012). Inorganic fertilizers are those that are either mined from mineral sources with little processing or generated industrially using chemical processes(Gupta & Hussain, 2014). After determining the nutrient the plant needs, an inorganic fertilizer containing that nutrient is utilized for effective short-term development (Ma et al., 2019). Fertilizers that are made in an industrial setting using chemical processes or that are mined from mineral resources with minimum processing (such as lime, potash, or phosphate rock) are known as inorganic fertilizers (e.g., urea).

A variety of chemical components are necessary for plants to flourish. The three that are present in air and water, carbon, hydrogen, and oxygen are the most significant. For plants to develop and produce at their best, they need macronutrients like potassium, phosphorus, and nitrogen, as well as micronutrients like boron, cobalt, copper, iron, manganese, and zinc, as well as secondary nutrients like sulfur, calcium, and magnesium (Mohammadbagheri et al., 2021). Calcium, boron, copper, zinc, and molybdenum are involved in enzymatic activities; N and S are involved in protein synthesis; and nutrients like nitrogen, phosphorus, potassium, magnesium, manganese, chlorine, and iron are directly involved in plant photosynthetic activities (Hasanuzzaman et al., 2018). Basically, the three macronutrients needed for plant growth are nitrogen, phosphorus, and potassium. They are essential for the fundamental building blocks. For instance, every amino acid contains nitrogen, and every molecule that makes up ATP, the primary energy source for all cells, as well as every molecule that makes up a cell's membrane, contain phosphorus (the membrane molecules known as phospholipids). Nitrogen is the most crucial nutrient for plant growth and is needed in the highest amount, despite the fact that all macro nutrients are significant and needed in the greatest amounts (Ali et al., 2022).

2.2 Sources of Nitrogen

Table 2.1. Nitrogen sources and their compositions (Zulfiqar et al., 2019)

Source	Nitrogen Content (%)
Anhydrous ammonia	82
Urea	46
Ammonium nitrate	33.5-34
Urea-ammonium nitrate solution	28-32
Calcium ammonium nitrate	21-27
Ammonium nitrate sulfate	26
Ammonium chloride	26
Aqua ammonia	20-25
Ammonium sulfate	21
Diammonium phosphate	18
Sodium nitrate	16
Calcium nitrate	15.5
Potassium nitrate	13
Ammonium thiosulfate	12
Monoammonium phosphate	10-11

Anhydrous ammonia has the largest concentration of nitrogen (N) among those inorganic fertilizers, as stated in Table 2.1 above, and it is inexpensive in many nations. However, because it is a gas and must be compressed to be stored as a liquid, it is difficult to handle and requires specialized equipment for storage, handling, and application. In addition, the pH change caused by this source may mean that lime is needed to keep the soil at the desired level (Herrera et al., 2016). All ammonia sources, not just anhydrous ammonia, can cause this later impact. The second-highest nitrogen concentration after anhydrous ammonia is found in urea ($CO(NH_2)_2$), which has the greatest nitrogen content of those solid nitrogenous fertilizers at 46%. Urea is a particularly competitive N source due to its advantageous handling, storage, and transport costs. As a result, it is currently the fertilizer that is used the most extensively worldwide.

2.3 Types of Fertilizers

Fertilizers are basically classified in to two: organic and inorganic fertilizers.

2.3.1 Organic fertilizer

They are formed using waste products from plants and animals. Examples include waste from the poultry and chicken meat processing sectors, animal and agricultural waste, vegetable trash, and so forth. By encouraging microbial growth and modifying the soil's physical and chemical composition for maximum productivity, organic fertilizers contribute to soil enrichment.

2.3.2 Inorganic fertilizer

Chemical compounds known as inorganic fertilizers are made up of nutrients needed for plant growth. These are what they are:

2.3.2.1 Nitrogenous fertilizer

For the crops, they provide as a supply of nitrogen. The leaf area index and leaf area are encouraged by nitrogen. In addition to being a constituent of vital cellular elements including amino acids, proteins, and nucleic acids, it makes the leaves' green hue more intense. In addition, it regulates P, K, and other nutrients, enhances the succulence of various crops, and promotes photosynthesis by increasing chlorophyll levels (Torres-olivar & Valdez-aguilar, 2014; Vargas et al., 2020). It boosts plant development and enhances yield as a result. Fertilizers that contain nitrogen include urea, ammonium sulfate, calcium ammonium nitrate, and others.

2.3.2.2 Phosphorus fertilizer

Phosphorus fertilizers are those that serve as the primary supply of phosphorus. Phosphorus boosts the quality of fruit, vegetable, and grain crops and is essential for seed production. It also speeds up ground cover for erosion protection (Mohammadbagheri et al., 2021). Single superphosphate, triple superphosphate, di-calcium phosphate, di-ammonium phosphate, and other phosphorus fertilizers are a few of the commercially available options.

2.3.2.3 Potassium fertilizer

Potassium increases protein production, early crop growth, and water usage effectiveness (Rawat et al., 2016). Potassium sulfate and muriate of potash (KCl) are two components of potassium-enriched fertilizer.

2.3.2 Urea fertilizer

The main source of nitrogen (N), one of the most crucial nutrients utilized in fertilizer manufacture, is urea ($CO(NH_2)_2$) fertilizer. Today's world population is about 48% alive thanks to fertilizers containing nitrogen (Lyu et al., 2021). Of all the solid nitrogenous fertilizers, urea has the largest nitrogen concentration (46% N). It has the greatest water solubility as well. In comparison to other nitrogenous fertilizers, urea offers a greater amount of nitrogen to plants and soil due to its high nitrogen content (Beig et al., 2020).The efficiency of urea fertilizer over a given period of time depends on how much nitrogen is absorbed by a crop. Urea combines with water to create ammonia when applied to soil, which increases the nitrogen content.

2.3.3 Limitations of using Commercial Fertilizers

Only 30–35% of the nutrients are absorbed by plants when chemical fertilizers are used directly on the plants, which has been demonstrated to have low utilization performance (Lawrencia et al., 2021). Unfortunately, between 40% and 70% of the nitrogen in urea is lost (Beig et al., 2020; Lawrencia et al., 2021), of which 2–10% is lost through leaching into water bodies and 2–20% is lost through volatilization, and 15–25% reacts with natural compounds in the soil. This loss of nitrogen is a major cause for urgent environmental concerns (Lawrencia et al., 2021).The soil's urease enzyme converts urea to the very unstable ammonium carbonate, which is then transformed to ammonia and released into the atmosphere as ammonia by carbon dioxide. The presence of water in the soil then causes a certain amount of ammonia to be transformed into ammonium. Furthermore, nitrifying bacteria such as Nitrobacteria and Nitrosomonas, which are extremely mobile in nature and leach into water bodies with rainwater, convert ammonium to nitrite and then to nitrate.

This process is illustrated in Figure 2.1 below.

$(NH_2)_2CO + 2H_2O + \text{Enzyme Urease} \longrightarrow (NH_4)_2CO_3$

$(NH4)_2CO_3 + H2O \longrightarrow 2NH_3 + CO_2 + H_2O$

$NH_3 + H_2O \longrightarrow NH_4^+ + OH^-$

$2NH_4^+ + 3O_2 + \text{Nitrosomonas bacteria} \longrightarrow 2NO_2^-$

$+2H2O + 4H^+$

$2NO_2^- + O_2 + \text{Nitrobacteria} \longrightarrow 2NO_3^-$

$2NO_3^- + \text{Microorganisms} \longrightarrow N_2 + N_2O$

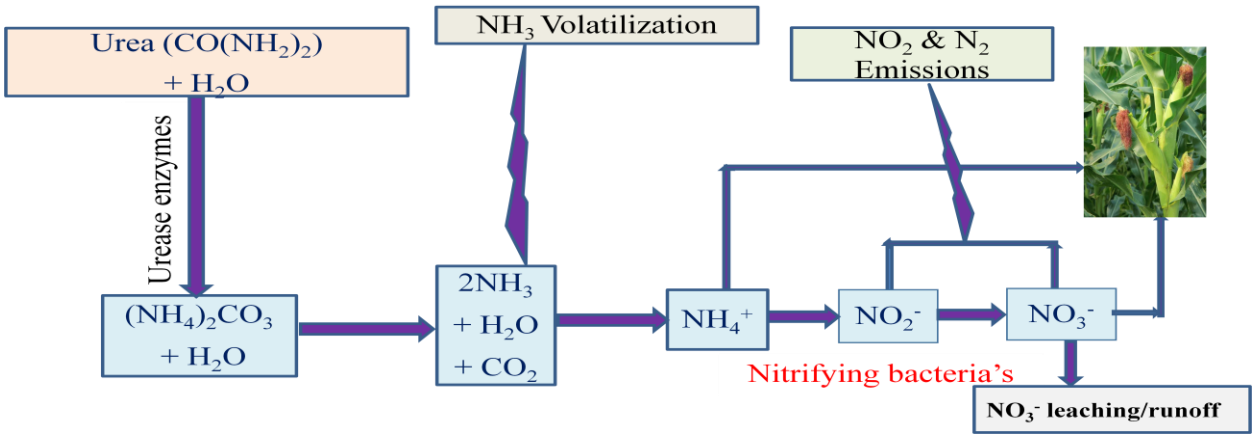

Figure 2.1. The loss of nitrogen from urea before the plants use it efficiently

Urea has a strong water affinity due to its molecular structure, which also allows it to absorb water from humid air. In the presence of even a small amount of water, the urease enzyme in the soil causes it to hydrolyze. A carbonyl functional group with two linked amino groups makes up urea. The amino groups split apart during hydrolysis, with each taking up a proton to create extremely volatile NH_3 (g), or, more ideally, can take up an additional proton to create $NH4^+$ (aq). In a typical urea application, this procedure takes one to four days to complete (Id et al., 2020). Therefore, the rate of urea hydrolysis needs to be managed in order to reduce nitrogen (N) losses to the atmosphere and water bodies, boost nitrogen usage efficiency (NUE) in crops, and maintain a sustainable and healthier ecosystem.

2.4 Slow or Controlled Release Fertilizers (S-CRFs)

By carefully coordinating N availability with N demand, plant nitrogen utilization efficiency is greatly increased. Therefore, the key to increasing crop uptake and reducing N losses is timing the N treatment to coincide with the crop's greatest uptake (Herrera et al., 2016). Slow or controlled-release fertilizers (S-CRFs) were recommended as a crucial strategy to improve the efficiency with which plants utilize nutrients and were afterwards taken into consideration to solve the issues brought on by the global population growth. Although it has been around since the 1950s, the 1980s and 1990s saw the majority of the advancements in the development of these items (Mayer,2010*)*.The three main stages of the S-CRF release process are water permeation, nutrient dissolution, and release of nutrients through the S-CRF system. The terms "controlled release fertilizers (CRF)" and "slow release fertilizers (SRF)" are defined differently by various academics.

Both SRFs and CRFs are used to characterize the delays in nutrient availability for plant uptake, according to Fertahi et al. (2021), however CRFs are typically associated with fertilizers coated or encapsulated with various materials to distinguish these two groups. While SRFs are made up of animal and plant manures and compost, which must first decompose through the action of microorganisms, CRFs have semi permeable coatings and hydrophobic encasing materials that enable a considerably more regulated rate and duration of nutrient release. However, because microbial organisms are so effective, the time delay of release in a slow release fertilizer cannot be adjusted. According to the Association of American Plant Food Control Officials (AAPFCO), a slow release fertilizer is one that "retains nutrients for a long time and delays their availability up to a period when the plants required nutrients, or a fertilizer that supplies nutrients to the plants for significantly longer periods than a standard fertilizer (rapidly available to the plants), such as urea or ammonium nitrate, potassium, or potash." Additionally, CRF is a subset of SRF, which belongs to the class of fertilizer with a physical barrier, according to Lawrencia et al. (2021). S-CRFs provide many benefits in terms of enhancing crops' ability to use nitrogen efficiently, raising agricultural output, and lowering fertilizer usage. To obtain the same yield, the fertilizer application rate can be reduced by 20–30% of the recommended amount (Lawrencia et al., 2021). Additionally, it lessens ecological, environmental, and health issues that are brought on by nutrient volatilization and leaching into the atmosphere and water bodies (Rajan et al., 2021). However, it is preferable to take into account the characteristics of the (soil type, pH, temperature, moisture, microorganisms present in the soil, etc.) when applying controlled release fertilizers, as well as characteristics like composition and solubility of the coating or encapsulating materials and coating thickness for CRFs created by coating commercial fertilizer with various coating materials.

2.5 Factors Affecting the Application of S-CRFs

2.5.1 Soil Temperature

The temperature of the soil is one of the crucial elements for the release of nutrients. The fertilizer release is too less when temperatures are below 10^{o}C (Rajan et al., 2021).The pace at which nutrients are released is affected by temperature (Naz & Sulaiman, 2016) .According to Husby et al. the nutrient release rate was at its highest between 35 and 40^{0}C. Because rising temperatures encourage NH_4^+ conversion to NH_3, NH_3 diffusion rate, urea hydrolysis, and organic N

mineralization, it was discovered that they are likely to contribute to high ammonia volatilization loss rates (X. Liu et al., 2020) .

2.5.2 Soil pH

The interactions of chemical species in the granule and the diffusion coefficient of the ions are significantly influenced by the release medium's acidic or alkaline nature (Lawrencia et al., 2021). The pH of the soil directly affects the nutrients' availability. When the pH of the soil is too low or too high, some nutrients become insoluble, which reduces their availability to the plant's root system. In comparison to neutral or slightly alkaline soils, most nutrients are more soluble in acidic soils (M. Liu & Wu, 2015) .

2.5.3 Granule Radius and Coating Thickness

In the sake of economic viability, expanding the S-CRFs' radius is typically recommended. For the appropriate dispersion of nutrients in the root zone, granules must always be the ideal size (Lawrencia et al., 2021). As the coating thickness rises, the nutrients released decrease. When there were coating faults and a porous coating film, even thicker coating films failed to produce satisfactory results. The diffusion coefficient decreases as coating thickness rises. Even though samples with coating flaws and very porous coating films had a significant mean coating thickness and the lowest coefficient of variance of coating thickness, the diffusion coefficient increased nonetheless. Since the urea release rate cannot be precisely regulated, acceptable release qualities of the controlled release urea require more than just an appropriate coating thickness (Azeem et al., 2020).

2.5.4 Activity of Microorganisms

S-CRF biodegradation is a complicated process that incorporates cascade events that are managed by biotic and abiotic environmental stimulus. (Panpatte & Jhala, 2018)'s description of the breakdown of biodegradable polymer coatings is as follows: The microbes attach to the polymer surfaces and secrete enzymes that break down the polymeric bonds, creating oligomers and dimers that break down into monomers. When these monomers are subsequently subjected to aerobic biodegradation, they are transformed into carbon dioxide, water, minerals, and biomass; when subjected to anaerobic biodegradation, they are transformed into carbon dioxide, methane, and moist

material. As a result, the amount of S-CRFs that degrade depends on whether soil microorganisms are present or not.

2.6 Mechanisms Followed to Develop S-CRFs

Nutrient availability can be delayed or plants can receive a steady supply of nutrients over long periods of time through a number of processes. These include membrane coatings that are either semi-permeable or impermeable, deep-planting fertilizers like urea super granules (USG), urea and nitrification inhibitors, and the use of nano-fertilizers.

2.6.1 Fertilizers Coated with Semi permeable or Impermeable Membranes

Over 95% of slow-release fertilizers have been replaced in recent years by coated fertilizers due to the rapid growth of coated fertilizers (Ruser & Schulz, 2015).To lessen the release of nutrients, it is necessary to create one or more layers of semi permeable or impermeable membranes on the surface of the fertilizer granules. There are numerous slow release effects because different membrane topologies have various characteristics. For slow-release coatings, a number of semi permeable or impermeable materials have been tried. Typically, these materials are divided into two categories: inorganic mineral compounds and organic polymeric polymers (Beig et al., 2020). Polymeric resins and thermoplastic polymers are examples of organic materials, whereas inorganic mineral-based compounds like gypsum, sulfur, and bentonite are categorized as inorganic coatings. An example of an impermeable substance is sulfur. Spraying sulfur over urea fertilizer creates a barrier that keeps soil water and rainwater away from the highly soluble urea until physical or microbiological activity causes cracks or fissures to form in the coating. The release of nutrients is slowed down and the pace at which fertilizer granules dissolve is decreased by covering urea with sulfur. However, due to high production costs and erratic release patterns, sulfur-coated fertilizers frequently fail to achieve the slow release guidelines (Herrera et al., 2016). Due to their notoriously fragile and easily damaged surfaces, sulfur-coated fertilizers are prone to cracking, which lets water in, premature urea granule disintegration, and nitrogen loss through leaching (Naz & Sulaiman, 2016) .Additionally, as elemental sulfur is extremely acidic, using it as a coating may promote soil acidification, which in turn may result in a lack of nitrogen (Dimkpa, Fugice, et al., 2020; Lawrencia et al., 2021). Disorders resulting from deficiencies in other nutrients, such as calcium or magnesium, may also be brought on by this acidity (M. Liu & Wu, 2015). Artificial polymers are membranes with small surface pores that are semi-permeable. Synthetic polymers are preferred over sulfur because of their

less propensity to have coating disturbances brought on by any physical or microbiological activities(Naz & Sulaiman, 2016).Additionally, coating polymers are relatively hydrophobic, allowing controlled moisture diffusion through their variably permeable membranes. As a result, the N release rates vary depending on the polymer's permeability, composition, and thickness as well as the soil's temperature, pH, and moisture content. When it comes to controlled release properties, synthetic polymers including polyethylene, polystyrene, polyacrylamide, and polysulfide show promising results. The majority of them have hydrophobic properties that allow controlled moisture flow across their porous membranes (Chen et al., 2018). Due to their high cost and lack of biodegradability, these materials could not be employed to manufacture controlled-release fertilizer on an industrial scale. The deposition of non-biodegradable residues from synthetic polymers could pose environmental risks (Dimkpa, Fugice, et al., 2020). In comparison to synthetic polymers, biopolymers such as starch, cellulose, lignin, vegetable oil, animal and vegetable gum, and rosin are noted for being less expensive, biodegradable in soil, and nontoxic; yet, they are binder films and somewhat weak coating barriers and primarily require changes (Fu et al., 2018).

2.6.2 Urease and Nitrification Inhibitor

Inhibitors of nitrification and urease have been studied recently as mitigation solutions to lower emissions and N losses from the use of agricultural fertilizer. Urease inhibitors function by impeding urease's active site, delaying the hydrolysis of urea, and reducing the quantity of nitrogen released into the atmosphere as NH_3. On the other side, nitrification inhibitors often work to stop soil-based bacteria like nitrobacter and nitrosomonas from nitrifying, which eventually limits N losses by lowering N_2O emissions and NO_3^- losses by leaching from soil (Cantarella et al., 2018). Inhibitors of urease and nitrification can both successfully lower nitrogen loss, as well as GHG emissions and water pollution. Urease inhibitors are made into solids by coating fertilizer products or applied separately to the soil, largely to lessen urea hydrolysis by urease enzymes, according to Cantarella et al. (2018). The most extensively used urease inhibitor is by far N-(n-butyl) Thiophosphoric Triamide (NBTPT), also marketed as Agrotain and created by Koch Agronomic Services. Ammonium thiosulfate (ATS), phenylphosphorodiamide and phenylphosphorodiamide (PPD and PPDA), hydroquinone, and calcium thiosulfate are further popular urease inhibitors (CTS). The nitrifying bacteria that produce the enzymes ammonia monooxygenase (AMO), hydroxylamine oxido-reductase (HAO), and nitric oxide reductase (NOR) are inhibited by a class of compounds known as nitrification inhibitors (Ruser & Schulz, 2015). The majority of nitrification inhibitors function by

blocking the enzyme ammonia monooxygenase during the first stage of nitrification, which involves the oxidation of NH_4^+ to hydroxylamine (NH_2OH) via the enzyme AMO. NH_2OH is then converted to NO_2 via the enzyme HAO, and the second stage involves blocking nitrobacterial nitrification, which oxidizes NO_2 to NO_3^- via the enzyme nitric oxide reductase. Nitrification inhibitors have drawn attention as a potential mitigation approach for reducing N_2O emissions and the water pollution brought on by the usage of fertilizers. Dicyclodiamide (DCD), 3, 4-dimethyl-1H-pyrazole phosphate (DMPP), carbon sulfide (CS_2), thioethers, and 2-ethynylpyridine are a few examples of nitrification inhibitors (Byrne et al., 2020). Inhibitors of nitrification and urea, however, change the osmotic strength of soil solutions. The flush of mineral N may be lessened by the delayed urea hydrolysis and lower osmotic shock (Abalos et al., 2014).

2.6.3 Urea Supper Granular Formulation

The production of USG fertilizer involves physically altering regular urea fertilizer. It was created by the International Fertilizer Development Center (IFDC), located in Muscle Shoals, Alabama, in the United States. Its nature and characteristics are comparable to those of urea, but its granule size is larger and more compact, and it has some slow hydrolysis-friendly circumstances. USG resembles commercial urea in composition and is spherical in shape with 46% nitrogen content. The granule weighs 1.8 g and has an average diameter of 11.5 mm (Hussain et al., 2017). Sarkar et al. (2021) claim that the usage of USG ensures greater nitrogen use throughout the plant's growing season and that using USG in place of commercial urea for cabbage and cauliflower can save 10–20% of the nutrient. However, deep placement of USG is required to prevent ammonia volatilization due to paddy soil's quick dissolving and the burning of seeds or plant roots (L. Liu et al., 2018).The USG's deep-placement strategy requires a lot of manpower and takes a long time, which has restricted its application in complex agricultural manufacturing systems.

2.6.4 Nano Fertilizers

In order to meet the essential nutrient needs of plants, nano-fertilizers are nutrients that have been encapsulated or coated with nano-material for regulated, gradual delivery of one or more nutrients. There are three approaches to encapsulate nutrients with nano-materials: coating commercial fertilizers with a thin layer of nano-particles; encapsulating plant nutrients in the nano-materials to create a new fertilizer; or preparing nutrients in the form of a nano-emulsion to be applied directly to plants (Zulfiqar et al., 2019).According to Madzokere et al. (2020), the use of nano-fertilizers

increased crop productivity by 6–17%. Nano-fertilizers containing zinc oxide, silicon dioxide, and titanium oxide nano-particles demonstrated novel performance characteristics, such as improved seed germination, shoot length, and healthy seedlings. While commercial fertilizers only perform the same thing in 4 to 10 days, NFs release their nutrition either alone or in combination with CF at a slow and consistent rate for 40 to 50 days (Seleiman et al., 2021). Seleiman et al. (2021) conducted a review and discovered that many NFs have already been created and have the potential to play a significant role in modern agriculture with regard to plant growth and development, including quality and yield, with a relatively small number of dosages compared to commercial fertilizers. The applied doses of NFs varied from 0.05 to 5000 mg/L, which is significantly less than CFs and has greater nitrogen utilization efficiency with little environmental contamination, according to Saha et al., (2021). The fact that the NFs dose ranges employed in various agricultural productions vary, however, is troubling. It suggests a lack of knowledge regarding the ideal NF dosages for specific crops. Therefore, the price of crop production as well as plant toxicity may increase as a result of the lack of NF prescribed levels. Risks to human health could result from the widespread release of nano-particles into the environment and food chain (Zulfiqar et al., 2019). The widespread use of nano-fertilizers as a source of plant nutrients is constrained by their expensive cost as well as a lack of production and supply in appropriate numbers. Other noted drawbacks of employing nano-fertilizers include the lack of appropriate risk management systems and uniformity, which are largely absent from the formulation process (Saha et al., 2021).

2.7 Advantages and Limitations of the S-CRF formulation Mechanisms

All of the aforementioned methods ultimately aim to maintain nitrogen in the soil as NH_4^+ and NO_3^- for a lot longer than the plant's uptake period. Urea nitrogen is used by plants as NH_4^+ and NO_3^-. The application of all the aforementioned processes to urea fertilizer, as illustrated in Figure 2.2 below, serves to decrease the activity of the urease enzyme and nitrifying bacteria, which helps to decrease the loss of nitrogen through ammonia volatilization, nitrous oxide emission, and surface runoff. Applying all three principles to commercial urea fertilizer improves plants by improving the efficiency with which they use nutrients (N), lowering the amount of fertilizer required, and minimizing adverse effects on the environment and human health.

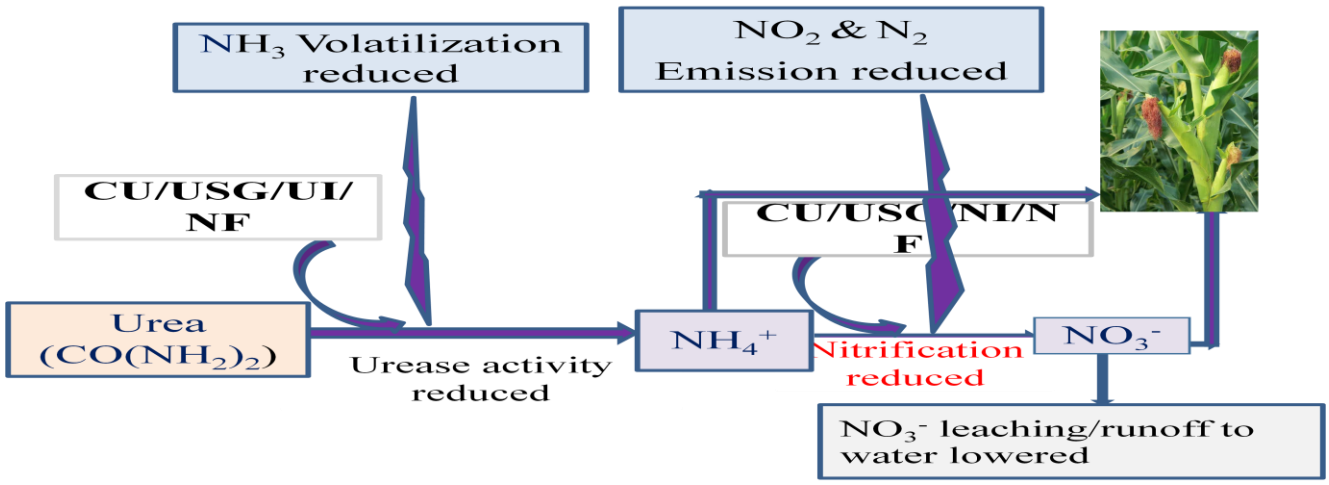

Figure 2.2. Effect of CU, USG, NF, UI, and NI to reduce the nitrogen transformation rate

As shown in the tables below (Tables 2.2 and 2.3), although the development of slow or controlled-release fertilizers using the aforementioned mechanisms plays a significant role in improving the nitrogen use efficiency of plants and lowering environmental and health problems, it has its own limitations, such as high processing costs and non-biodegradability, and is primarily still susceptible to nutrient loss because of the easily crackable nature of coating materials.

Table 2.2. Advantages of using S-CRF formulation mechanisms

Mechanisms	Advantages	Reference
Sulfur coating	➢ S coating of urea could significantly reduce ammonia (NH_3) volatilization from soil. ➢ High S-induced N recovery from soil by Plants.	➢ (Naz & Sulaiman, 2016) ➢ (Beig et al., 2020)

Polymercoating	❖ It has a hydrophobic nature, permitting controlled diffusion of moisture through their permeable membrane. ❖ Least affected by soil properties.	❖ (Dimkpa, Fugice, et al., 2020)
Urea super Granule	❖ Reduce the ammonia volatilization loss ❖ Reduce the usage of fertilizer in the fields.	➢ (Sarkar et al., 2021)
Urease and Nitrification Inhibiter	❖ Inhibits urease enzymes and microorganisms that causes N losses in the form of N_2O, NO and NH_3. ❖ Reduce burning of seed due to a high Concentration $NH4^+$ and $NO3^-$.	➢ (Abalos et al., 2014) ➢ (Cantarella et al., 2018)
Nano fertilizers	❖ Improves the nutrient-use efficiency and decreasing nutrient loss through Evaporation and leaching.	❖ (Seleiman et al., 2021) ❖ (Madzokere et al., 2020)

Table 2. 3. Limitations of using S-CRF formulation mechanisms

Techniques used	Drawbacks	Reference
Coating using Sulfur	➢ High production cost and irregular release pattern. ➢ S is relatively acidic; can result in soil Acidification.	➢ (Naz & Sulaiman, 2016) ➢ (Beig et al., 2020) ➢ (Dimkpa, Andrews, et al., 2020) ➢ (Lawrencia et al., 2021)
Polymer- coating	❖ Highly expensive ❖ Mostly non-degradable ❖ Pollutant ❖ Toxic	➢ (Dimkpa, Andrews, et al., 2020)
Urea super Granule	❖ Labor-intensive and time-consuming	➢ (L. Liu et al., 2018)
Urease and Nitrification Inhibiter	❖ Decreased osmotic shock along with delayed urea hydrolysis might reduce the flush of mineral N.	➢ (Abalos et al., 2014)
Nano fertilizers	❖ High cost of production ❖ Lack of information regarding the optimum dosages of NFs for particular crops causes to increase crop production cost as well as the plant toxicity.	➢ (Zulfiqar et al., 2019)

A variety of S-CRFs have recently been created by covering fertilizer with various coating materials. Over 95% of slow-release fertilizers come from it (Fu et al., 2018). In addition to being coated with semi permeable and impermeable membranes such as sulfur, gypsum, polymer, and lignin, urea has also been coated with urease and nitrification inhibitor materials to create slow-release fertilizers and nano fertilizers, such as N-(n-butyl) Thiophosphoric Triamide (NBTPT) inhibitor (Antille et al., 2015; Byrne et al., 2020; Janke et al., 2020; M. J. Khan et al., 2014; Shan et

al., 2021; Skorupka & Nosalewicz, 2021) and with neem oil (Ali et al., 2022; Kumar et al., 2020; Mohanty et al., 2021; Singh, 2012) and also urea coated with Nano particles (Dimkpa, Andrews, et al., 2020; T. Li et al., 2020; Shan et al., 2021; Umar et al., 2022). Although different coating materials can reduce nitrogen loss through leaching and volatilization, there is still a tendency for loss in most coated fertilizers because an irregular release of nutrients occurs when the coating materials are removed through any physical, chemical, or biological activity. It is also challenging to predict the thickness of a coating layer that can give plants the right amount of nitrogen at the right time. The nutrient (nitrogen) is sensitive to loss as a result of its erratic release brought on by the dissolution of coating layers that happens when the coated urea is exposed to water and soil, as shown in Figure 2.3 below.

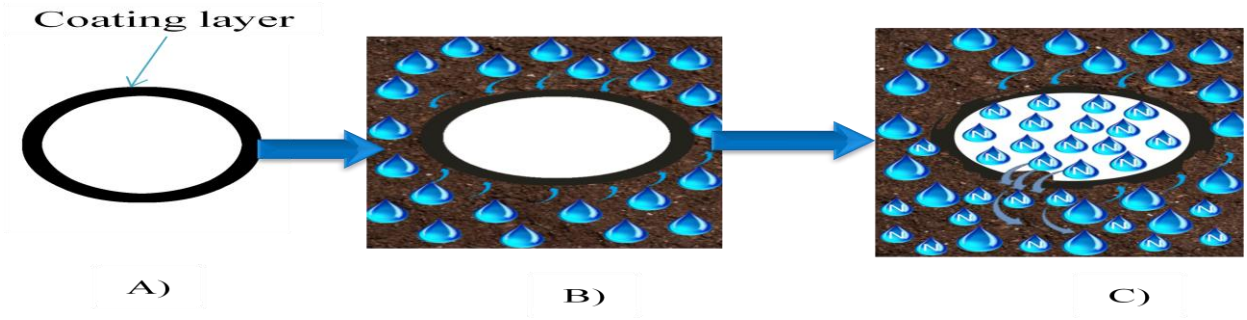

Figure 2.3. Irregular release of nitrogen due to disintegration of coating materials, A) coated urea, B) coated urea exposed to soil and water, C) irregular release of nitrogen (Dimkpa, Fugice, et al.,2020)

First, it is preferable to select coating materials that take into account their interactions with various soil properties and soil microorganisms, as well as their biodegradability, affinity for urea, permeability property to allow water and urea solution, capability to delay immediate urea escape from the coating surface, and ability to release nitrogen in a way that meets a crop's nutritional needs. The second crucial method for resolving issues with coating materials is to create a controlled nitrogen release fertilizer using industrial-grade urea granules straight out of the bag rather than covering it with coating materials later. The nitrogen from urea can be released regularly when it is encased in a biodegradable matrix, as demonstrated in the Figure 2.4 below. In this instance, urea powder was dispersed into a hydrophobic and biodegradable adhesive to create a bio-adhesive that is encapsulated in urea for a controlled release of nitrogen.

This adhesive can address issues with coating materials disintegrating through any physical, chemical, or biological activity and can improve the efficiency with which plants utilize nitrogen.

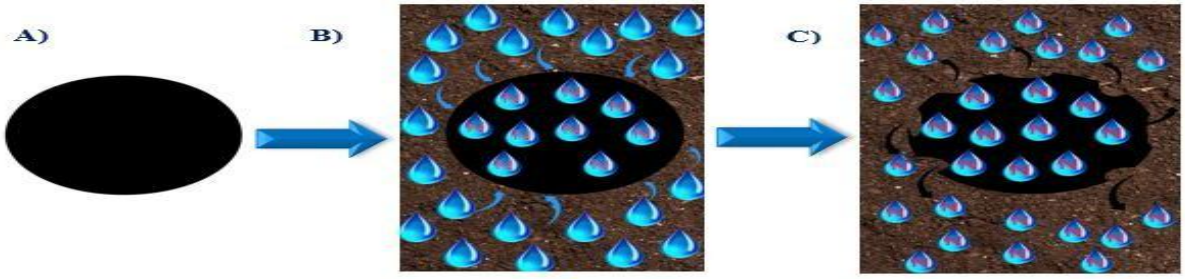

Figure 2.4. The Nitrogen release from the newly formulated fertilizer, A) urea encapsulated in a bio-encapsulating agent, B) when it is exposed to soil &water, C) release of nitrogen through degradation (Dimkpa, Fugice, et al., 2020).

Table 2.4. Matrix materials used for the formulation of slow-release fertilizer with its formulation methods

Nº	Matrix material/+ Modifier	Formulation Methods	References
1	Natural bentonite + binder: corn starch or Hydroxyl- propyl methyl-cellulose	Melt blending	(Hermida and Agustian, 2019)
2	Acetylated lignin sulfonate	Spray-coating	(Sadeghi et al., 2017)
3	Gypsum & Sulfur magnesium lime	Coating	(Babadi et al., 2015)
4	Phosphogypsum + Paraffin wax + span	Coating	(Yu & Li, 2019)
5	Polyvinyl alcohol + biochar	Melt blending	(Chen et al., 2018)
6	Polyurethane + mesoporous silica	Coating	(L. Li et al., 2016)
7	Polystyrene + Wax; Polyurethane	Coating	(Y.-c. Yang et al., 2012)
8	Bio-based Polyurethane (PU) + Isocyanate, acrylonitrile	Coating	(Bortoletto-Santos et al., 2020)

2.7 Lignin

The second-most prevalent natural polymer is lignin, a biodegradable, renewable macromolecule polymer that is derived from plants (H. Wang, Wang, et al., 2019). However, a number of variables, including the type of plant and leaf, stage of development, and extraction procedure, contribute to the complexity of lignin's structure. Ether bonds are prevalent in the natural lignin structure. Technical lignin is mostly produced as a by-product in the pulp and paper, cellulosic ethanol, and other bio-refinery industries (Ragauskas et al., 2014). For instance, around 150

million tons of chemical pulps are produced worldwide each year, along with about 70 million tons of lignin (Chakar & Ragauskas, 2004). The three-dimensional network structure of lignin, a type of organic polymer, includes phenolic and aliphatic hydroxyl, carboxyl, and methyl groups (H. Wang, Wang, et al., 2019). Entropy calculations reveal that lignin is where 40% of the energy produced biologically by the components of plants is kept. As a result, one of the most abundant green resources available to mankind in the twenty-first century is lignin. Technical lignin has recently been employed as an intriguing candidate in the physicochemical synthesis of novel materials and chemicals (Cortés-Triviño et al., 2018). Overall, technical lignin's high-end use is important for reducing environmental pollution and advancing the use of ecological resources because it not only provides raw materials for other industries but also has significant environmental benefits. But because of its variability, research and development of lignin-based products go quite slowly. The majority of technical lignin is utilized as low-grade fuel and burned directly in the bio-refinery to generate heat and electricity, which prevents it from fully utilizing the lignin structure characteristic and achieving value-added lignin usage. Technical lignin has only been partially transformed into value-added products. Numerous researches published recently suggested that polyurethanes, antioxidants, and phenol-formaldehyde resins may all benefit from the use of some technical lignin (Qiao et al., 2015). However, the largest obstacle to the development and use of lignin is its poor purity and complicated structure (Kai et al., 2016). Technical lignin is noteworthy for having intriguing qualities like gradual element release, chelating of metal ions, adhesiveness, dispersability, and other qualities (Sipponen et al., 2017; C. Wang et al., 2016). For the growth and development of crops, it can be converted into humus in the soil to cultivate the soil, enhance soil structure, and reduce the effects of soil illnesses (Neff et al., 2002; Sipponen et al., 2017). Additionally, lignin can be altered to create lignin-based slow or controlled-release fertilizers, which can greatly increase the effectiveness with which nutrients are utilized while simultaneously lowering the current market price of these fertilizers (Lapierre et al.,1994). In general, chemical (Esterification reaction, and other chemical changes), coating (without or with chemical modifications), and chelation alterations are used to create lignin-based slow or controlled release fertilizers (Lapierre et al., 1994; Mulder et al., 2011; Sipponen et al., 2017). This work has been interested to valorize Lignosulfonate and to adapt modification techniques used to create lignin-based slow or controlled release fertilizers. It then focuses on examining the releasing impact of fertilizers to serve as a guide for the growth of

the fertilizer business in the future. Depending on the species, the amount of lignin in biomass might range from 10 to 40 weight fraction. In general, woody biomass has larger lignin content than herbaceous biomass. Lignin can be divided into three categories: hardwood, softwood, and herbaceous lignins, depending on the make-up of the building blocks. S-units and G-units make up the majority of the lignin in hardwood. Most of the G-unit in softwood lignin is present. Herbaceous lignin differs from the other two forms of lignin chemically because it contains all three monolignols and has a minor excess of H-unit. Lignin has larger carbon content than cellulose, according to the chemical formula, and it can hold up to one-third of the biomass' total energy.

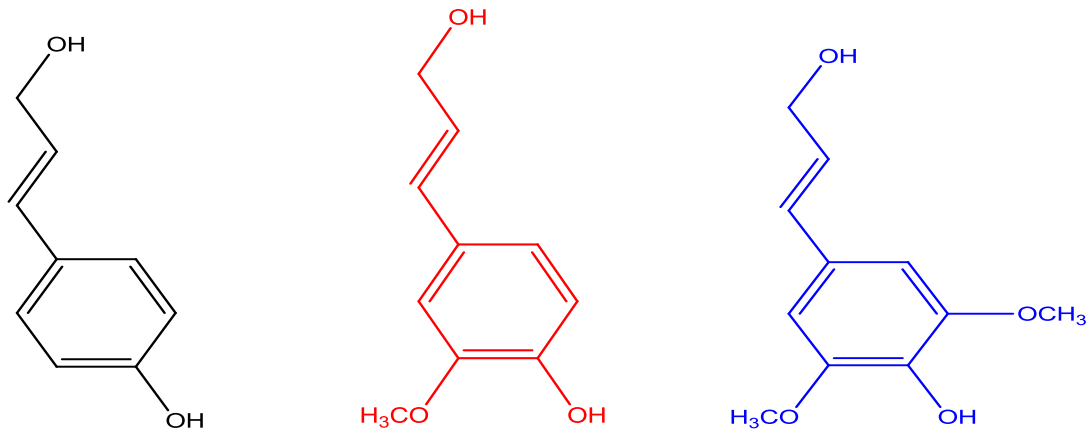

P-Coumaryl alcohol *Coniferyl-alcohol* *Sinapyl alcohol*

H-unit G-unit S-unit

Figure 2.5. Major Monolignols of Lignins

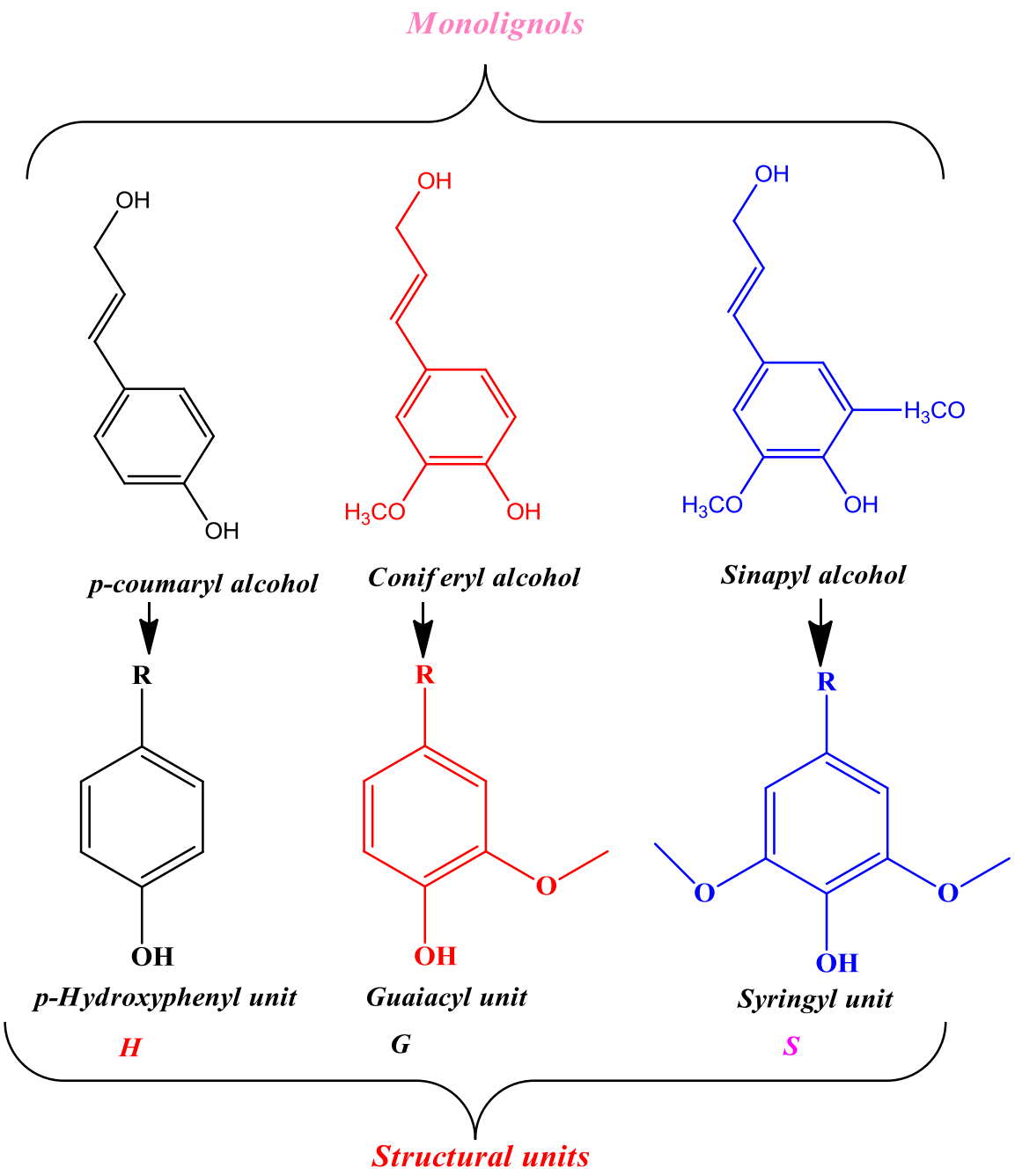

Figure 2.6. Structural units of Lignin along with its monolignols

There are differences between lignins from different plants (softwoods, hardwoods, and non-woods) in terms of the proportion of each phenylpropanoid unit and the strength of the carbon-carbon bonds between the lignin units. On the other hand, lignins from the same source can be different in terms of their structures and functions depending on the conditions under which they

are extracted (Bykov, 2018). Softwoods lignins are primarily comprised of guaiacyl with only small amounts of hydroxyl phenyl and syringyl units. Hardwood lignins are often referred to as guaiacyl-syringyl lignins, as they contain both types of lignins. Hardwoods also contain small amounts of hydroxyl phenyl lignin (Moshinsky, 1959). Although, the ratio of phenylpropanoid units in non-wood lignins varies, they normally contain all three precursors, guaiacyl, syringyl and p- hydroxyl phenyl (Derkacheva & Sukhov, 2008). The overall content of p-hydroxyphenyl is higher in annual crops than in softwoods and hardwoods (Brodin, 2019). A radical coupling method is used to polymerize the carbon-carbon or ether bonds that connect the monomers. Several different linkage types may occur at any of several different sites on each phenolic unit. The most prevalent linkage types in a lignin molecule are β-O-4, α-O-4, β-5, 5-5, 4-O-5, β-1, β-β and Di benzodioxocin (Figure 2.7) (Gordis, 1940; Karhunen et al., 1995) which is around one-third of the linkages comprising of carbon-carbon and two-thirds are ether linkages (J. K. Sameni, 2015).

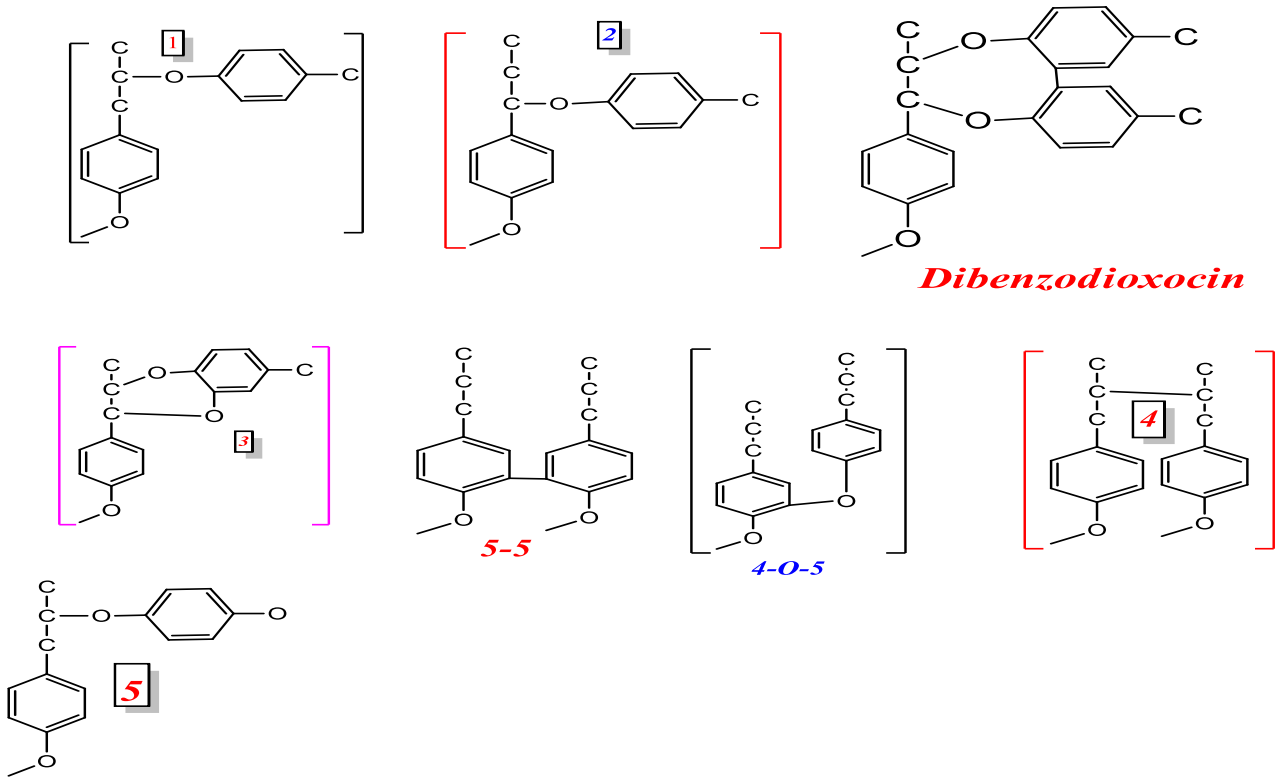

Figure 2.7. The most common inter-monomeric linkages between lignin units: 1) β-O-4, 2) α-O-4, 3) β-5, 4) β-β, 5) β-1

2.7.1 Types and Industrial sources of lignin

When lignocellulosic biomasses are utilized as raw materials for pulp manufacturing or second-generation ethanol production, different pretreatments or separation methods yield technical lignin as a byproduct. Depending on the method employed to isolate the technical lignin's chemical characteristics, such as composition and molecular weight, the molecular structure may be compromised, leading to the production of various types of lignin with various uses in bio-refinery platforms. Physical characteristics like solubility, hydrophobic and hydrophilic properties of lignin also make a difference. Due to these variations, each technical lignin must be taken into account separately (Kumar et al., 2020; Vishtal & Kraslawski, 2011). The primary commercial source of lignin is the pulp mill. The extraction operations, depending on the technology utilized, may take place in acid, alkaline medium, or organic solvents. The pulping techniques are used to separate the wood fibers. In each procedure, the lignin gradually fractures into low-molecular-weight pieces (Doherty et al., 2011). Kraft, sulfite, soda, and organosolv are the primary industrial processes (on a pilot scale). Depending on the method employed, native lignin may undergo significant structural and functional degradation, with a reduction in the quantity of aliphatic OH groups, β-O-4, and β-β bonds. Degraded compounds like phenolic hydroxyl groups, carboxylic acids, and carbonyl groups can also be produced (Capanema & Balakshin, 2015). Therefore, the extraction process and the sources of raw material (softwood, hardwood, or grasses) both have an impact on the structure of technical lignin (José Borges Gomes et al., 2020). In general, lignin separation process is clearly depicted by the following picture.

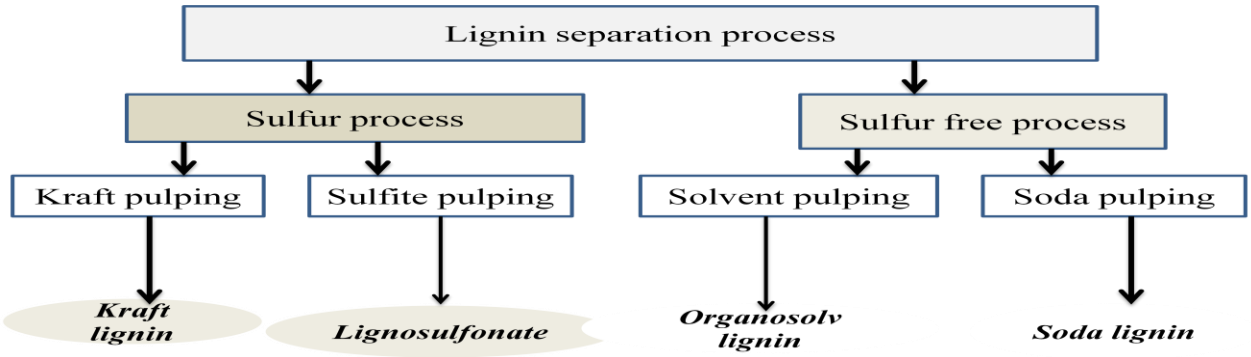

Figure 2.8. Lignin extraction process along their products (Ruwoldt, 2020)

2.7.1.1 Kraft lignin

The Kraft process is based on the use of an alkaline cooking mixture with the goal of removing the lignin from the lignocellulosic materials. Sodium hydroxide (NaOH) and sodium sulfide are the primary reagents at extremely high temperatures (140–170^{0}C) (Na_2S). After the lignocellulosic material has been de-lignified, a black fluid that contains lignin that has decomposed, oxidized inorganic compounds, and other organic components is produced. It could serve as a feedstock and serve as a source of technical lignin (Doherty et al., 2011; Kumar et al., 2020). The Kraft lignin produced by the Kraft pulping process is extremely condensed, has a significant amount of C-C bonds, and is separated from the Kraft black liquor by acidification. Kraft lignin may contain sulfur impurities in its structure as a result of the chemical reagents used during the Kraft pulping process. Due to the venous nature of sulfur, these impurities within its structure may render its utilization impractical or even inhibit the activity of catalysts (Doherty et al., 2011). Since aryl bonds are broken during cooking, a lot of phenolic hydroxyls are present in Kraft lignin. During the delignification process, oxidative circumstances might result in the creation of catechol and quinone structures as well as an increase in carboxylic groups. Ash and sugars are present in minor amounts in Kraft lignins (Kumar et al., 2020; Lin et al., 2014). There are aliphatic thiol groups as well as both high polydispersity and low molecular weight(Lin et al., 2014). Since the industries won't be able to use all of the black liquor produced, numerous studies are being done on how to turn it into high-value-added products (Luong et al., 2012). The structure of Kraft lignin is elaborated as follows.

2.7.1.2 Lignosulfonate lignin

It is lignin that was obtained by the sulfite pulping procedure. When wood is pulped, an alkaline earth metal sulfite mixture de-lignifies it by interacting with the lignin to create a water-soluble sulfonated system, which is then hydrolyzed by acids to destroy the lignin. A sulfonated compound with a variety of functional groups is created when the lignin is broken down during the sulfite process, giving it special colloidal characteristics (Vishtal & Kraslawski, 2011). A higher amount of ash roughly 4-8% than Kraft lignin is present in lignosulfonates of lignin, which are also water soluble and have a high molecular weight. As colloidal suspensions, stabilizers, dispersants, binders, detergents, adhesives, and feed components as well as surfactants and cement additives, it has been put to use in these applications (Conference et al., 2014). Based on interest there are different types of lignosulfonate lignin; such as, sodium

lignosulfonate, calcium lignosulfonate, magnesium lignosulfonate, aluminium lignosulfonate, ammonium lignosulfonate, and etc,. In this research, Sodium lignosulfonate was applied and modified for further urea encapsulation. The modification of this lignin type is due to it is susceptible for dissolution, improve its solubility. The chemical structure of used lignosulfonate in this work was depicted in the figure 2.9 below.

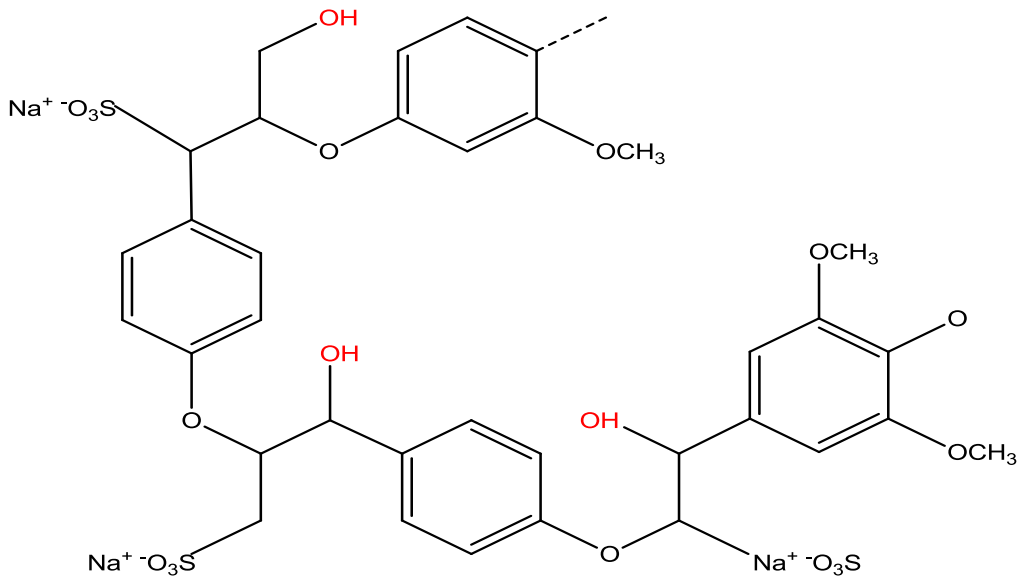

Figure 2. 9. Structure of sodium lignosulfonate

2.7.1.3 Soda lignin

Because they are based on the same conditions and principles as the current Kraft pulping technology and are compatible with it, soda-based procedures are an intriguing delignification method. However, they do not employ sulfur. The soda pulping method makes use of the primary chemical used in the sodium hydroxide (NaOH) process. Due to its lack of sulfur, soda lignin differs significantly from Kraft lignin and lignosulfonates. The presence of vinyl ethers is another distinctive characteristic (Vishtal & Kraslawski, 2011). For the synthesis of polymers, dispersants, and phenolic resins, soda lignin has been used (Conference et al., 2014). The lack of sulfur makes it applicable in fields like animal nutrition (Baurhoo et al., 2008). On the other hand, soda pulping is a rarer procedure because to its poor pulp yield performance.

2.7.1.4 Organosolv lignin

Organosolv delignification process aims to isolate the lignin from the carbohydrates in the lignocellulosic biomass using organic solvents for solubilizing the lignin. It is also interesting for many byproducts application for being possible sulfur free processes depending on the used solvents (Yáñez-S et al., 2014). Lignin extracted by organosolv process may have high purity, chemical reactivity, sulfur free and no toxicity. Low molecular weight, homogenous structure that resembles native lignin and polydispersity are its other characteristics (Vishtal & Kraslawski, 2011). According to some studies, more severe organosolv procedures result in a 36–56% reduction in the molar mass of extracted lignin relative to untreated lignin. Additionally, it is possible to see a decrease in the amount of aliphatic hydroxyl groups and an increase in syringyl phenolic units and condensed phenolic structures (Yáñez-S et al., 2014). Because it is extremely hydrophobic, organo soluble lignin is highly soluble in organic solvents but practically insoluble in water. It must be precipitated in order to remove organosolv lignin from the solvent, which commonly entails adjusting temperature, pH, and concentration (Vázquez et al., 1997).

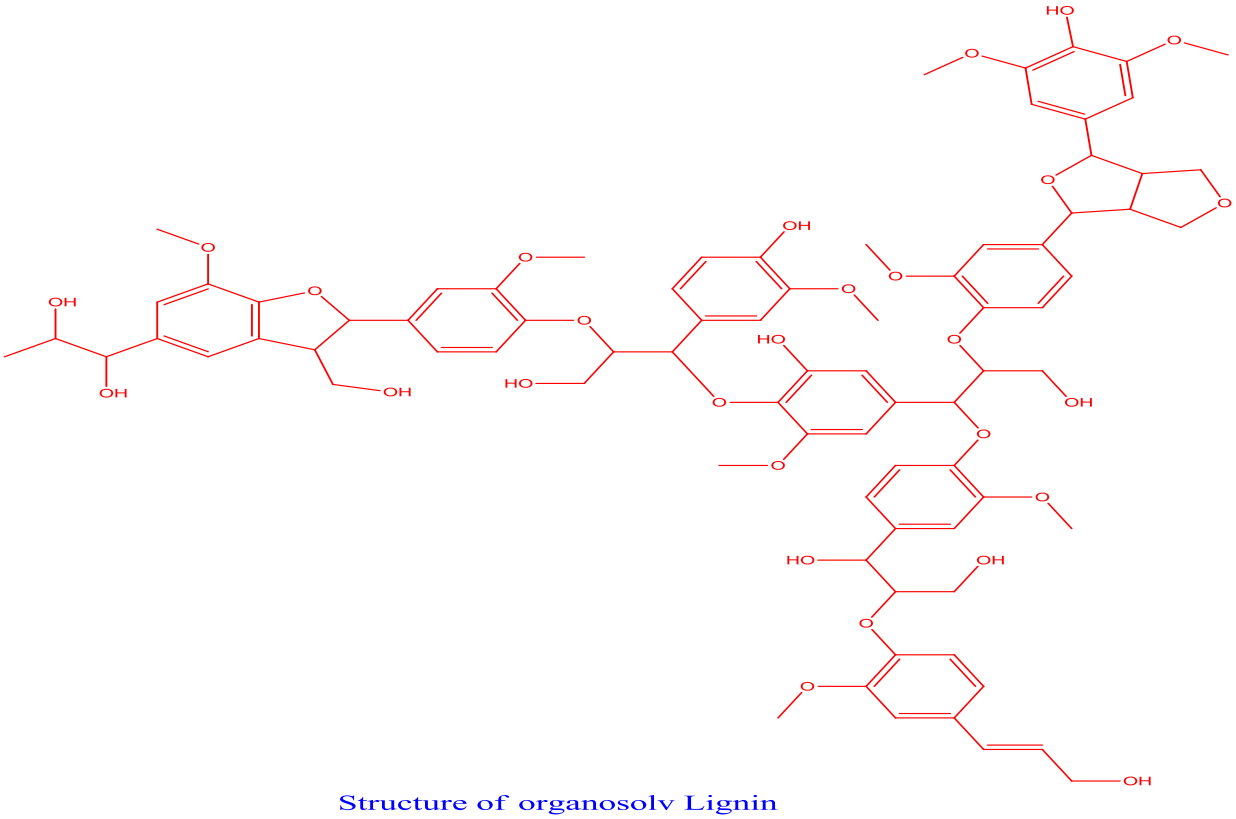

Figure 2.10. Structure of organosolv lignin

2.8 Lignin Functionalization/Modification

In addition to its macromolecular structure, the presence of numerous functional groups indicates the degree of lignin's complexity. The phenyl propanoid structure is decorated with functional groups like alcohols, phenols, and ethers, making the biopolymer amenable to chemical alterations. Additionally, the initial functional groups themselves may react with a variety of organic molecules as acids, nucleophiles, or electrophiles. Because of this, lignin structure can undergo a wide variety of changes, including those that alter its molecular mass distribution, increase its reactivity by adding highly reactive functional groups (such as phenolic and aliphatic hydroxyls), and enhance its compatibility with some synthetic polymeric matrices. Amination, methylation, phenolation, acetylating or esterification, and nitration are a few of these processes. Aside from that, depending on the new functional groups connected to the lignin macromolecule, enhanced solubility and hydrophobicity may be attained.

2.8.1 Amination

The elemental analysis of lignin shows that nitrogen is not a common element in the composition (Ge et al., 2015; X. Wang et al., 2014). However, introducing reactive sites that can be employed as intermediaries for lignin functionalization by using amines to graft nitrogen into the lignin structure appears to be an attractive alternative. Because amino groups are positively charged and ionizable under acidic circumstances, lignin is extremely reactive in aqueous fluids (B. Wang et al., 2018). Additionally, amino groups can change Kraft lignin, a hydrophobic technical lignin, into a very hydrophilic substance, enhancing its foamability, emulsifying abilities, durability, and mechanical strength (Liu et al. 2016). Additionally, because aminated lignins are capable of absorbing both cationic and anionic ions, they can be utilized to remove dyes and heavy metals from aqueous systems (X. Wang et al., 2014; Xu et al., 2017). By adding amine groups to the lignin, its molecular mass is increased and its TG is decreased. Technical lignins are tailored for a variety of value-added applications by increasing properties like reactivity, solubility, and surface tension.

2.8.2 Methylation

Methylation increases the methoxylation degree of lignin without appreciably changing their molecular mass distribution because methyl groups are relatively common in lignin as part of

methyl (-OCH_3) groups (Sen et al., 2015; Shen et al., 2020). As a result, lignin is more readily available for particular polymer synthesis applications because to methylation's increased solubility in organic solvents (Xiong et al. 2020). Brauns (1939) developed the first lignin methylation procedure as a way to characterize lignin. Using diazomethane in dioxane and then dimethyl sulfate in sodium hydroxide, the native spruce lignin was methylated. Due to methylation, lignin was rendered insoluble in bisulfite, affecting both phenolic and enolic hydroxyl groups. Today, one of the most popular methods for altering lignin is methylation in dimethyl sulfoxide (DMSO), which results in derivatives that are less reactive and thermally stable than the original hydroxylated lignin (Shen et al., 2020; X. Wang et al., 2014). Additionally, polymeric substances like polyethers, polyesters, polyethylene, and natural rubber respond better to methylated lignin (X. Wang et al., 2014). During the conversion of lignin, hydroxyl groups can also be shielded by methylation from undesirable reactions. In order to prepare lignin for pyrolysis and thermal conversion, methylation can be a valuable pretreatment method.

2.8.3 Phenolation

Lignin is altered via phenolation, or aromatic condensation, in an acidic media (Taleb et al., 2020; Thébault et al., 2020). This is due to an increase in the concentration of phenolic hydroxyl groups, which increases the number of reactive sites for the production and functionalization of polymers (Mou et al., 2020). However, for applications in bio-processing, a rise in free phenolic hydroxyl groups may be detrimental as these reactive sites may block hydrolyses like cellulases (Mou et al. 2020). Multiple reaction pathways are involved in lignin phenolation (F. Zhang et al., 2019). By creating reactive sites on the C_α and C_γ side chains of lignin, dehydration in an acidic media produces stable benzylic carbocations that can be condensed by phenol addition. The other pathways entail the removal of C_γ formaldehyde, the creation of enols, and the addition of phenol in para or ortho locations (Jiang et al., 2018; Londono-Zuluaga et al., 2018).

2.8.4 Nitration

The common method for performing lignin nitration is non-aqueous solvents. The most popular nitrating agents are sulfuric acid, acetic anhydride, or nitric acid in concentrated acetic acid (Meister, 2002). The resulting nitro-lignin (NL) is an amorphous powder with an average

molecular mass of between 600 and 2000 Da with colors ranging from yellow to brown. Large-scale lignin de-alkylation is caused by nitration, and nitrogen incorporation is typically around 7 wt% (Meister, 2002; L. Zhang & Huang, 2001). In binary water-aprotic solvent combinations, Lakhmanov et al. (2020) nitrated lignin using nitric acid. The nitrating agent also included acetyl nitrate, a mixture of acetic and nitric anhydrides. When nitration was carried out using nitric acid, 1,4-dioxane, acetonitrile, and tetrahydrofuran were used to provide the highest yield of nitrated lignin (83 to 101%) and the highest nitrogen content (4.3 to 4.5%), respectively.

2.8.5 Esterification

One of the key methods for functionalizing Aliphatic and aromatic OH in lignin is esterification. Typically, multiple anhydrides and acid chlorides are used in a pyridine or dioxane medium to produce lignin esters (L. Y. Liu et al., 2019). Since Fischer conducted the first high-temperature reaction of carboxylic acids with alcohols, this process has undergone a number of changes to produce high yields from a wide variety of reagents and raw materials. Because lignin has a number of reactive sites and is susceptible to structural changes when exposed to acids and heat, the Fischer approach can be challenging for lignin (L. Y. Liu et al., 2019). Additionally, depending on the reaction conditions, partial esterification frequently happens (Luo et al., 2018). Lignin that has been esterified exhibits different characteristics, including improved thermal and oxidative stability, a lower melting point, increased hydrophobicity nature and greater solubility in non-polar organic solvents. Lignin is thereby improved in terms of compatibility with hydrophobic matrices like polyolefins and aliphatic polyesters (Buono et al., 2016; J. Sameni et al., 2017; Shayesteh et al., 2020).The fact that toxic solvents are used and hazardous wastes (halogenated species) are produced, especially for homogeneous catalytic systems, is a downside of the majority of lignin esterification techniques .The traditional process of esterification known as acetylation often involves the use of acetic anhydride or acetyl chloride with pyridine as a catalyst. However, acetic acid is recommended for usage as the acylating agent because it is accessible, affordable, and sustainable (Shayesteh et al., 2020). Acetic acid was used as both a solvent and an acetylating agent in a study by de Oliveira et al. (2020) on the acetylation of Kraft lignin. Products were studied by FTIR, NMR (^{1}H, ^{13}C, and ^{31}P), and hetero-nuclear single quantum correlation after reactions were carried out under microwave heating (HSQC). Compared to unaltered Kraft lignin, the resultant lignin acetates displayed high solubility in

organic solvents (chloroform, ethyl acetate, and dichloromethane). This technique allowed for the selective acetylation of aliphatic OHs. This led to an increase in antioxidant capacity when compared to commercial antioxidants like butylated hydroxytoluene (BHT), which opened the door for its use as a green, sustainable antioxidant additive. A summary of recent studies regarding lignin esterification is found in the following Table 2.5. Even if various acids can be used as solvent and acetylating agent, acid anhydride is important for acetylating agent due to its process enhancement. In this thesis, acetic anhydride is selected as acetylating agent along with pyridine as a catalyst for sodium lignosulfonate modification.

Table 2.5. Lignin Esterification of different types of lignins

Lignin type	Reagents	Reaction parameter	Potential applications	Source
Alkali lignin	5% citric acid	RT/3 h/ 1% sodium hypophosphite	Nanofiller in polymeric matrices	(He et al., 2018)
Kraft and Proto bind lignin from agricultural fiber soda pulping	Butyric or crotonic anhydride	120 °C/24 h/ 1-MIM	Lignin-based polymeric materials	(Luo et al., 2018)
Soluble or insoluble Kraft Lignin in Water	Methacryloyl chloride, DMF Maleic anhydride	(a) 7 °C/24 h/ Et_3N (b) 85 °C/3.5 h	Pressure sensitive adhesive	(Nasiri et al., 2020)
Low Sulfur content alkali lignin	10% (aq.) polyvinyl alcohol, 10% (aq.) maleic acid	180 °C/ 0.5 h	Natural fibers reinforced composites	(Ko et al., 2020)

Lignosulfonates	Acetic anhydride-pyridine (1:1, v/v)	100 °C/48 h	Not suggested	(Shayesteh et al., 2020)
Eucaypt lignin and industrial Bioethanol residue lignin	Acetic anhydride-pyridine (1:1, v/v)	RT/ 24 h	Solubility Investigation	(J. Sameni et al., 2017)
Kraft lignin	Glacial acetic acid andH_2SO_4 (0, 0.5, 1.0 and 2.0% v/v)	110 °C/ 0.08-0.33 h/ Microwave reactor	Additive with highantioxidant capacity	(de Oliveira et al., 2020)
Lignin containing micro-fibrilled Cellulose	K_2CO_3 (0.3 g) and acetic anhydride (6mL)	90 °C/1 h	Bio-composites forpacking and biomedical Products	(Yetiş et al., 2020)
Softwood Kraft lignin	2/3 mL acetic anhydride/gram of lignin	0.25 h	Carbon fibers	(M. Zhang & Ogale, 2014)
Pine Kraft lignin	Mixture of Choline chloride/acetic anhydride (1:5, v/v)	0.05-1 h; Heating	Pretreatment for pyrolysis	(T. Li et al., 2020)

The following reaction mechanism is the acetylation of lignin with acetic anhydride.

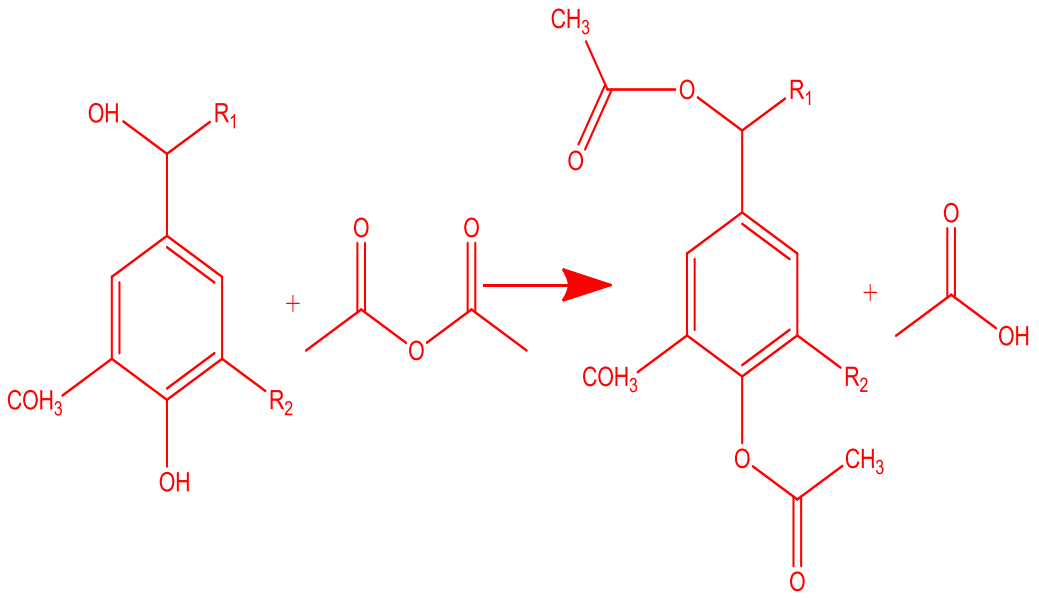

Figure 2.11. Acetylation process of lignin by acetic anhydride

Table 2.6. Applications of different Types of Lignin

Functional products	Potential application	Reference
Lignin monomers and dimers, aromatic phenols, alkyl phenols, aromatic aldehydes, aromatic alcohols, acids, aryl ketones, antioxidants, dispersants, PU, phenolic resins, vanillin	Industrial chemicals, bio-based adhesives, multifunctional materials, building blocks for bio-based products	(Cao et al., 2018; Kalami et al., 2017; Solt et al., 2019; H. Wang, Pu, et al., 2019)
Biochar, bio-oil, syngas, activated carbon, carbon fibers, carbon black	Light-weight polymer composites, adsorbents, electrochemical devices, automotive	(A. Khan et al., 2018; Puziy et al., 2018)
3D Printing resin (anionic surfactant), Scaffolds, lignin nanotubes, hydrogel	Biomedical applications, tissue engineering, drug	(Aro & Fatehi, 2017; Askvik et al., 1999;

	delivery	Figueiredo et al., 2018; Myrvold, 2014; Thakur & Thakur, 2015)
Li-ion, Na-ion batteries (electrodes), super capacitors, solar cells	Energy devices, batteries, fuels cells	(Hydrogel, 2011)
Bitumen, cement additive, dispersant, reinforcement	Construction pavements, cement panels	(Kalami et al., 2017; Puziy et al., 2018)
Soil conditioner, in fertilizers and pesticides as controlled release agent, sequestering agent, material absorbing soil contaminants, fire retardant	Agriculture, textiles, soil reclamation, water purification, fire suppression	(Kalami et al., 2017; Puziy et al., 2018) (Aso et al., 2013; Ge & Li, 2018; Ouyang et al., 2009)

2.9 Adhesive

In order to hold or bind at least two materials together in a way that is suitable for the application, adhesives are a diverse group of chemicals (Cui & Liu, 2021). The property of adhesion is the main mechanism by which the adhesive functions, and surface adherence and cohesion are necessary for bonding. Intermolecular interactions are what create adhesion, which is the attraction between two different substances. Material connecting with an adhesive is known as bonding. A variety of adhesives are used with diverse materials and in varied situations to bond different sorts of material (Banea & Da Silva, 2009).

2.9.1 Adhesive classification

Adhesive can be classified based on their origin as follows:

2.9.1.1 Synthetic adhesives: Epoxies, polyurethanes, cyanoacrylates, polyimides, silicones, acrylics, polyamides, cyanoacrylates, polyacrylates, polyvinyl acetate (PVA), nitrile, and neoprene are examples of common synthetic adhesives.

2.9.1.2 Natural/Organic adhesives (glues)

Animal glue: Boiling animal bones and connective tissues that contain protein produces animal glue.

Casein: Skimmed milk is the source of casein. The protein found in cow's milk makes up the majority of casein.

Fish glue: which includes protein, is used to make fish glue (collagen).

Aqueous dextrin-based vegetable glues (such as tapioca paste, soybean glue, starch glue, and) Latex adhesive made of natural rubber Natural rubber glues are made from plant-derived, water-based latex emulsions.

2.10 Physicochemical Properties of Lignosulfonate

2.10.1 Interaction with other components

The presence of ionic functional groups has a significant impact on interactions with other surfactants and polymers because lignosulfonates' anionic groups exhibit strong electrostatic interactions. It is by no means simple to study inter-species interactions because they frequently have opposing impacts. Cooperative adsorption might result, for instance, from the interaction between lignosulfonates and cationic surfactants (Askvik et al., 1999). While precipitation would lower the surfactant bulk concentration, such mixing is also possible. Because lignosulfonate and anionic surfactants are electrostatically attracted to one another, their adsorption at the interface is likely to be competitive. Yet, because both species also enhance ionic strength, the surfactants are salting out and being drawn to the contact. An early investigation by Ström and Stenius demonstrated that interactions between lignosulfonate and cationic polyelectrolyte can produce soluble complexes, colloids, and macroscopic precipitates (Stenius,1981). Fractionated lignosulfonate was also used by the authors in their investigation, which demonstrated that lignosulfonate with a low molecular weight only generated colloids, but lignosulfonate with a larger molecular weight produced a flocculated precipitate.

2.10.2 Gelling and precipitation in aqueous solution

Many modifications that weaken the solubility of lignosulfonate can lead to its precipitation from solutions. Another electrolyte may be added to cause precipitation by salting out (Ruwoldt et al.,

2020). With a few exceptions, the salting-out tendency for different ions, as reported, is consistent with both the Schulze-Hardy rule and the Hofmeister series (Myrvold, 2013; Ruwoldt et al., 2020).The fact that the common ion effect and screening effects could not account for the observed effects was also examined. Due to the fact that many solvents are miscible with water but are ineffective solvents for lignosulfonates (Myrvold, 2014), adding a solvent to an aqueous solution can also result in the precipitation of lignosulfonates (Vainio et al., 2012). For instance, a popular technique to extract lignin from alkali black liquor during wood pulping is technical lignin precipitation by pH lowering (Sixta, 2008). If the ratio of sulfonic to carboxylic acid groups is too low, lignosulfonate precipitation can occur because both the phenolic and carboxylic acid groups are largely un dissociated at pH-3 or lower (Deng et al., 2010; Yan et al., 2010).

2.10.3 Chemical modification

Controlling the production parameters during sulfite pulping and post-separation modification are two ways to modify the chemical composition of lignosulfonates (Aro & Fatehi, 2017). One of two reasons why lignosulfonates are frequently subjected to chemical modification is:

1. Modification of the physicochemical parameters, for instance, to enhance the performance and compatibility of the dispersant Functional group addition or substitution is one way to achieve this, but depolymerization and polymerization are also viable options.

2. By changing the availability and abundance of specific functional groups, one can increase the utilization of and compatibility with polymer compositions. Lignosulfonate may be included in a larger polymer matrix as a quasi-monomer. It has also been proved that the modified lignin can be used as filler by mixing it with thermoplastic substances.

2.10.4 Solubility in different solvents

Due to the high concentration of sulfonate groups, lignosulfonate is more water soluble than other types of technical lignin (Ross & Mazza, 2010). Solutions of 53 wt% in water have been observed (Myrvold, 2013), indicating that lignosulfonate is almost completely soluble in water. Myrvold conducted additional research on the solubility of several lignosulfonate samples in various solvents (Myrvold, 2016). In addition to being soluble in water, the author demonstrated that lignosulfonates are also well-soluble in ethylene glycol, propylene glycol, dimethyl

sulfoxide (DMSO), methanol-water, and dioxane-water mixes that contain more than 20% water. Dimethyl form-amide, methanol, cyclohexylamine, and acetic acid all have low solubility. Hardwood lignosulfonates were shown to have Hansen solubility parameters that were greater than those of softwood lignosulfonates at greater distances from water (Myrvold, 2016).

CHAPTER THREE

METHODOLOGY

3.1 Equipment

Different materials and tools were used, including an analytical balance, a pH meter, a ball mill, a hot plate, heating mantle, sieve, Rotary evaporator, chiller, a measuring cylinder, water bath, beaker, three neck flask, plastic funnel, fine mesh cloth, filter paper, copper wire, spatula, mirror glass, syringe, oven, and a mixer, for the modification/acetylation and characterization of lignosulfonate and the encapsulation of urea in acetylated lignosulfonate. Instruments like FTIR, manual pelletizer machine, and the Automatic Kjeldhal Analyzer were employed for analysis as well as characterization.

3.2 Chemicals

Commercial urea granules (sized 1-4 mm) with 46% nitrogen content were purchased from Ethiopian government fertilizer dealers. Commercial Lignosulfonate (alkaline) (TCI) was purchased from Tokyo Chemical Industry, India. From the department lab, other substances, including sodium phosphate dibasic, sodium bicarbonate, sodium carbonate, and solvents like Dichloromethane, pyridine, acetic anhydride, ethanol, acetone, and de-ionized water, were obtained.

3.2.1 Methodology Framework

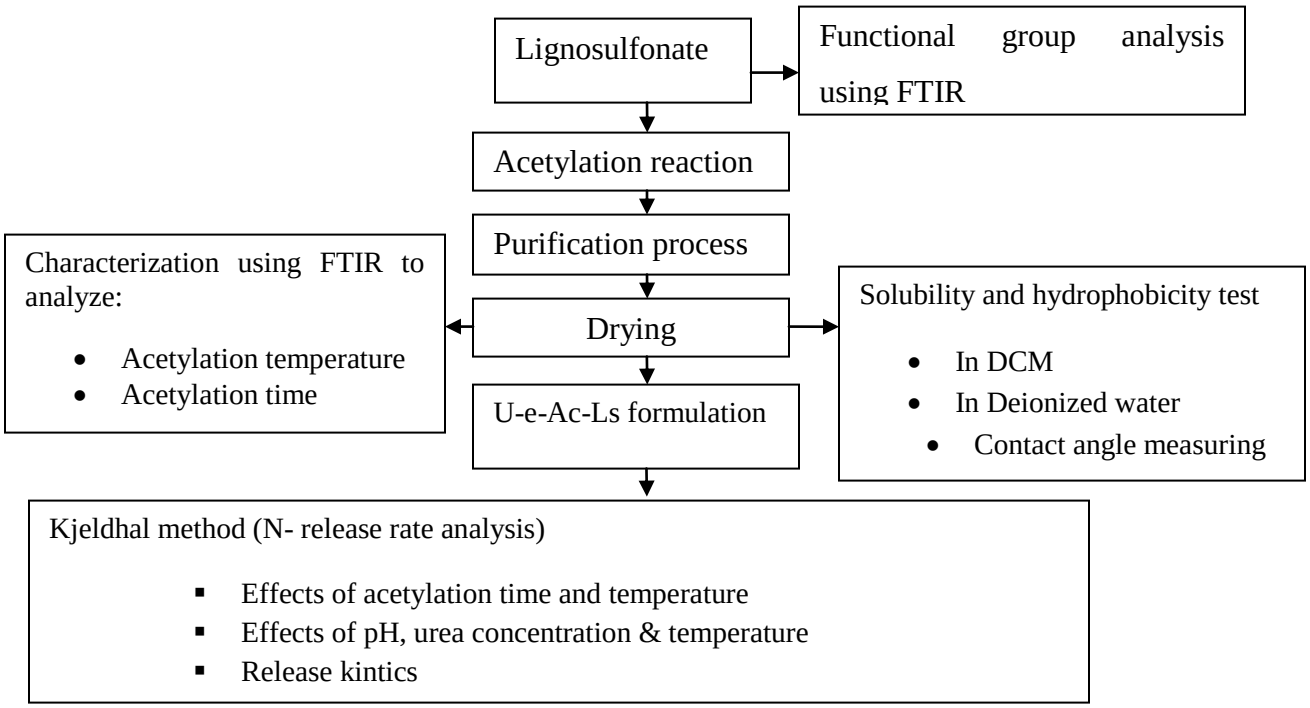

Figure 3.1. General overview of Methology

3.3 Methods

3.3.1 Lignosulfonate modification/Acetylation process

The acetylation procedure was conducted according to (Buono et al., 2016) with some modifications. A weighed amount of Lignosulfonate is acetylated using a pure pyridine-acetic anhydride (1:1, v/v) combination at different temperatures (60-100 ^{0}C) on a hot plate for different reaction times (6 hr, 12 hr, and 24 hr.). To quench the reaction, 40 mL of deionized water was added. Then, the samples were allowed to be cooled and filtered using a vacuum filter, and the residue was washed repeatedly until it reached neutral pH to remove excess acetic anhydride, acetic acid and catalyst. Then, the sample was washed with ethanol (50 mL) and removed the used ethanol using a rotary evaporator. Finally, the residue was suspended in acetone and dried at 50 ^{0}C for 12 hrs. Then the acetylated lignin was prepared in powder form for further characterization. The overall Acetylation process is explained in Figure 3.2.

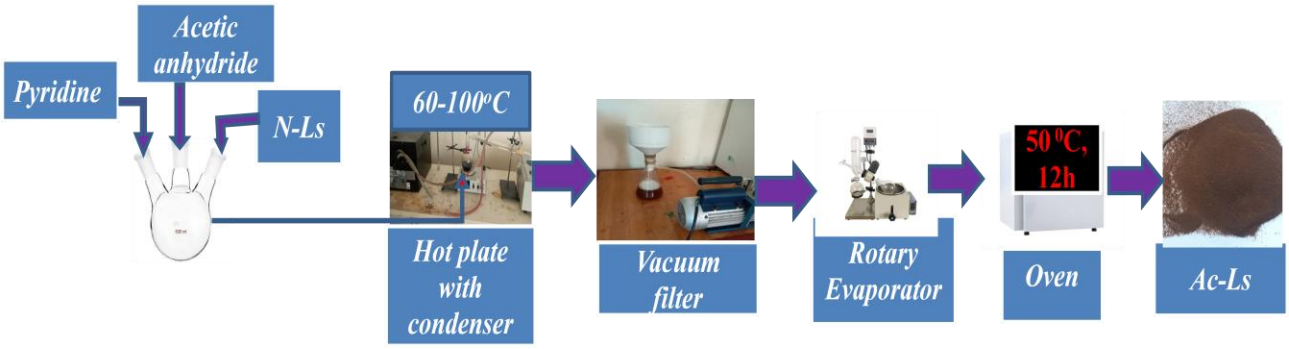

Figure 3.2. Overall representation of the Lignosulfonate Acetylation Process

3.4 Characterization of Modified Lignosulfonate

3.4.1 Solubility test

As illustrated in Figure 3.3 below, the solubility of the acetylated and un-acetylated lignosulfonate was assessed by dissolving it in DCM and deionized water at 25 °C and stirring the solutions for 15 minutes. When the solutions were filtered, the residual weight was estimated by subtracting the filter paper's initial weight from the weight of a filter paper with dried residue. Eventually, the following formulae were used to calculate the percentage solubility of acetylated and un-acetylated lignosulfonate (Tripathi & Katiyar, 2018).

$$\text{Percentage solubility (\%)} = \frac{W2-W1}{W2} \quad \text{(1)}$$

Where: W_2- total weight of dissolved sample in the DCM/Deionized water

W_1- weight of residue left on the filter

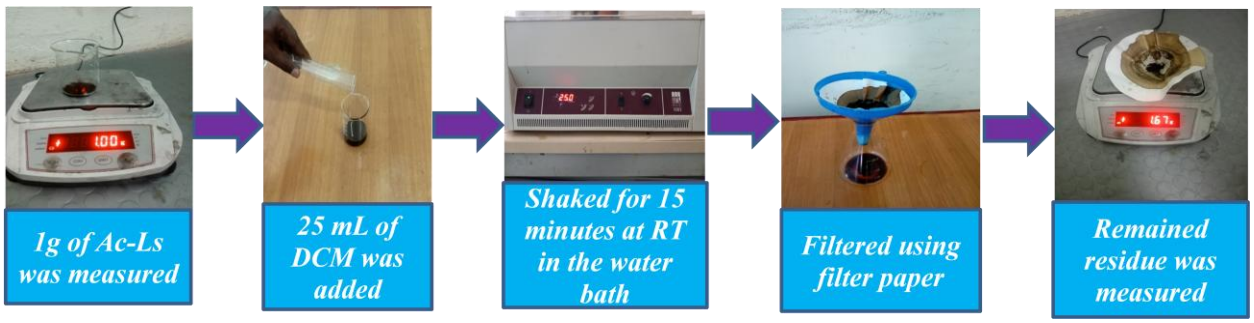

Figure 3.3. Solubility testing procedures for Ac-Ls

3.4.2 Effects of Time on Lignosulfonate Acetylation

The effects of reaction time were investigated by examining the FTIR result of the acetylated Lignosulfonate at different acetylation times (i.e., 6hr, 12hr and 24hr). Based on the FTIR spectrum of acetylated products at different reaction times, the stretching of the expected functional group (i.e., hydroxyl group) on the structure of Lignosulfonate was confirmed. Additionally, the appearance (increasing) of carbonyl groups on the structure of acetylated product as the absorbance of the hydroxyl group reduced was analyzed separately.

3.4.3 Effects of Temperature on Lignosulfonate Acetylation

By analyzing the FTIR spectrum of acetylated Lignosulfonate at different acetylation temperature (i.e., 60, 80, and 100 ^{0}C), the effects of temperature on the acetylation of Lignosulfonate was investigated. The effects of temperature on hydroxyl stretching and the increasing/appearance of the carbonyl group were actually differentiated. Additionally, the acetylation reaction of Lignosulfonate with acetic anhydride as for substitution of Hydroxyl by carbonyl group affected by acetylation temperature was depicted on the peak of FTIR. The effect of acetylation temperature, thereby impacting the hydrophobicity of the sample, was also observed.

3.4.4 Measurement of Contact Angle

The surface hydrophobicity behavior of Acetylated lignosulfonate (Ac-Ls) is typically explained using the contact angle created when the water droplet and the Ac-Ls come into contact. The (Le & Nguyen, 2020) method was simply modified to perform contact angle measurement. A clean, dry glass slide was sprayed with the synthetic Ac-Ls (2.5 x 10 cm). At room temperature, the glass sheet was cured for three hours. The contact angle of the water drop was then determined using the image-J software program after a drop of water was applied to the glass sheet's surface and photographed (Shayesteh et al., 2020).

3.4.3 FTIR Analysis for the Acetylated Lignosulfonate

Using an FTIR spectroscopic instrument, the presence of the predicted functional groups and the transformation and substitution of functional groups were further confirmed. In the range of 4000 to 400 cm^{-1}, the attenuated total reflectance FTIR with the model name FTIR-6600 type A and serial number A013861790 was employed.

3.4.4 Encapsulation of Urea into Acetylated Lignosulfonate

Commercial urea granules ranging in size from 1-4 mm were first ground using a ball mill grinder at 350 rpm for 15 minutes. Then it sieved to obtain a powder with a size of approximately 35 mesh sieves, as illustrated in Figure 3.4 below. After that, by distributing urea powder into Ac-Ls produced by solubilizing in dichloromethane(1:5 w/v ratio),urea-encapsulated acetylated lignosulfonate (U-e-Ac-Ls) was synthesized. Continuous mixing was carried out for 15 minutes at 30 ^{0}C to distribute it evenly. From the preliminary experiment, the mixing temperature was chosen. After heating and mixing the mixture, a pelletizing machine was used to formulate pellets of U-e-Ac-Ls. Before final product characterization, the U-e-Ac-Ls were prepared.

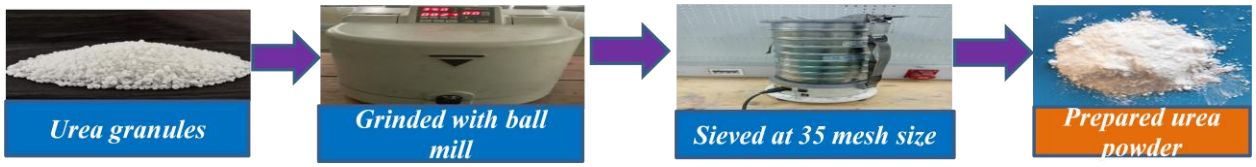

Figure 3.4. Urea powder preparations procedure

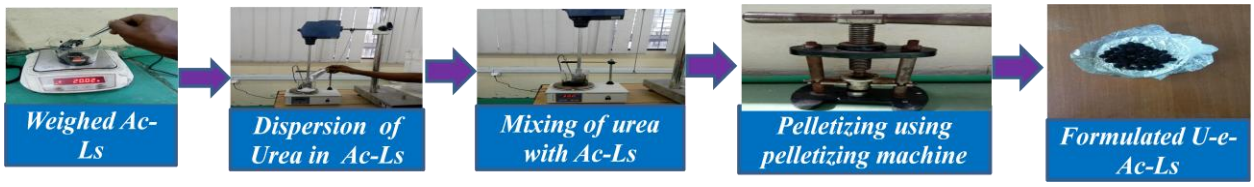

Figure 3.5. The overall procedures of U-e-Ac-Ls formulation

3.5 Characterization of U-e-Ac-Ls

Based on the FTIR spectrum result and the result of Nitrogen release rate at different acetylation times and temperatures (shown in appendix-1A&B) of Ac-Ls of various ranges of acetylation time, the sample acetylated for 12hrs of reaction time at 100 ^{o}C was chosen for the urea encapsulation and characterization of U-e-Ac-Ls was proceed using this sample for further analyzing. In deionized water, the nitrogen release rate from the U-e-Ac-Ls was tested. 10 grams of each of the U-e-Ac-Ls with the amount of urea concentration (60%, 70% and 80% urea) were put in fine mesh cloth bags and immersed in 100 mL of deionized water in a different glass beaker, properly covered, at room temperature, in order to study the impact of Ac-Ls that encapsulate pure urea of various concentration and to select the appropriate urea concentration

for the nitrogen release rate. A copper wire was used to hang the bags. Following three hours of incubation, the samples were carefully removed using the pre-attached copper wire, and the solutions were thoroughly smashed. The percentage of nitrogen released of each sample was then calculated using Kjeldhal method using 10 mL of the solution from each beaker (Affendi et al., 2020; Jintakanon et al., 2008; Taha et al., 2016). The percentage of nitrogen released for each of U-e-Ac-Ls at various urea concentrations and that of pure urea after each interval of incubation time was clearly analyzed as shown in Appendix, and then used to calculate the amount of nitrogen released into deionized water from U-e-Ac-Ls sample. For each distinct sample, this was carried out in duplicate. Equation (2) below was used to determine the amount of nitrogen released after determining the percentage of nitrogen released into distilled water (Silva et al., 2021).

$$\text{Nitrogen released (\%)} = \frac{C*V}{M} * 100 \quad ----------(2)$$

Where: C is the concentration of nitrogen in leachate (g/mL) obtained from Kjeldhal method, and V is the leachate volume in each sampling (mL). M-is the final concentration released in the experiment.

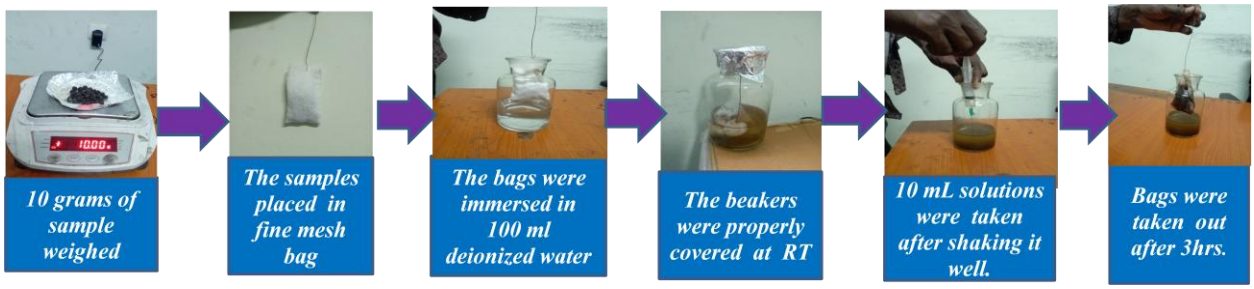

Figure 3.6. Process of preparing the sample for Nitrogen release rate analysis

3.5.1 Effects of Acetylation Temperature and Time on Nitrogen Release Rate

The effects of acetylation temperature (60, 80 and 100 ^{0}C) and acetylation time (6, 12 and 24 hrs) on nitrogen release rate were analyzed separately. The impact of acetylating lignosulfonate at different times and at different temperatures on the nature of the nitrogen release rate was studied in deionized water. To confirm the effects of acetylation temperature and time on the nitrogen release rate, the same process of preparing the sample and analysis was considered, as

shown in Figure 3.6 above. The effects of substituting O-H groups by C=O as temperature and time increased were also identified in the nitrogen release rate analysis.

3.5.2 Effect of Temperature, pH and Urea concentration on Nitrogen Release Rate

The U-e-Ac-Ls sample that contains 70% of urea concentration was chosen from the nitrogen release rate results of method 3.4.4 based on the quality of their release rate (i.e., highly released, medium released, and low released) after 3 hours of incubation in a deionized water. The effect of pH, temperature, and concentration of urea on nitrogen release rate was determined by varying the values of those parameters on the selected U-e-Ac-Ls. The procedure for determining the nitrogen release rate is similar to that in method 3.4.4. Glass beakers containing 100 mL of deionized water were placed in the water bath at various temperatures (i.e., 25 ^{0}C, 35 ^{0}C, and 45 ^{0}C) in order to assess the impact of temperature on the rate at which nitrogen is released. The U-e-Ac-Ls (10 g) that contained the concentration of urea (70%) were plunged into the glass beakers and properly covered. Using the pre-attached copper wire, the cloth bags containing the samples were then removed from the glass beakers at certain intervals (i.e., at 1, 4, 7, 10, 13, 16, 19, 22, and 25 hrs.) and the solutions in beaker were then well shaken. Finally, the Nitrogen content was determined using a Kjeldhal method by collecting 10 mL of solution from each beaker (Sadeghi et al., 2017). Then, using the Kjeldhal method, the amount of fraction of nitrogen released into deionized water from the sample at various time intervals was computed. Also, the method for evaluating the impact of medium's temperature on nitrogen release rate was used to determine the influence of pH, except that it used three distinct buffer solutions (pH 4, 7, and 10) and was carried out at room temperature. In addition, the length of incubation during which the samples were removed increases by 3 hours and analyzed until the time reaches 25 hrs of incubation time (expected that highly released sample reaches its equilibrium condition) (i.e., at 1, 4, 7, 10, 13, 16, 19, 22, and 25 hrs). Similarly, the influence of urea concentration on the rate at which this synthesized U-e-Ac-Ls release nitrogen was assessed by altering only the quantity of urea encapsulated in Ac-Ls (i.e., 60%, 70%, and 80% urea concentration) first at room temperature. Here, the samples were incubated for up to 25 hours before being removed (i.e., at 1, 4, 7, 10, 13, 16, 19, 22 and 25 hrs). Every experiment was carried out twice, and average results were recorded.

3.5.1.1 Buffer Solution Preparation

According to (Rodrı, 2018), three buffer solutions at pH 4, 7, and 10 were prepared to determine how pH affected the N release rate. The pH 4 solution was prepared by combining 79 mL of 0.2 M sodium phosphate dibasic and 123 mL of 0.1 M citric acid in 1 liter of deionized water. 2 L of deionized water should be mixed with 436 mL of 0.2 M sodium phosphate dibasic and 65 mL of 0.1 M citric acid to prepare a pH 7 solution. In addition, 2.25 L of deionized water was combined with 50 mL of 0.1 M sodium bicarbonate and 50 mL of 0.1 M sodium carbonate to prepare a buffer solution pH 10.

3.5.2 Nitrogen Release Rate Test in the Soil

According to Xiaoyu et al. (2013), the nitrogen release rate test in soil was conducted by burying U- e-Ac-Ls at room temperature. To measure the nitrogen release rate in the soil, plastic bottles with identically sized bottom holes were made for the U-e-Ac-Ls that were chosen and for pure urea. A fine mesh cloth was placed over the cleaned sand in each individual plastic bottle before 400 g of soil with 20% moisture content was added. This was done to prevent soil from entering the leachate. 10 g of each U-e-Ac-Ls (70% urea concentration) and 7 g of pure urea were put in separate fine mesh cloth bags before being buried in the ready plastic bottles 5 cm under the soil. The prepared bottles were gently covered with 200 mL of deionized water at various points throughout the incubation process (i.e., at 1, 5, 10, 15, 20, 25, and 30 days), and the leachate was collected at the bottom of each plastic bottle. The nitrogen release rate (%) was then computed using equation (2) above after calculating the percent of nitrogen released during each incubation time by measuring the itrogen content of leachate using Kjeldhal method.

Figure 3.7. Experimental procedure of analyzing nitrogen release rate for pure urea and U-e-Ac-Ls in the soil

3.5.3 Soil Degradation Rate Test

The soil degradation tests of the U-e-Ac-Ls were compared to commercial urea fertilizer to evaluate the biodegradability of U-e-Ac-Ls. A different plastic bottle was prepared and filled with 400 g of soil for each of the commercial urea fertilizers and U-e- Ac-Ls. Soil moisture was kept at 20% throughout the incubation period. In order to prevent sample loss throughout the experiment, 2 g of both U-e-Ac-Ls and commercial urea fertilizer were packed in fine mesh fabric bags (5 x 6 cm in size) before being buried 5 cm beneath the soil's surface in plastic bottles. The weight loss from U-e-Ac-Ls and commercial urea fertilizer was recorded over the 25-day incubation period in the soil as part of the soil degradation test. The samples were excavated, washed, and dried for two hours at room temperature at each predetermined time interval (1, 4, 7, 10, 13, 16, 19,22 and 25 days). The dried samples were then weighed, and equation (3) below was used to calculate the percentage of degradation (Llive et al., 2020). This procedure is shown in Figure 3.7 below. This experiment was used to compare the nature of degradation of U-e-Ac-Ls and that of pure urea.

$$\text{Degradation rate (\%)} = \frac{W1-W2}{W1} * 100 \quad \text{(3)}$$

Where: W_1 and W_2 are the weights of the dried samples before and after the burying in the soil, respectively.

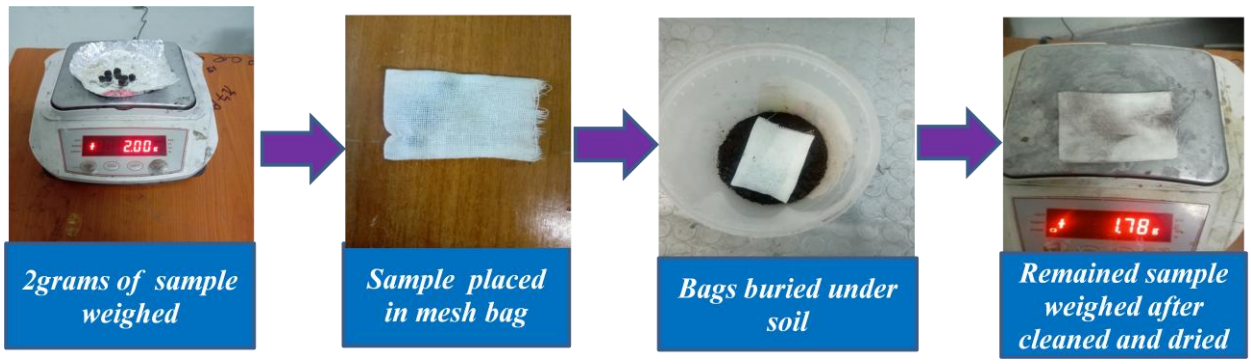

Figure 3.8. Soil degradation test procedure for U-e-Ac-Ls and pure urea

3.5.4 Studying the Behaviors of Nitrogen Release Kinetics

Here, to study the release rate behaviors of total nitrogen from U-e-Ac-Ls, the total nitrogen released rate value of the sample of pH-7 that contains (70% urea) conducted at room temperature was considered. Since the procedure is the same, this value was considered to

analyze the nitrogen release kinetics. Moreover, analyzing all samples was tedious, time, and energy-consuming. Hence, only the nitrogen release rate values of the sample with pH-7 (70% urea) conducted at room temperature were evaluated. Nitrogen in a sample was calculated using the nitrogen percentage content of urea. Using equation (4) below, the nitrogen release rate from the sample at each time interval was then determined (Ding et al., 2016).

$$\text{Nitrogen release rate (\%)} = \frac{C*V}{M} * 100 \quad ----------(4)$$

Where C is the concentration of nitrogen in leachate (g/mL) obtained from Kjeldhal method, V is the leachate volume in each sampling (mL), and M is the nitrogen present in a fertilizer (g). Based on the data generated, further study of the release behaviors of the samples was conducted. Moreover, the four distinct model equations listed below were used to assess the release kinetics behavior of U-e-Ac-Ls (Adebayo et al., 2021).

a. Korsmeyer-Peppas

$$\frac{Mt}{M\infty} = Kit^{n} \quad ----------(5)$$

Where: K_i, t, and n are diffusion content, time and diffusion exponent indicative of the release mechanism respectively. Mt/M∞ is the fraction of nitrogen released at time t. The n value is used to characterize different release mechanisms.

b. Higuchi kinetic model

$$Qt = KHt^{1/2} \quad ----------(6)$$

c. Zero-order kinetic model

$$Qt = Kot \quad ----------(7)$$

d. First-order kinetic model

$$Qt = Q0e^{-Kt} \quad ----------(8)$$

Where: Qt is the amount of nutrient release at time t, Q_0, is the amount of nutrient initially in the formulated fertilizer, t is the time, K_H is the Higuchi dissolution constant, K_0 and K is the zero order and first order release constant respectively.

CHAPTER FOUR

4. RESULT AND DISCUSSION

The physiochemical properties of U-e-Ac-Ls, which were synthesized from Ac-Ls for a regulated dissolution rate, are significantly influenced by the properties of Ac-Ls. It is, therefore, preferable to look at the basic characteristics of Ac-Ls before studying U-e-Ac-Ls, especially those features that are directly related to the target of its application (i.e., controlling the nitrogen release rate), such as the solubility and hydrophobicity of Ac-Ls. This chapter went into great length about the impact of various Ac-Ls synthesizing parameters (such as reaction temperature and acetylation time) on its Hydrophobicity and on the rate at which urea releases that cause nitrogen releases after being encapsulated. Also, the effect of hydrophobicity on the end product's solubility was briefly discussed. This information was crucial for controlling the rate at which the final product dissolves (U-e-Ac-Ls). The impact of various factors, including pH, temperature, and urea concentration, as well as other supporting factors, including FTIR analyses of Ac-Ls, nitrogen release rate in soil, soil degradation rate test, the impact of urea concentration on its degradation rate, nitrogen release rate in water, and its release kinetics behavior tests, were also covered in detail.

4.1 Characterization of Acetylated Lignosulfonate

4.1.1 Acetylation Mechanism During synthesis of Ac-Ls

The acetylation reaction was carried out using a convection heating system when a combination of acetic anhydride and Lignosulfonate was placed on the hotplate at a specific temperature during the synthesis of the Ac-Ls. Carbonyl groups were produced on the functional groups of Lignosulfonate structure as well as on the functional groups of the OH during the acetylation reaction, which is caused by the substitution system. In Lignosulfonate, the free hydroxyl groups that induce a reaction to occur with the ester end groups of acetic anhydride molecules were carboxylic acid functional groups (Shayesteh et al., 2020). Figure 4.1 below provides a schematic representation of how Ac-Ls were formed. By performing the FTIR analyses, the anticipated interactions between Lignosulfonate and acetic anhydride and the substitution of Hydroxyl group by the carbonyl group were confirmed.

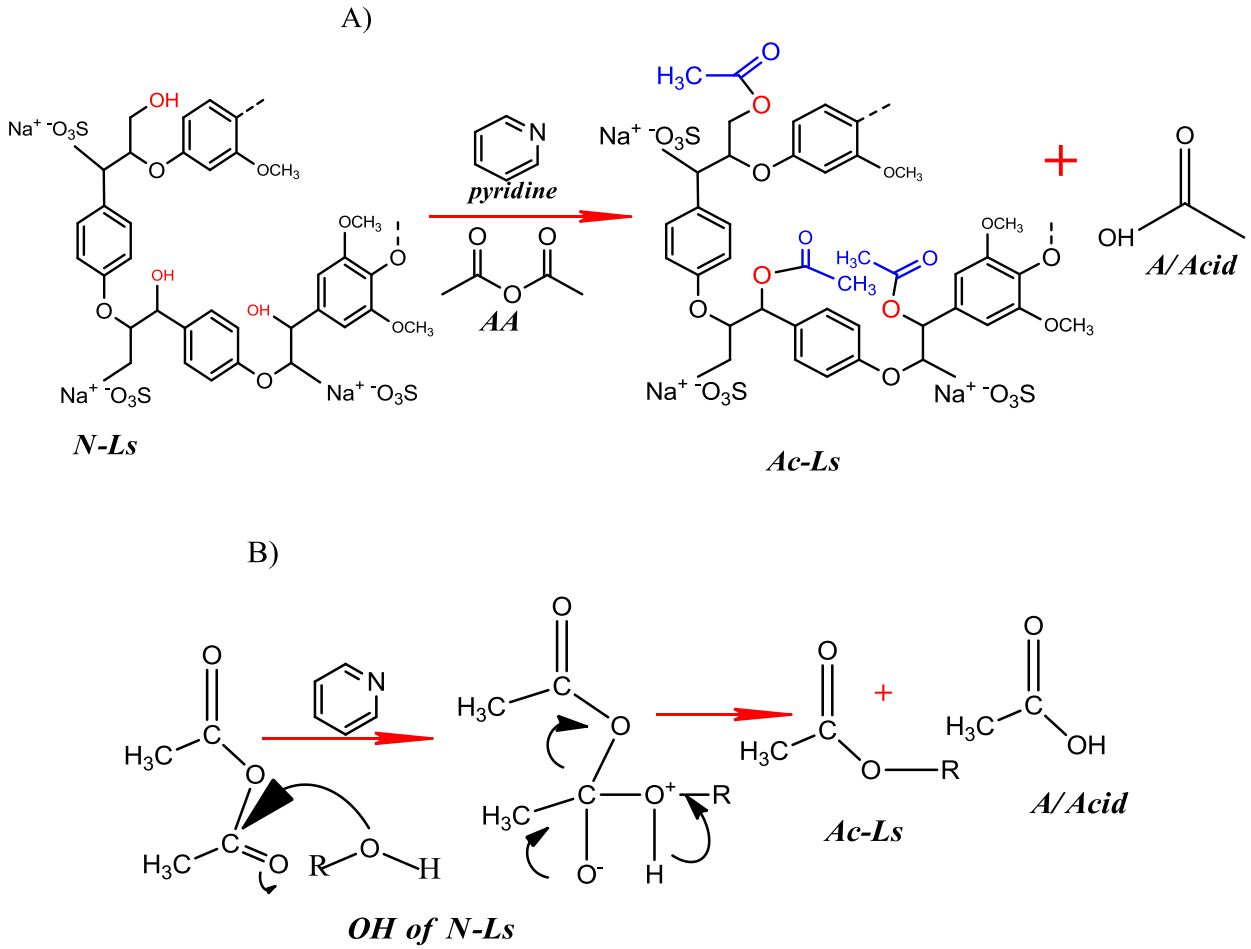

Figure 4.1. Acetylation reaction of lignosulfonate with Acetic anhydride: A) Overall N-Ls Acetylation B) Illustration of acetylation route

The primary step in the acetylation route for the reaction of O-H groups lignosulfonate with AA molecules begins from the nucleophilic attacking on the acyl carbon center of AA molecules by lone pair of aliphatic/phenolic OH groups (Hill, Jones, et al., 1998). Here, the purpose of using pyridine is to promote forming of a pyridine salt intermediate and facilitate the reaction.

As illustrated in Figure 4.1 above, the oxygen attached to acyl carbon is protonated by the acid. The resulting positive charge is relaxed to the adjacent carbonyl carbon, the double bond gets broken and the positive center of OH groups is attached to the acyl carbon. The oxygen atom connecting AA molecules attached to Hydrogen of OH groups and forms A/Acid. In this manner, the Ac-Ls product and acetic acid are synthesized as a by-product.

To select one sample for additional characterization, it is preferable to first assess the functional group analysis for further experimental duty because conducting the FTIR analysis and other physiochemical characterizations of all synthesized Ac-Ls is challenging and time-consuming. As seen below in Figure 4.2, the functional group of molecules of N-Ls and Ac-Ls were differentiated using FTIR spectrum. This shows the effects of acetylation reaction on the molecular structure of lignosulfonate. Moreover, due to the reaction carried out between O-H groups of lignosulfonate and carboxylic acid parts of acetic anhydride, the hydroxyl part of Lignosulfonate was reduced and new carbonyl groups was developed on the structure of Ac-Ls. The OH functional group was found in the 3500-3200 cm^{-1} wave numbers; compared to the normal lignosulfonate, the absorbance of O-H of Ac-Ls reduced and a new C=O functional group was developed at 1748 cm^{-1} wave number. C-H group band change also appeared in the range of 3000-2800 cm^{-1} wave number. The peak at 1582 and 1509 cm^{-1} indicates asymmetric groups of C-H on the structure of N-Ls. Due to the molecular vibration, these peaks were shifted to 1594 and 1506 cm^{-1} on the structure of Ac-Ls (Priyanto et al., 2018). The weak band at 1455 cm^{-1} from the spectrum of N-Ls indicates the presence of sulfite group (SO_3) and shifted to 1466 on the FTIR spectrum of Ac-Ls. Here, the peak at 1509 cm^{-1} from N-Ls and 1506 from Ac-Ls shows the typical aromatic skeletal vibration combined with C-H in-plane deformation, whereas the intensity peak at 1582 and 1594 show the aliphatic C-H stretching in CH_3 and phenolic O-H (Priyanto et al., 2018). The band at 1748 from Ac-Ls FTIR spectrum indicates the newly formed carbonyl groups because of acetylation carried out on the structure of N-Ls (Shayesteh et al., 2020). The peak at 1131 from N-Ls shifted to 1190 from Ac-Ls showing the presence of C-O on the structure. The presence of S=O ranges was also indicated at 1033 from N-Ls and shifted to 1030 from Ac-Ls (Priyanto et al., 2021). Additionally, to boost the aromatic substitution the out-of-plane stretching vibration of C-H was developed at 903 cm^{-1} wave numbers on the Ac-Ls structure. The S-O peak range was depicted at 617 and shifted to 753 cm^{-1} wave number on the structure of acetylated lignosulfonate.

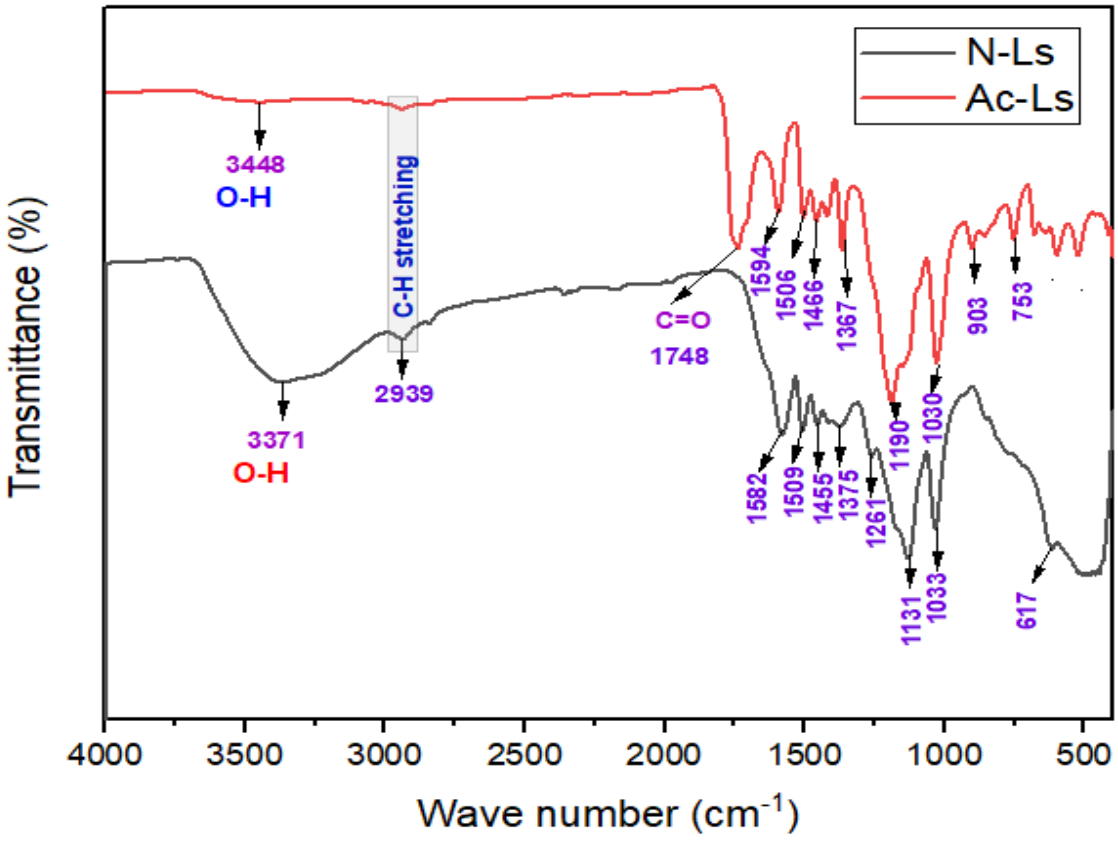

Figure 4.2. FTIR Spectrums of normal and acetylated lignosulfonate

4.1.2 Effect of Reaction Temperature on Lignosulfonate Acetylation

According to FT-IR studies, temperature plays an effective role in Ls acetylation reaction. The absorption peak of the hydroxyl group, which arises between 3200 and 3500 cm^{-1}, declines with rising temperature. This reduction of the Hydroxyl group only by itself does not demonstrate that the reaction of lignosulfonate is enough for effective acetylation; rather, the peak of the C=O functional group must develop simultaneously. The replacement of hydroxyl groups by carbonyl groups must account for some of the hydroxyl group drops. The peak strength of the hydroxyl group does drop during the process at temperatures above 60 °C, showing that this is a sign of the acetylation reaction because, at the same time peak of the C=O group has been seen. The C=O group's absorption peak, which shows the development of lignosulfonate acetylation, elaborates that the reaction that took place between Hydroxyl groups of lignosulfonate and acyl carbon of acetic anhydride shows the effective acetylation reaction that resulted in the increment of newly emerged carbonyl groups and reduction of hydroxyl groups on the structure of modified

lignosulfonate in a tangible way as shown in the Figure 4.3 below. Additionally, it shows that the C=O functional group's absorption peak is becoming stronger as the temperature rises from 60 to 100 °C. In order to perform the acetylation reaction with the polymer's hydroxyl group, the hydrogen bond must be broken because the hydroxyl group forms vast hydrogen bonding networks (Hill, Hill, et al., 1998). The polymer hydrogen bonds typically dissociate at higher temperatures, which speeds up the process (Nwankwere, 2016). Based on Figure 4.3 below, at temperatures above 60 °C, the peak of the carbonyl group is increased while the OH group's absorption peak is accentuated. This observation appears to be caused by an interaction between lignosulfonate and acetic anhydride (Adebajo & Frost, 2004; Onwuka et al., 2019). In addition, the greater temperature might make the reaction between hydroxyl groups of Ls and that of carboxylic acid to be enhanced, which would cause a faster reduction of Hydroxyl groups and significant appearances of carbonyl groups (Otromke et al., 2019; Peng et al., 2019). From Figure 4.3 below, as the acetylation temperature increased, the peak of the O-H group become declines and that of C=O becomes progressed well. For instance, the O-H band of N-Ls was at 3371 cm^{-1}; after acetylation at 60 ^{o}C it became at the band of 4438 cm^{-1} and shifted to 4443 cm^{-1} when acetylated at 80^{o}C. it also shifted to 4448 cm^{-1} when acetylation temperature increased to 100^{o}C. At the same time peak of the carbonyl group was increased to 1733, 1736 and 1740 cm^{-1} when the acetylation temperature increased to 60 ^{o}C, 80 ^{o}C and 100 ^{o}C, respectively.

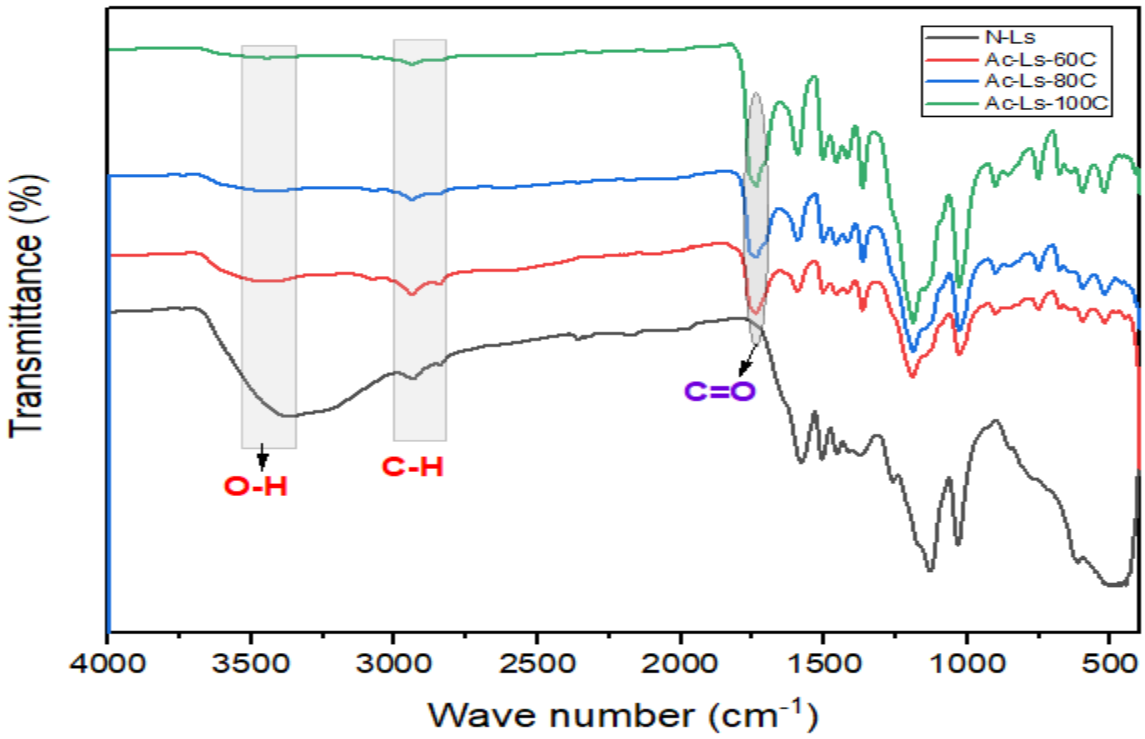

Figure 4.3. FTIR Spectrums of N-Ls and Ac-Ls at different acetylation temperatures

4.1.3 Effect of Reaction Time on Lignosulfonate

The significance of reaction time was explored by looking at the FTIR spectra of the products of Lignosulfonate (Ls) acetylation with acetic anhydride over a range of times (6, 12, 24 hrs). By decreasing the hydroxyl functional groups, the carbonyl functional groups should also be visible in the FT-IR spectrum to confirm the acetylation reaction. As depicted from the FTIR spectrum, with increasing reaction time, the carbonyl functional group increases; on the contrary, the hydroxyl functional groups decrease simultaneously. Additionally, the C-H groups stretching become vary as the acetylation reaction time increases; for instance, wave number 2933 cm^{-1} shows for the normal lignosulfonate whereas, after 6hrs of acetylation, it stretches to become narrow when the acetylation time of Lignosulfonate increased to12 hrs, and smoothly appeared when acetylation time increased to 24hrs of reaction duration. The carbonyl groups also strengthened to 1735, 1737 and 1741 cm^{-1} when acetylation was carried out at 6hrs, 12hrs, and 24hrs, respectively. At the same time, when the acetylation time increased to 6hrs, 12hrs, and 24hrs, the O-H group peak shifted to 4439,4445, and 4450 $cm^{-1,}$ respectively. This is due to the fact that as the acetylation time increases, the possibility of contact time of reaction of

Lignosulfonate with Acetic anhydride get increased, and hence the chance of substitution of O-H group with C=O becomes high (Shayesteh et al., 2020).

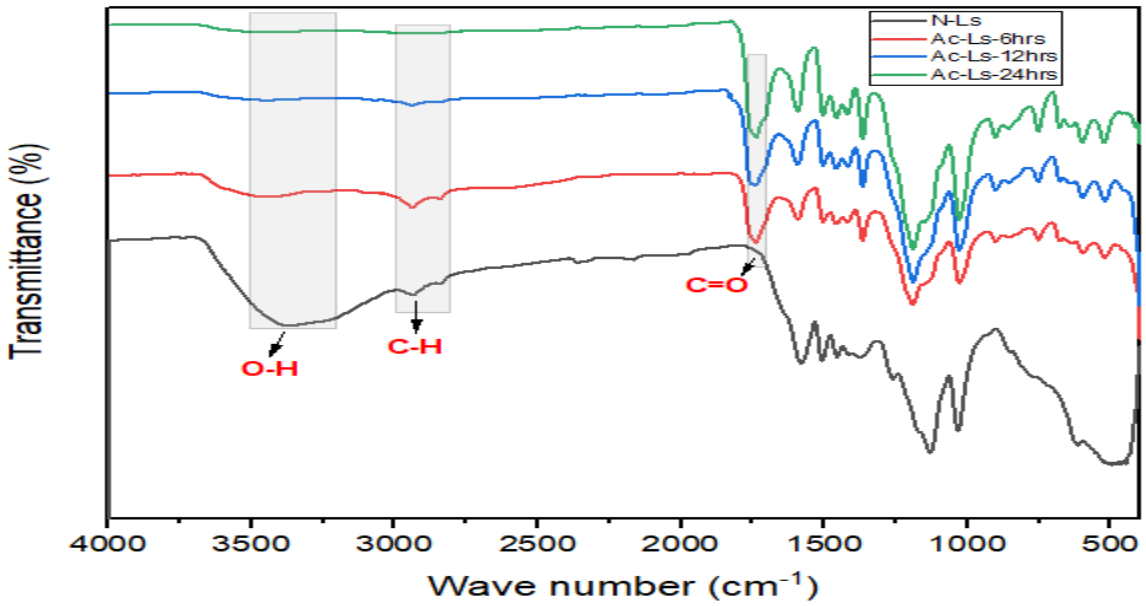

Figure 4.4. FTIR Spectrums of N-Ls and Ac- Ls at different acetylation time

4.1.4 Solubility and Hydrophobicity Test

The solubility test was conducted using DCM and deionized water, and the hydrophobicity was assessed using a contact angle measurement. The values of the contact angles are directly correlated with the hydrophobicity (Riveiro et al., 2018). According to the experimental findings, the hydrophobicity and percentage solubility of Ac-Ls in DCM were positively impacted by its acetylation and tendency of solubility (Shayesteh et al., 2020). The contact angle's recorded data for both N-Ls and Ac-Ls are found in appendix-22. Based on the contact angle values, the hydrophilicity and hydrophobicity of N-Ls and Ac-Ls characteristics are observed. As shown in Table 4.1 below, as the Lignosulfonate becomes acetylated, so does the contact angle value and percentage solubility in DCM increase. Moreover, the solubility of un-acetylated or normal lignosulfonate is high in deionized water and becomes less for acetylated lignosulfonate. This is because the acetylated one has many hydrophilic polar groups of Ls replaced by hydrophobic ester groups of acetic anhydride, which increases the hydrophobicity of Ac-Ls (Shayesteh et al., 2020). According to a contact angle measurement, a surface is hydrophilic if the contact angle is less than 60^0 and has a hydrophobic nature if it is larger than 60^0 (Fertahi et al., 2021). The Ac-

Ls contact angle is measured at 74^{o}, showing that the modified lignosulfonate has hydrophobic characteristics. While the N-Ls have a hydrophilic character, as indicated by their contact angle (14^{0}). Additionally, the solubility of Ac-Ls in DCM was become higher as compared to deionized water. Moreover, the solubility of N-Ls in deionized water was higher as compared to DCM. This generally shows the hydrophilicity of N-Ls and becomes hydrophobic after acetylation (Ac-Ls).

Table 4.1. Solubility and contact angle of N-Ls and Ac-Ls

Sample used	Percentage (%) of solubility		Contact Angle (^{0})
	In DCM	In Deionized water	
N-Ls	41.27	79.51	14
Ac-Ls	70.13	22	74

4.2 Analysis of Synthesized U-e-Ac-Ls

4.2.1 Effects of Acetylation Time on Nitrogen Release Rate

The effects of Lignosulfonate acetylation time were illustrated using Figure 4.2 below. This figure was drawn based on the result of nitrogen release rate at different incubation times in appendix-1A. As the acetylation time increases, so does the reduction of the intensity of hydroxyl groups and the increment of carbonyl groups. As a result, it decreases the solubility of acetylated lignosulfonate and reduces the solubility of urea encapsulated in acetylated lignosulfonate. Thus, as the acetylation time increases, the nitrogen release rate decreases. This scenario is explained in Figure 4.5 below.

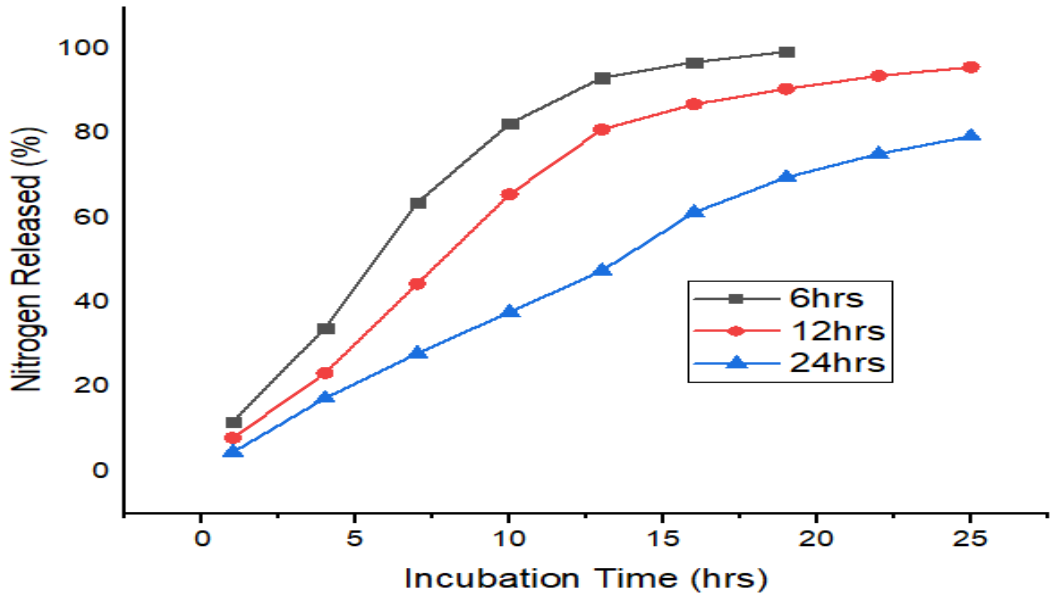

Figure 4.5. Effects of acetylation time on the nitrogen release rate

For the sample encapsulated in Ac-Ls for 6hrs, the total nitrogen was almost completely released (99.455%) within 19hrs of incubation periods. Whereas the sample encapsulated in Ac-Ls for 12hrs released 90.65% of its nitrogen within the same time of incubation, and for the acetylation, time increased to 24hrs, only released 69.65% of its nitrogen within the same time of incubation (19hrs). This is due to the fact that as acetylation time increased, the substitution of hydroxyl groups by carbonyl was more progressed. As a result, the hydroxyl group that causes solubility was masked by carbonyl groups and reduced the release rate of nitrogen.

4.2.2 Effects of Acetylation Temperature on the Nitrogen Release Rate

The effect of acetylation temperature is elaborated in Figure 4.6 below. This illustration graph was drawn using the nitrogen release rate percentage in appendix-1B. As seen from the figure, the acetylation temperature has its own impact on the nitrogen release rate. As the acetylation temperature gets increased, the substitution of hydroxyl groups by carbonyl groups progresses and reduces the solubility nature of lignosulfonate. Thus, the sample encapsulated in Ac-Ls at low temperature was soluble compared to the one encapsulated in Ac-Ls at high temperature. For instance, the sample encapsulated in Ac-Ls at 60 ^{o}C released its nitrogen almost completely (99.775%) within 19hrs of incubation, while the one encapsulated in Ac-Ls at 80^{o}C releases 97.035% of its total nitrogen within the same time of incubation and the sample encapsulated in

Ac-Ls at 100 ^{o}C releases 91.885% of its total nitrogen within the same time of incubation (19hrs). All these impacts of acetylation temperature on the nitrogen release rate are illustrated in Figure 4.6 below.

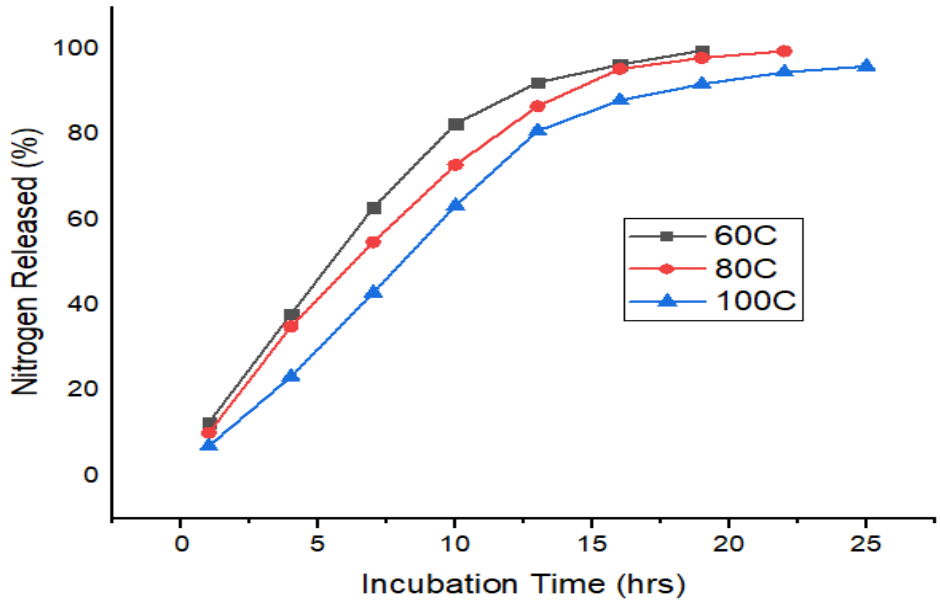

Figure 4.6. Effects of acetylation temperature on the nitrogen release rate

4.2.3 Effect of pH on the Nitrogen Release Rate

The evaluation of the nitrogen release rate for the synthesized U-e-Ac-Ls in buffer solution at pH 4, 7, and 10 at room temperature is illustrated in Figure 4.7 below. The data from the experimental results, which are summarized in Appendix-2, 3&4, were used to draw the figures. Because soil is made up of alkaline and silica-based minerals, the pH values were chosen by taking into account extreme pH values (4 and 10); as a result, soil pH is often close to 7 (Heuchan et al., 2019; Rodrı, 2018). As seen from this experiment, it was found that the nitrogen release rate reduces as the pH of the medium rises. Figure 4.7 demonstrates that at pH 4, the amount of nitrogen released from a sample almost completely (99.82%) within 19 hours of incubation periods in a solution, while the amount of nitrogen released at pH 7 and pH 10 was (95.4%) and (82.19%) respectively within the same period of incubation time (19hrs). A sample at pH-4 highly released and released 99.82% nitrogen at pH 4 within 19hrs, whereas 99.48% of its nitrogen after 22 hours of incubation at pH 7, as shown in Figure 4.7 below respectively, whereas 97.55% of nitrogen was released within 25hrs of incubation at pH 10. The protonation

of the urea's amino groups determines how pH affects the rate at which nitrogen is released from U-e-Ac-Ls. Urea can either be protonated or deprotonated, depending on the pH of the medium. When the pH of the solution medium dropped, more H^+ ions were conducted into the solution, and as a result, the amino groups in urea were protonated by those H^+ ions. The carboxyl groups of Ac-Ls are unable to connect easily with the urea molecules because H^+ ions from the solution have taken up the bond sites of the amino groups of urea. As a result, urea's amino groups are present at pH 4 in their ionized form (NH_3^+). Due to electrical repulsion between non-ionized carboxyl groups (-COOH) of Ac-Ls and ionized amino groups (NH_3^+) of urea as a result of the H^+ ions occupying the bond sites, rapid release results. On the other hand, the carbonyl groups in the Ac-Ls are anticipated to be in both their ionized (-COO-) and non-ionized (-COOH) forms when the buffer solution is made to pH 7. The amine groups in urea continue to be in their non-ionized state (NH_2) when the buffer solution is made to pH 7 (Rodrı, 2018). The connection between the amine groups of urea and the carboxyl groups of Ac-Ls through hydrogen bonding increases as a result. This slows down the rate at which nitrogen is released. The carboxyl groups of Ac-Ls were anticipated to acquire their ionized (-COO-) forms when the pH increased. However, the amino groups of urea were not protonated and remained in the form of primary amine (NH_2). As a result, when the pH of a medium reaches pH 10, the contact through hydrogen bonding between the carbonyl groups of Ac-Ls and the amine groups of urea increases. The amount of nitrogen released into the medium gradually decreases as the number of hydrogen bonds between Ac-Ls and urea rises. Even while the pH of the medium had an impact on U-e-Ac-Ls, the extent of that impact varied from sample to sample. When we observe the nitrogen release rate of all samples at a specific time of incubation, like at 19 hrs, to understand the effect of pH on the nitrogen release rate of each individual sample separately. In particular, when the pH is dropped from pH 10 to pH 4, it increases by 17.63%. The fact that the amino group of urea takes a long time to protonate with the H^+ of a solution at a lower pH (pH 4) and the aminogroups of urea prefer to bond with H^+ in the solution rather than with that of carboxylic groups. The carboxylic groups of Ac-Ls exist in ionized state and suggests that the carboxyl groups of Ac-Ls can bind to non-ionized amine groups of urea by hydrogen bonding simply at higher pH.

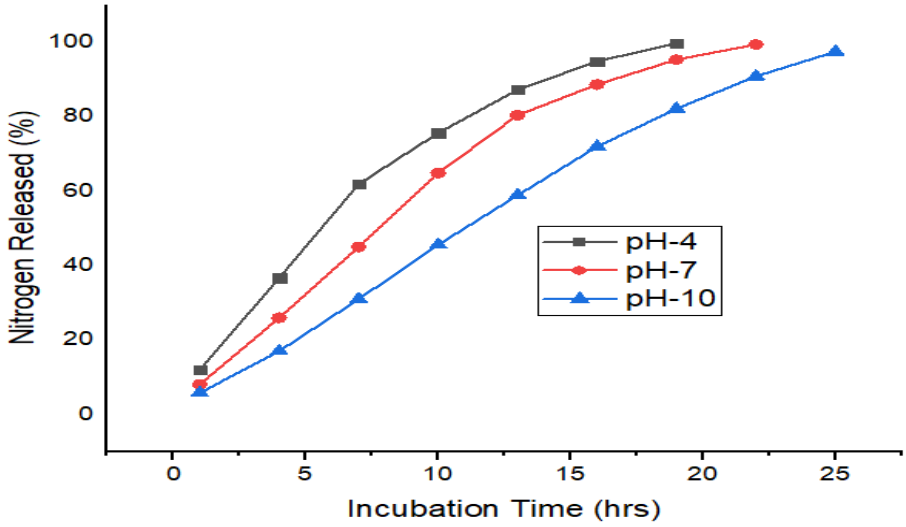

Figure 4.7. Effects of pH on Nitrogen release rate

4.2.4 The Effect of Temperature on Nitrogen Release Rate

The effects of medium temperatures on nitrogen release rates are shown in Figure 4.8 below as a function of temperature at 25 ^{0}C, 35 ^{0}C, and 45 ^{0}C, respectively. The experimental result data, which is tabulated in Appendix-5, 6&7, was used to plot the graph. The temperature ranges were chosen based on the literature (Rodrı, 2018) and (Harris et al., 2017), and as shown in (Harris et al., 2017), the high nutrient release rate was reported at the range of 35 ^{0}C - 40 ^{0}C. Therefore, 25 ^{0}C and 45 ^{0}C were selected as an extreme value to study the nutrient release rate in this case. Figure 4.8 demonstrates how the temperature rises cause an increase in the rate of nitrogen release in U-e-Ac-Ls. This is because, at a greater temperature, the urea molecules' kinetic energy rises, increasing their average molecular diffusion rate and, ultimately, nitrogen release rate. When the temperature rises, the hydrogen bonds are more prone to break down because they have weaker energies than ordinary valence bonds (Rodrguez-Félix et al., 2012). As seen in figure 4.8, at 25 ^{0}C, 78.845% of the nitrogen in a sample was released into deionized water within 16 hours of incubation time. While throughout these 16 hours of incubation, at 35^{0}C and 45^{0}C, 86.37% and 99.83% of the nitrogen in a sample was released, respectively. The first hours of release periods were when the effect of temperature on the nitrogen release rate was most pronounced, as seen in Figure 4.8. This phenomenon is thought to be caused by the system getting additional energy, which facilitates the dissociation of connections through hydrogen

bonding between the amino group of urea and the carbonyl group of Ac-Ls, leading to an increase in the rate of nitrogen release. And as shown in Figure 4.8, all samples' nitrogen release rates become slow after around ten hours at each temperature condition. This is due to the fact that under the experimental conditions, the urea bound to an insoluble Ac-Ls component could only be released after being converted into soluble, which is a highly laborious process.

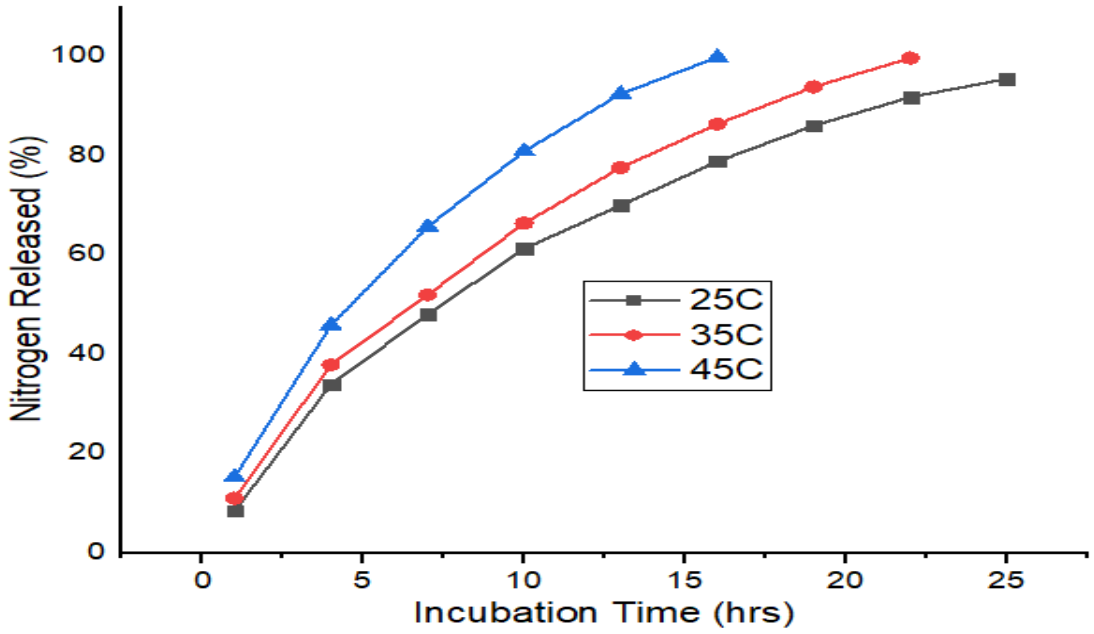

Figure 4.8. Effects of Temperature on the nitrogen release rate

4.2.5 Effects of Urea concentration on the Nitrogen Release Rate

The influence of urea concentrations on the rate of nitrogen release of the U-e-Ac-Ls is shown in Figure 4.7 below, at 60%, 70%, and 80% of urea concentrations, respectively. Based on the early experiment results, the values of the urea concentrations were chosen. The experimental result data tabulated in Appendix 7, 8, and 9 was used to plot the figures. From the experiment, it was found that the rate at which nitrogen is released from U-e-Ac-Ls likewise increases when the urea concentration encapsulated into the synthesized Ac-Ls increases. The nitrogen from the sample was released almost completely (99.905%) within 22 hours of incubation when U-e-Ac-Ls contained 80% of urea. But, the nitrogen released from the sample containing 70% urea concentration was 89.90% throughout this incubation period (22 hours). The sample contain 60% of urea released 84.13% of nitrogen within the same time of incubation periods (22hrs). As

shown in Figure 4.9 below, when the amount of urea contained in U-e-Ac-Ls increases to 70%, the nitrogen release rate increases compared to the one containing 60% urea. And when the amount of urea contained in U-e-Ac-Ls further increases to 80%, a highly released sample, it took only 22hrs to release 99.905% of nitrogen, whereas the sample containing 60% urea, taken 25hrs of incubation time to release 87.975 % of nitrogen and the sample containing 70% urea released 93.5% of its nitrogen within 25hrs of incubation time. This is a result of the Ac-Ls molecular chains expanding as the amount of urea contained within each Ac-Ls rises. As a result, the distance between the molecular chains increases, and the surface strength of the material decreases. As a result, more water was able to enter Ac-Ls through the openings and its surface, increasing the rate at which nitrogen is released.

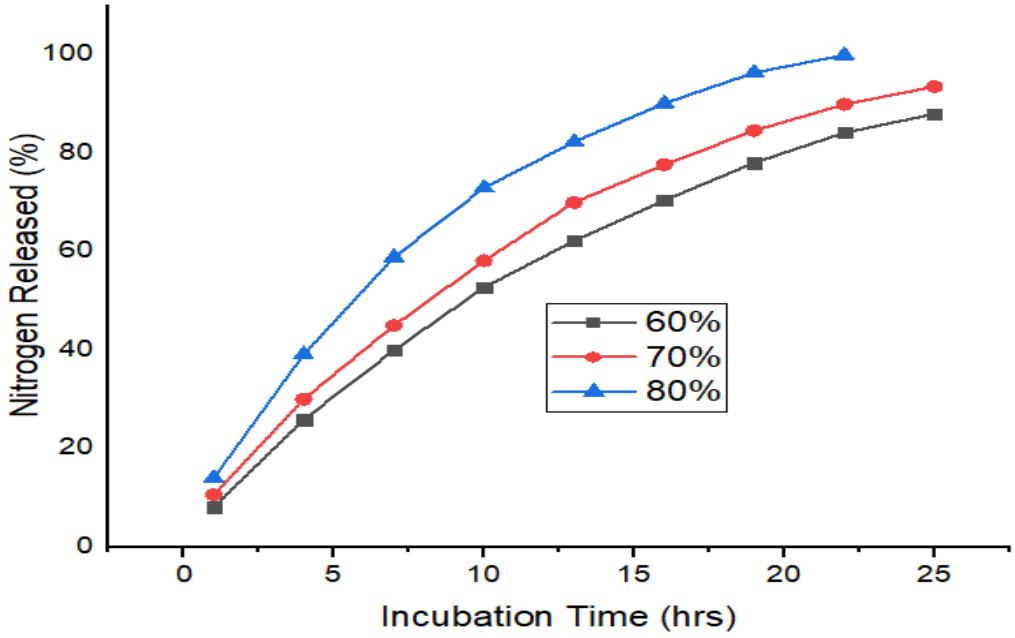

Figure 4.9. Effects of urea concentration on Nitrogen release rate

4.2.6 Nitrogen Release Rate in the Soil

The nitrogen release rate of U-e-Ac-Ls that contain 70% urea concentration and commercial urea fertilizer in soil were also evaluated, as shown in Figure 4.10 below. The figure was plotted from the experimental result data tabulated in Appendix-15. The experimental results showed that the nitrogen release rate in soil was slower compared to its release rate in deionized water. This is due to the fact that the sample in the soil was in an environment of extreme conditions. During

the release process, the U-e-Ac-Ls surface was connected with soil particles, in this way the soil condition around the U-e-Ac-Ls might be changed. Hence, this leads to decreased free water exchange rate between the soil and the U-e-Ac-Ls, reducing the water diffusion rate into the U-e-Ac-Ls. Consequently, the nitrogen release rate of U-e-Ac-Ls in the soil becomes less relative to that in water. Besides, as the nitrogen release rate test in the deionize water condition was static and in the soil condition was dynamic, the water might leach out with less absorbency of urea. As a result, the release of nitrogen into leachate was reduced (Gungula et al., 2021). Figure 4.10 shows that the nitrogen release rate of pure urea in the soil rapidly reaches its equilibrium within the first 10 days of incubation. Whereas, from U-e-Ac-Ls, the high released amount releases 98.67% of nitrogen after 30 days of incubation, demonstrating that U-e-Ac-Ls was able to effectively reduces the nitrogen release rate in the soil over a period of time (30 days) almost 3 times longer than that was observed for a pure urea fertilizer (10days). At this long time incubation (30 days), the percentages of nitrogen released showed that the synthesized U-e-Ac-Ls played the role of nutrient release reduction. The observed release rate of nitrogen of pure urea was 63.36% within 24hrs of incubation. This also implies more than half of the essential nutrient N from pure urea was released within this short time (24hrs), which is very fast relative to plants' nutrient requirement for their long lifetime.

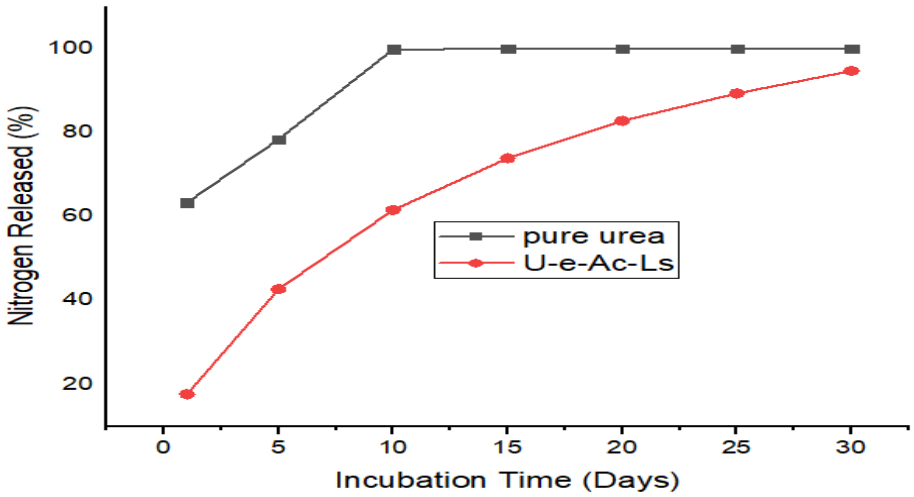

Figure 4.10. Nitrogen release rate in the soil

4.2.7 Soil Degradation Rate of U-e-Ac-Ls relative to Pure Urea

The soil degradation experiment (70% urea) was conducted to understand the degradation rate of U-e-Ac-Ls relative to the commercial urea fertilizer. The results of soil degradation rate of U-e-Ac-Ls and commercial urea fertilizer are shown in Figure 4.9 below, in which the figure was plotted from the experimental result data's tabulated in Appendix- 11 and 13 (the sample contains 70% urea concentration). As illustrated in Figure 4.9, it was observed that the weight loss of U-e-Ac-Ls and pure urea increases with the increase in incubation time. The commercial urea (pure urea) degrades completely within 4 days of incubation in the soil i.e., its weight loss reaches 100% within 4 days of incubation. Whereas the U-e-Ac-Ls loses only 40.17% of its weight within the first 4 days of incubation. As illustrated in Figure 4.9 below, the U-e-Ac-Ls fertilizer showed less degradation, i.e., 94.86 % within 25 days, compared to pure urea, which loses its 100% of the weight. This is because the fertilizer encapsulated in U-e-Ac-Ls influences its soil degradation rates. The formulated in U-e-Ac-Ls was densely packed together and hence its molecular chains were densely packed well. As a result, microorganisms in the soil cannot easily access it to break down, causing it to slow down its degradation rate compared to pure urea.

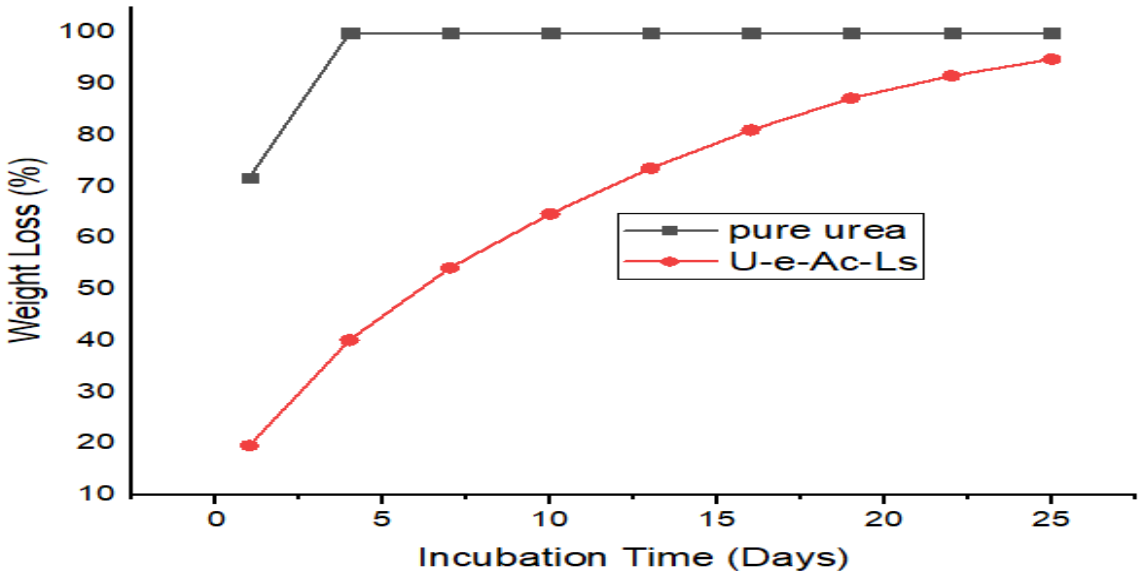

Figure 4.11.Weight loss (%) for the selected U-e-Ac-Ls and pure urea exposed to soil for 25 days

4.2.8 The Effects of Urea Concentration on the Urea Degradation Rate Test

Figure 4.12 below shows the effect of urea concentration (i.e., at 60%, 70%, and 80%) on the soil degradation rate of U-e-Ac-Ls. Figure 4.12 was plotted from the experimental result data's tabulated in Appendix-11, 12 & 13 below. The experimental results indicate that, as the urea concentration increases, the soil degradation rate also increases in U-e-Ac-Ls. As illustrated in Figure 4.9 below, the sample containing 60% urea concentration takes 25 days to lose 92.92% of its weight, but when its urea concentration becomes 70% it loses 94.86% of its weight within the same incubation time. When urea concentration further increased to 80%, the degradation rate increased to 96.82% within the same time. This is because as the amount of urea encapsulated in Ac-Ls increases, the Ac-Ls molecular chains expand and their molecular bond strength gets low. As a result, the microorganisms in the soil can effectively break down easily. In general, in this soli degradation experiment, the result demonstrates not only its nitrogen release rate in water but also its soil degradation was greatly affected by the amount of urea encapsulated in Ac-Ls.

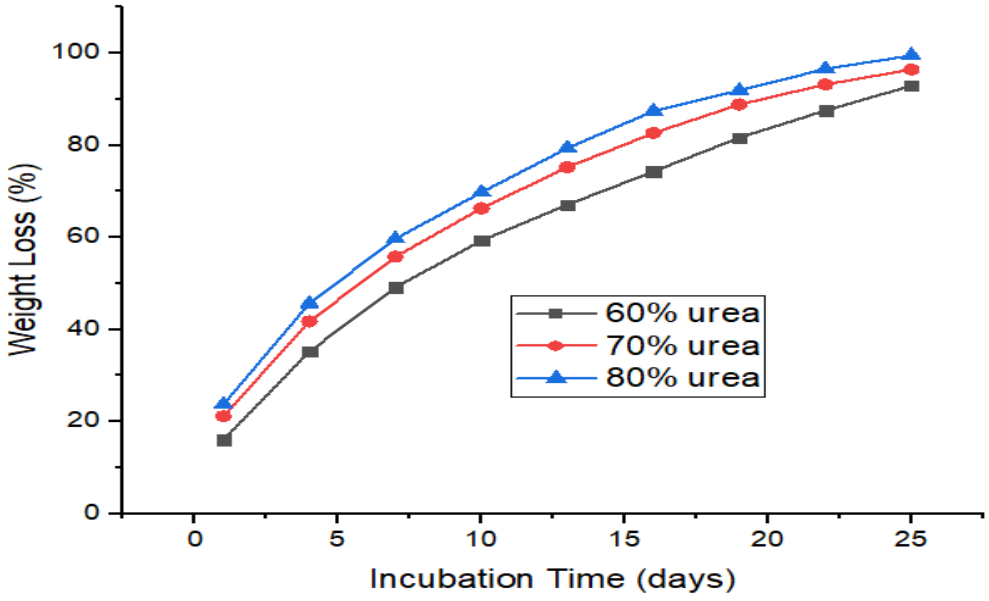

Figure 4.12. The effects of urea concentration on the soil degradation rate

4.2.9 Studying Behaviors of Nitrogen Release Kinetics

The total nitrogen release percentage evaluated at pH-7 sample was considered in studying the behaviors of nitrogen release rate kinetics. In this case, the release kinetics of U-e-Ac-Ls was

analyzed by considering and evaluating different mathematical linear fit models. In this approach, the nitrogen release rate of the sample was evaluated at pH-7 and commercial urea in the pH-7 medium. The experimental results data, which are tabulated in Appendix-3, were used to plot the figure. In an hour, pure urea releases 98.12 % of its nitrogen content. These results are almost identical to those reported in the literature by Gungula et al. (2021) (97%) and Muslim et al. (2015) (100%). However, after an hour of incubation time in pH-7 medium, the nitrogen release rates for U-e-Ac-Ls were 8.075% and within 25hrs of incubation, 99.48% of nitrogen was practically released. The percentage of nitrogen release rate was calculated by Kjeldhal method analysis and accordingly shown in appendix-16. The nitrogen release kinetics for each equation in the mathematical model are displayed in Table 4.2 below, and the graphs of their linear fits are presented in Appendix-17 through 19. Due to a significant discrepancy between experimental findings and model calculation data beyond 60% nitrogen release, only fractions of nitrogen release below 60% were employed in the Korsmeyer-Peppas model (Mechanisms, 2021). Diffusion control, erosion control, or a combination of those controls can be applied to the nutrient release mechanism. A good fit to the Korsmeyer-Peppas equation shows a mixed influence of diffusion and erosion mechanisms for nutrient release, and the Higuchi model is relevant if the release of nutrients is predominantly controlled by diffusion through water-filled pores in the matrix (Limmatvapirat et al., 2008). With the correlation coefficient ($R^2 > 0.99$), it is possible that the release mechanism in question is a diffusion-controlled release. However, the release kinetics has a best fit on Korsmeyer-Peppas equation relative to the other model equations with correlation coefficient ($R^2 > 0.99$), implying the release mechanism was not a pure diffusion-controlled release rather, it was a combined effect of diffusion and erosion release mechanisms. Additionally, the diffusion type can be identified by computing the release exponent (n). For anomalous transport (non-Fickian diffusion release), the value of the release exponent (n) lies between 0.45 and 0.89, the value of n is 0.89 for case II transport across swollen matrixes, and the value of n is higher for super case II transport compared to 0.89 (Ahmed et al., 2019; Bhuyan et al., 2018). The value of the release exponent (n) in this instance, as shown in Table 4.2 below, was greater than 0.89 (n = 0.897), indicating that the nitrogen released from the U-e-Ac-Ls followed the super case-II transport mechanism. The Ac-Ls chains' macromolecular relaxation and erosion process accomplishes this (Limmatvapirat et al., 2008; Nanocellulose et al., 2021).

Table 4.2. Release Kinetics modeling data for formulated U-e-Ac-Ls

Kinetic Models		Formulated U-e-Ac-Ls
Korsmeyer-Peppas	K_i (hr^{-n})	0.0799
	N	0.8974
	R^2	0.99867
Higuchi	K_H ($g/hr^{0.5}$)	0.8665
	R^2	0.9843
Zero order	K_o (g/hr)	0.1449
	R^2	0.9491
First order	K (g/hr)	-0.1045
	R^2	0.7821
Fit Model		Korsmeyer-Peppas
Types of diffusion		Super case-II Transport

Nitrogen likely diffuses from the U-e-Ac-Ls through its eroding outer layer, releasing droplets with dissolved nitrogen into the aqueous media. The findings from the analysis of the nitrogen release mechanism using different kinetic models support the conclusion that the erosion and diffusion mechanisms collaborated to produce the nitrogen release kinetics from the U-e-Ac-Ls.

5. CONCLUSIONS AND RECOMMENDATIONS

5.1 Conclusions

By encapsulating urea in a biodegradable acetylated lignosulfonate (Ac-Ls), slow dissolution rate fertilizer with an improved soil degradation rate was successfully formulated. Different physiochemical approaches were used to characterize the properties of synthesized Ac-Ls and the urea-encapsulated acetylated lignosulfonate (U-e-Ac-Ls). On the Acetylation of lignosulfonate, the influence of independent reaction variables (such as acetylation temperature and acetylation time) was investigated. The findings show that as acetylation temperature and acetylation time increased, the reduction peak of hydroxyl and appearance of carbonyl groups on the structure of Acetylated lignosulfonate increased simultaneously and confirmed using FTIR spectrum. It also investigated how the acetylation of lignosulfonate affects the solubility and hydrophobicity of lignosulfonate in dichloromethane. The findings show that when lignosulfonate gets acetylated, its percentage of solubility in dichloromethane (70.13%) and its hydrophobicity (74^{o}) (evaluated using contact angle measurement) gets increased. Moreover, the percentage of solubility of lignosulfonate in deionized water (79.51%) was higher as compared to in DCM (41.27%) and its hydrophobicity was found to be 14^{o} (evaluated using contact angle measurement) before acetylated. It was also determined how medium's pH, temperature, and urea concentration affected U-e-Ac-Ls released rate of nitrogen. Since an increase in temperature induces an increase in the rate of urea's molecular diffusion in the Ac-Ls, the rate of nitrogen release also rises as the temperature rises. Similar to this, the rate at which nitrogen is released increases as urea concentration within the Ac-Ls increases. This results from the Ac-Ls' molecular chains expanding due to the significant urea enclosed within them. However, the amount of nitrogen released from U-e-Ac-Ls decreases when the medium's pH rises because there is greater contact between the amine groups of urea and the carboxyl groups of Ac-Ls. Also, the release rate of nitrogen and soil degradation rate of formulated urea-encapsulated acetylated lignosulfonate (U-e-Ac-Ls) were investigated. In contrast to the U-e-Ac-Ls, which lose just 40.17% of their weight within the first four days of incubation, commercial urea (pure urea) totally degrades within four days of incubation in the soil. This shows that the U-e-Ac-Ls were decomposed in the soil, but it took more time than the commercial urea fertilizer to decay entirely. Additionally, the soil degradation rate increases with the urea concentration

encapsulated in Ac-Ls. Using the Kjeldhal method, the total nitrogen release rate of U-e-Ac-Ls in comparison to pure urea in water was investigated. And four different kinetic models were studied to examine the kinetics of nitrogen release from U-e-Ac-Ls. With correlation values (R^2 > 0.99) for the formulated U-e-Ac-Ls and a value of the release exponent (n) that was larger than 0.89, the Korsmeyer-Peppas equation offers the best match among those model equations. This suggests that the super case-II transport mechanism was used for the nitrogen release from the U-e-Ac-Ls, and that the release kinetics of nitrogen from these materials was a result of both diffusion and erosion-regulated releases mechanisms. In general, this research demonstrated a successfully controlled dissolution rate fertilizer that totally degrades in the soil, leaving no residue that could harm the soil's structure or nutrient balance.

5.2 Recommendations

- This study observed the effects of acetylation reaction time and temperatures. Whereas the effects of the ratio of acetic anhydride to pyridine on the lignosulfonate and the degrees of acetylation should be studied.
- By encapsulating urea in hydrophobic and biodegradable Ac-Ls in this study, an efficient control of the release rate of nitrogen in the water was achieved. However, additional research on the usefulness of this technique should be done by sowing crops and observing the yield.
- Though the acetylation reaction on the lignosulfonate molecules was studied using FTIR spectrum, it is also better to emphasize the structure of un-acetylated and acetylated lignosulfonate using C-NMR spectroscopy.
- The impact of variables like pH, temperature, and urea concentration on the rate of nitrogen release is visible in the current study of U-e-Ac-Ls. But it's important to consider the impact of several other factors, including degrees of acetylation, the urease enzyme and other soil-based microorganisms, to understand more about the nitrogen release rate.
- It is better to apply the U-e-Ac-Ls in different soil types, to understand in which soil pH it is appropriate for plant growths.
- Although the synthesized Ac-Ls, employed to create a U-e-Ac-Ls, exhibits good characteristics in their binding efficiency, solubility, and hydrophobicity tests, it still requires additional evaluation in other applications other than as a urea holding matrix.

Special Acknowledgement

The researcher immensely appreciate for the financial support funded to accomplish this research work. This research project is funded by Adama Science and Technology University at grant number, ASTU/SM-R/578/22.

REFERENCES

Abalos, D., Jeffery, S., Sanz-Cobena, A., Guardia, G., & Vallejo, A. (2014). Meta-analysis of the effect of urease and nitrification inhibitors on crop productivity and nitrogen use efficiency. *Agriculture, Ecosystems and Environment*, *189*, 136–144.

Abd El-Aziz, M. E., Salama, D. M., Morsi, S. M. M., Youssef, A. M., & El-Sakhawy, M. (2022). Development of polymer composites and encapsulation technology for slow-release fertilizers. *Reviews in Chemical Engineering*, *38*(5), 603–616.

Adebajo, M. O., & Frost, R. L. (2004). Acetylation of raw cotton for oil spill cleanup application: An FTIR and 13C MAS NMR spectroscopic investigation. *Spectrochimica Acta - Part A: Molecular and Biomolecular Spectroscopy*, *60*(10), 2315–2321.

Adebayo, E. F., Tame, V. T., Mavakumba, H., & Joseph, J. (2021). *2 3 4 5*. *October*.

Affendi, N. M. N., Mansor, N., & Mathialagan, R. (2020). Development and characterization of allicin using palm stearin as a binder on urea granules. *Journal of Plant Nutrition*, *43*(5), 621–628.

Ali, I., Adnan, M., Iqbal, A., Ullah, S., Khan, M., Yuan, P., Zhang, H., Nasar, J., Gu, M., & Jiang, L. (2022). Effects of Biochar and Nitrogen Application on Rice Biomass Saccharification, Bioethanol Yield and Cell Wall Polymers Features. *International Journal of Molecular Sciences*, *23*(21), 13635.

An, X., Wu, Z., Qin, H., Liu, X., He, Y., Xu, X., Li, T., & Yu, B. (2021). Integrated co-pyrolysis and coating for the synthesis of a new coated biochar-based fertilizer with enhanced slow-release performance. *Journal of Cleaner Production*, *283*, 124642.

Antille, D. L., Hoekstra, N. J., & Lalor, S. T. J. (2015). *Communications in Soil Science and Plant Analysis Field-Scale Evaluation of Calcium Ammonium Nitrate , Urea , and Urea Treated with N- (N-Butyl) Thiophosphoric Triamide Applied to Grassland in Ireland*. *June*, 37–41.

Areskogh, D., Li, J., Gellerstedt, G., & Henriksson, G. (2010). Structural modification of commercial lignosulphonates through laccase catalysis and ozonolysis. *Industrial Crops*

and Products, *32*(3), 458–466.

Aro, T., & Fatehi, P. (2017). Production and Application of Lignosulfonates and Sulfonated Lignin. *ChemSusChem*, *10*(9), 1861–1877.

Askvik, K. M., Are Gundersen, S., Sjöblom, J., Merta, J., & Stenius, P. (1999). Complexation between lignosulfonates and cationic surfactants and its influence on emulsion and foam stability. *Colloids and Surfaces A: Physicochemical and Engineering Aspects*, *159*(1), 89–101.

Aso, T., Koda, K., Kubo, S., Yamada, T., Nakajima, I., & Uraki, Y. (2013). Preparation of novel lignin-based cement dispersants from isolated lignins. *Journal of Wood Chemistry and Technology*, *33*(4), 286–298.

Azeem, B., KuShaari, K., Naqvi, M., Keong, L. K., Almesfer, M. K., Al-Qodah, Z., Naqvi, S. R., & Elboughdiri, N. (2020). Production and characterization of controlled release urea using biopolymer and geopolymer as coating materials. *Polymers*, *12*(2).

Banea, M. D., & Da Silva, L. F. M. (2009). Adhesively bonded joints in composite materials: An overview. *Proceedings of the Institution of Mechanical Engineers, Part L: Journal of Materials: Design and Applications*, *223*(1), 1–18.

Baurhoo, B., Ruiz-Feria, C. A., & Zhao, X. (2008). Purified lignin: Nutritional and health impacts on farm animals-A review. *Animal Feed Science and Technology*, *144*(3–4), 175–184.

Beig, B., Niazi, M. B. K., Jahan, Z., Hussain, A., Zia, M. H., & Mehran, M. T. (2020). Coating materials for slow release of nitrogen from urea fertilizer: a review. *Journal of Plant Nutrition*, *43*(10), 1510–1533.

Brodin, I. (2009). *Chemical Properties and Thermal Behaviour of Kraft Lignins*.

Buono, P., Duval, A., Verge, P., Averous, L., & Habibi, Y. (2016). New Insights on the Chemical Modification of Lignin: Acetylation versus Silylation. *ACS Sustainable Chemistry and Engineering*, *4*(10), 5212–5222.

Bykov, I. (2008). Characterization of Natural and Technical Lignins using FTIR Spectroscopy. *Construction*, 43.

Byrne, M. P., Tobin, J. T., Forrestal, P. J., Danaher, M., Nkwonta, C. G., Richards, K., Cummins, E., Hogan, S. A., & O'Callaghan, T. F. (2020). Urease and nitrification inhibitors-As mitigation tools for greenhouse gas emissions in sustainable dairy systems: A review. *Sustainability (Switzerland)*, *12*(15), 1–35.

Cantarella, H., Otto, R., Soares, J. R., De, A. G., & Silva, B. (2018). Agronomic Efficiency of NBPT as a Urease Inhibitor: A review. *Journal of Advanced Research*.

Cao, L., Yu, I. K. M., Liu, Y., Ruan, X., Tsang, D. C. W., Hunt, A. J., Ok, Y. S., Song, H., & Zhang, S. (2018). Lignin valorization for the production of renewable chemicals: State-of-the-art review and future prospects. *Bioresource Technology*, *269*, 465–475.

Capanema, E. A., & Balakshin, M. (2015). Plantrose lignins: a new type of technical lignins. *18th International Symposium on Wood, Fibre and Pulping Chemistry*, *September*, 120–123.

Chakar, F. S., & Ragauskas, A. J. (2004). Review of current and future softwood kraft lignin process chemistry. *Industrial Crops and Products*, *20*(2), 131–141.

Chen, S., Yang, M., Ba, C., Yu, S., Jiang, Y., Zou, H., & Zhang, Y. (2018). Science of the Total Environment Preparation and characterization of slow-release fertilizer encapsulated by biochar-based waterborne copolymers. *Science of the Total Environment*, *615*, 431–437.

Conference, I. S., Tatras, H., Republic, S., & Polymers, S. (2014). *the Approach the Isolation of Lignins and Its Characterization*.

Contents, T. O. F. (n.d.). *ENVIRONMENTAL TECHNOLOGY & INNOVATION*.

Cortés-Triviño, E., Valencia, C., Delgado, M. A., & Franco, J. M. (2018). Modification of alkali lignin with poly(ethylene glycol) diglycidyl ether to be used as a thickener in bio-lubricant formulations. *Polymers*, *10*(6).

Cui, C., & Liu, W. (2021). Recent advances in wet adhesives: Adhesion mechanism, design

principle and applications. *Progress in Polymer Science*, *116*, 101388.

de Oliveira, D. R., Avelino, F., Mazzetto, S. E., & Lomonaco, D. (2020). Microwave-assisted selective acetylation of Kraft lignin: Acetic acid as a sustainable reactant for lignin valorization. *International Journal of Biological Macromolecules*, *164*, 1536–1544.

Deng, Y., Wu, Y., Qian, Y., Ouyang, X., Yang, D., & Qiu, X. (2010). Adsorption and desorption behaviors of lignosulfonate during the self-assembly of multilayers. *BioResources*, *5*(2), 1178–1196.

Derkacheva, O., & Sukhov, D. (2008). Investigation of lignins by FTIR spectroscopy. *Macromolecular Symposia*, *265*(1), 61–68.

Dimkpa, C. O., Andrews, J., Fugice, J., Singh, U., Bindraban, P. S., Elmer, W. H., Gardea-Torresdey, J. L., & White, J. C. (2020). Facile Coating of Urea With Low-Dose ZnO Nanoparticles Promotes Wheat Performance and Enhances Zn Uptake Under Drought Stress. *Frontiers in Plant Science*, *11*(February), 1–12.

Dimkpa, C. O., Fugice, J., Singh, U., & Lewis, T. D. (2020). Development of fertilizers for enhanced nitrogen use efficiency – Trends and perspectives. *Science of the Total Environment*, *731*, 139113.

Ding, H., Zhang, Y. S., Li, W. H., Zheng, X. Z., Wang, M. K., Tang, L. N., & Chen, D. L. (2016). Nutrients Release from a Novel Gel-Based Slow/Controlled Release Fertilizer. *Applied and Environmental Soil Science*, *2016*.

Doherty, W. O. S., Mousavioun, P., & Fellows, C. M. (2011). Value-adding to cellulosic ethanol: Lignin polymers. *Industrial Crops and Products*, *33*(2), 259–276.

El Assimi, T., Blažic, R., Vidović, E., Raihane, M., El Meziane, A., Baouab, M. H. V., Khouloud, M., Beniazza, R., Kricheldorf, H., & Lahcini, M. (2021). Polylactide/cellulose acetate biocomposites as potential coating membranes for controlled and slow nutrients release from water-soluble fertilizers. *Progress in Organic Coatings*, *156*(April).

Fertahi, S., Ilsouk, M., Zeroual, Y., Oukarroum, A., & Barakat, A. (2021). Recent trends in organic coating based on biopolymers and biomass for controlled and slow release

fertilizers. *Journal of Controlled Release*, *330*(September 2020), 341–361.

Figueiredo, P., Lintinen, K., Hirvonen, J. T., Kostiainen, M. A., & Santos, H. A. (2018). Properties and chemical modifications of lignin: Towards lignin-based nanomaterials for biomedical applications. *Progress in Materials Science*, *93*, 233–269.

Fu, J., Wang, C., Chen, X., Huang, Z., & Chen, D. (2018). Classification research and types of slow controlled release fertilizers (SRFs) used - a review. *Communications in Soil Science and Plant Analysis*, *49*(17), 2219–2230.

Galloway, J. N., Townsend, A. R., Erisman, J. W., Bekunda, M., Cai, Z., Freney, J. R., Martinelli, L. A., Seitzinger, S. P., & Sutton, M. A. (2008). Transformation of the nitrogen cycle: Recent trends, questions, and potential solutions. *Science*, *320*(5878), 889–892.

Ge, Y., & Li, Z. (2018). Application of Lignin and Its Derivatives in Adsorption of Heavy Metal Ions in Water: A Review. *ACS Sustainable Chemistry and Engineering*, *6*(5), 7181–7192.

Ge, Y., Song, Q., & Li, Z. (2015). A Mannich base biosorbent derived from alkaline lignin for lead removal from aqueous solution. *Journal of Industrial and Engineering Chemistry*, *23*, 228–234.

Gordis, R. (1940). The composition and structure of amos. *Harvard Theological Review*, *33*(4), 239–251.

Gungula, D. T., Andrew, F. P., Joseph, J., Kareem, S. A., Barminas, T., Adebayo, E. F., Saddiq, A. M., Tame, V. T., Dere, I., Ahinda, W. J., & Ator, R. (2021). Jo ur na l P re. *Results in Materials*, 100223.

Gupta, A., & Hussain, N. (2014). A critical study on the use, application and effectiveness of organic and inorganic fertilizers. *Journal of Industrial Pollution Control*, *30*(2), 191–193.

Hammad, H. M., Khaliq, A., Abbas, F., Farhad, W., Fahad, S., Aslam, M., Shah, G. M., Nasim, W., Mubeen, M., & Bakhat, H. F. (2020). Comparative Effects of Organic and Inorganic Fertilizers on Soil Organic Carbon and Wheat Productivity under Arid Region. *Communications in Soil Science and Plant Analysis*, *51*(10), 1406–1422.

Harris, J. R., Fanelli, J., Niemiera, A., Wright, R., Hall, S., & Inst, V. P. (2000). *Morphology during Adventitious Rooting of Artemisia , Gaura , and Nepeta quent Field Performance of Stem Cuttings of Loblolly Pine Rooting of Softwood Cuttings from Dormant Woody Stems POSTER SESSION 13 (Abstr . 349 – 367) Nutrition*. *35*(3), 451–480.

Hasanuzzaman, M., Fujita, M., Oku, H., Nahar, K., & Hawrylak-Nowak, B. (2018). Plant nutrients and abiotic stress tolerance. *Plant Nutrients and Abiotic Stress Tolerance*, 1–590.

He, X., Luzi, F., Yang, W., Xiao, Z., Torre, L., Xie, Y., & Puglia, D. (2018). Citric Acid as Green Modifier for Tuned Hydrophilicity of Surface Modified Cellulose and Lignin Nanoparticles. *ACS Sustainable Chemistry and Engineering*, *6*(8), 9966–9978.

Herrera, J. M., Rubio, G., Häner, L. L., Delgado, J. A., Lucho-Constantino, C. A., Islas-Valdez, S., & Pellet, D. (2016). Emerging and established technologies to increase nitrogen use efficiency of cereals. *Agronomy*, *6*(2), 11–18.

Heuchan, S. M., Fan, B., Kowalski, J. J., Gillies, E. R., & Henry, H. A. L. (2019). Development of Fertilizer Coatings from Polyglyoxylate-Polyester Blends Responsive to Root-Driven pH Change. *Journal of Agricultural and Food Chemistry*, *67*(46), 12720–12729.

Hill, C. A. S., Hill, B. C. A. S., Jones, D., Strickland, G., & Cetin, N. S. (1998). *Kinetic and Mechanistic Aspects of the Acetylation of Wood with Acetic Anhydride v*. *52*, 623–629.

Hill, C. A. S., Jones, D., Strickland, G., & Cetin, N. S. (1998). Kinetic and Mechanistic Aspects of the Acetylation of Wood with Acetic Anhydride. *Holzforschung*, *52*(6), 623–629.

Hussain, M. J., Karim, A. J. M. S., Solaiman, A. R. M., Islam, M. S., & Rahman, M. (2017). Effect of Urea Super Granule and Prilled Urea on Yield and Yield Attributes of Broccoli (*Brassica oleracea* var. *italica* L.). *The Agriculturists*, *14*(2), 95–112.

Hydrogel, T. L. (2011). *Preparation and characterization of a temperature-sensitive lignin-based hydrogel*. *6*, 4942–4952.

Id, C. J. R., Jolley, V. D., Blair, T. A., Sutton, L. E., & Hopkins, B. G. (2020). *Nitrogen release rates from slow- and controlled-release fertilizers influenced by placement and temperature*. 1–21.

Janke, C. K., Moody, P., & Bell, M. J. (2020). Three-dimensional dynamics of nitrogen from banded enhanced efficiency fertilizers. *Nutrient Cycling in Agroecosystems*, *118*(3), 227–247.

Jiang, X., Liu, J., Du, X., Hu, Z., Chang, H. M., & Jameel, H. (2018). Phenolation to Improve Lignin Reactivity toward Thermosets Application. *ACS Sustainable Chemistry and Engineering*, *6*(4), 5504–5512.

Jintakanon, N., Opaprakasit, P., Petchsuk, A., & Opaprakasit, M. (2008). Controlled-release materials for fertilizer based on lactic acid polymers. *Advanced Materials Research*, *55–57*, 905–908.

José Borges Gomes, F., de Souza, R. E., Brito, E. O., & Costa Lelis, R. C. (2020). A review on lignin sources and uses. *Journal of Applied Biotechnology & Bioengineering*, *7*(C), 100–105.

Kai, D., Tan, M. J., Chee, P. L., Chua, Y. K., Yap, Y. L., & Loh, X. J. (2016). Towards lignin-based functional materials in a sustainable world. *Green Chemistry*, *18*(5), 1175–1200.

Kalami, S., Arefmanesh, M., Master, E., & Nejad, M. (2017). Replacing 100% of phenol in phenolic adhesive formulations with lignin. *Journal of Applied Polymer Science*, *134*(30), 2–10.

Karhunen, P., Rummakko, P., Sipilä, J., Brunow, G., & Kilpeläinen, I. (1995). Dibenzodioxocins; a novel type of linkage in softwood lignins.

Khan, A., Nair, V., Colmenares, J. C., & Gl, R. (2018). Lignin-Based Composite Materials for Photocatalysis. *Topics in Current Chemistry Collection-Lignin Chemistry*, 1–31.

Khan, M. J., Malik, A., Zaman, M., & Khan, Q. (2014). *Nitrogen use efficiency and yield of maize crop as affected by agrotain coated urea in arid calcareous soils Impact of Agrotain coated urea on maize yield Materials and Methods*. *33*(1), 1–6.

Ko, H. U., Kim, J. W., Kim, H. C., Zhai, L., & Kim, J. (2020). Esterified PVA-lignin resin by maleic acid applicable for natural fiber reinforced composites. *Journal of Applied Polymer Science*, *137*(26), 1–9.

Kreetachat, T., Damrongsri, M., Punsuwon, V., Vaithanomsat, P., Chiemchaisri, C., & Chomsurin, C. (2007). Effects of ozonation process on lignin-derived compounds in pulp and paper mill effluents. *Journal of Hazardous Materials*, *142*(1–2), 250–257.

Kumar, A., Anushree, Kumar, J., & Bhaskar, T. (2020). Utilization of lignin: A sustainable and eco-friendly approach. *Journal of the Energy Institute*, *93*(1), 235–271.

Lamsen, M. R. (2019). *TRACE : Tennessee Research and Creative Exchange Encapsulation of Vitamin D3 in Gum Arabic to Improve Application in Beverages and Enhance Bioavailability*.

Lapierre, C., Monties, B., Meier, D., & Faix, O. (1994). Structural investigation of kraft lignins transformed via oxo-ammoniation to Potential nitrogenous fertilizers.

Lawrencia, D., Wong, S. K., Low, D. Y. S., Goh, B. H., Goh, J. K., Ruktanonchai, U. R., Soottitantawat, A., Lee, L. H., & Tang, S. Y. (2021). Controlled release fertilizers: A review on coating materials and mechanism of release. *Plants*, *10*(2), 1–26.

Le, P. T., & Nguyen, K. T. (2020). Hydrophobizing cellulose surfaces via catalyzed transesterification reaction using soybean oil and starch. *Heliyon*, *6*(11), e05559.

Li, L., Sun, Y., Cao, B., Song, H., Xiao, Q., & Yi, W. (2016). Preparation and performance of polyurethane/mesoporous silica composites for coated urea. *Materials and Design*, *99*.

Li, T., Yin, Y., Wu, S., Ma, H., & Zhang, F. (2020). Effect of pre-acetylation of hydroxyl functional groups by choline chloride/acetic anhydride on subsequent lignin pyrolysis. *Bioresource Technology*, *317*(July), 124034.

Limmatvapirat, S., Limmatvapirat, C., & Puttipipatkhachorn, S. (2008). *Modulation of drug release kinetics of shellac-based matrix tablets by in-situ polymerization through annealing process*. *69*, 1004–1013.

Lin, X., Zhou, M., Wang, S., Lou, H., Yang, D., & Qiu, X. (2014). Synthesis, structure, and dispersion property of a novel lignin-based polyoxyethylene ether from kraft lignin and poly(ethylene glycol). *ACS Sustainable Chemistry and Engineering*, *2*(7), 1902–1909.

Liu, J., Liu, H. F., Deng, L., Liao, B., & Guo, Q. X. (2013). Improving aging resistance and mechanical properties of waterborne polyurethanes modified by lignin amines. *Journal of Applied Polymer Science*, *130*(3), 1736–1742.

Liu, L., Shen, T., Yang, Y., Gao, B., Li, Y. C., Xie, J., Tang, Y., Zhang, S., Wang, Z., & Chen, J. (2018). Bio-based Large Tablet Controlled-Release Urea: Synthesis, Characterization, and Controlled-Released Mechanisms. *Journal of Agricultural and Food Chemistry*, *66*(43), 11265–11272.

Liu, L. Y., Hua, Q., & Renneckar, S. (2019). A simple route to synthesize esterified lignin derivatives. *Green Chemistry*, *21*(13), 3682–3692.

Liu, M., & Wu, L. (2015). *" Smart " Fertilizer with Temperature- and pH-Responsive Behavior via Surface-Initiated Polymerization for Controlled Release of Nutrients*.

Liu, X., Chen, L., & Hua, Z. (2020). *Comparing ammonia volatilization between conventional and slow-release nitrogen fertilizers in paddy fields in the Taihu Lake region*. 8386–8394.

Llive, L. M., Perullini, M., Santagapita, P. R., Schneider-teixeira, A., & Deladino, L. (2020). Controlled release of fertilizers from Ca (II) -alginate matrix modified by yerba mate (Ilex paraguariensis) waste. *European Polymer Journal*, *138*(August), 109955.

Londono-Zuluaga, C., Du, J., Chang, H. M., Jameel, H., & Gonzalez, R. (2018). Lignin Modifications and Perspectives towards Applications of Phenolic Foams: A Review. *BioResources*, *13*(4), 9158–9179. https://doi.org/10.15376/BIORES.13.4.9158-9179

Lora, J. H., & Glasser, W. G. (2002). Recent industrial applications of lignin: A sustainable alternative to nonrenewable materials. *Journal of Polymers and the Environment*, *10*(1–2), 39–48. https://doi.org/10.1023/A:1021070006895

Luo, S., Cao, J., & McDonald, A. G. (2018). Cross-linking of technical lignin via esterification and thermally initiated free radical reaction. *Industrial Crops and Products*, *121*(December 2017), 169–179. https://doi.org/10.1016/j.indcrop.2018.05.007

Luong, N. D., Binh, N. T. T., Duong, L. D., Kim, D. O., Kim, D. S., Lee, S. H., Kim, B. J., Lee, Y. S., & Nam, J. Do. (2012). An eco-friendly and efficient route of lignin extraction from

black liquor and a lignin-based copolyester synthesis. *Polymer Bulletin*, *68*(3), 879–890.

Lyu, Y., Yang, X., Pan, H., Zhang, X., Cao, H., Ulgiati, S., Wu, J., Zhang, Y., Wang, G., & Xiao, Y. (2021). Impact of fertilization schemes with different ratios of urea to controlled release nitrogen fertilizer on environmental sustainability, nitrogen use efficiency and economic benefit of rice production: A study case from Southwest China. *Journal of Cleaner Production*, *293*, 126198. https://doi.org/10.1016/j.jclepro.2021.126198

Ma, Z., Yue, Y., Feng, M., Li, Y., Ma, X., Zhao, X., & Wang, S. (2019). Mitigation of ammonia volatilization and nitrate leaching via loss control urea triggered H-bond forces. *Scientific Reports*, *9*(1), 1–9. https://doi.org/10.1038/s41598-019-51566-2

Madzokere, T. C., Murombo, L. T., & Chiririwa, H. (2020). Nano-based slow releasing fertilizers for enhanced agricultural productivity. *Materials Today: Proceedings*, *45*, 3709–3715. https://doi.org/10.1016/j.matpr.2020.12.674

Mechanisms, R. (2021). *A Slow-Release Fertilizer of Urea Prepared via Melt Blending with Degradable Poly (lactic acid): Formulation*.

Meister, J. J. (2002). Modification of lignin. In *Journal of Macromolecular Science - Polymer Reviews* (Vol. 42, Issue 2). https://doi.org/10.1081/MC-120004764

Mohammadbagheri, Z., Rahmati, A., & Hoshyarmanesh, P. (2021). Synthesis of a novel superabsorbent with slow-release urea fertilizer using modified cellulose as a grafting agent and flexible copolymer. *International Journal of Biological Macromolecules*, *182*, 1893–1905. https://doi.org/10.1016/j.ijbiomac.2021.05.191

Mohanty, S., Nayak, A. K., Bhaduri, D., Swain, C. K., Kumar, A., Tripathi, R., Behera, K. K., & Pathak, H. (2021). Field Crops Research Real-time application of neem-coated urea for enhancing N-use efficiency and minimizing the yield gap between aerobic direct-seeded and puddled transplanted rice. *Field Crops Research*, *264*(February), 108072.

Moshinsky, M. (1959). No Titleيب ل يد. *Nucl. Phys.*, *13*(1), 104–116.

Mou, H., Huang, J., Li, W., Wu, X., Liu, Y., & Fan, H. (2020). Study on the chemical modification of alkali lignin towards for cellulase adsorbent application. *International*

Journal of Biological Macromolecules, *149*, 794–800.

Mulder, W. J., Gosselink, R. J. A., Vingerhoeds, M. H., Harmsen, P. F. H., & Eastham, D. (2011). Lignin based controlled release coatings. *Industrial Crops and Products*, *34*(1), 915–920. https://doi.org/10.1016/j.indcrop.2011.02.011

Myrvold, B. O. (2013). Salting-out and salting-in experiments with lignosulfonates (LSs). *Holzforschung*, *67*(5), 549–557. https://doi.org/10.1515/hf-2012-0163

Myrvold, B. O. (2014). The Hansen Solubility Parameters of Some Lignosulfonates. *World Academy of Science, Engineering and Technology International Journal of Energy and Power Engineering*, *1*(October), 261.

Myrvold, B. O. (2016). Differences in solubility parameters and susceptibility to salting-out between softwood and hardwood lignosulfonates. *Holzforschung*, *70*(11), 1015–1021.

Nanocellulose, P., Particles, H., & Krajnc, M. (2021). *Bacteriophage Delivery Systems Based on Composite*.

Nasiri, A., Wearing, J., & Dubé, M. A. (2020). The use of lignin in emulsion-based pressure-sensitive adhesives. *International Journal of Adhesion and Adhesives*, *100*(October 2019).

Naz, M. Y., & Sulaiman, S. A. (2016). NU SC. *Journal of Controlled Release*.

Neff, J. C., Townsend, A. R., Gleixner, G., Lehman, S. J., Turnbull, J., & Bowman, W. D. (2002). Variable effects of nitrogen additions on the stability and turnover of soil carbon. *Nature*, *419*(6910), 915–917. https://doi.org/10.1038/nature01136

NUTRIENT RELEASE PATTERNS OF CONTROLLED RELEASE FERTILIZERS USED IN. (2010). 1–80.

Nwankwere, E. T. (2016). *Sorption Studies of Crude Oil on Acetylated Rice Husks Sorption studies of crude oil on acetylated rice husks*. *August*.

Onwuka, J. C., Agbaji, E. B., Ajibola, V. O., & Okibe, F. G. (2019). Thermodynamic pathway of lignocellulosic acetylation process. *BMC Chemistry*, *13*(3), 1–11.

Otromke, M., White, R. J., & Sauer, J. (2019). Hydrothermal Base Catalyzed Depolymerization and Conversion of Technical Lignin – An Introductory Review. *Carbon Resources Conversion*. https://doi.org/10.1016/j.crcon.2019.01.002

Ouyang, X., Ke, L., Qiu, X., Guo, Y., & Pang, Y. (2009). Sulfonation of alkali lignin and its potential use in dispersant for cement. *Journal of Dispersion Science and Technology*, *30*(1), 1–6. https://doi.org/10.1080/01932690802473560

Panpatte, D. G., & Jhala, Y. K. (n.d.). *Nanotechnology for Agriculture : Crop Production & Protection*.

Peng, C., Zhang, G., Han, J., & Li, X. (2019). Hydrothermal conversion of lignin and black liquor for phenolics with the aids of alkali and hydrogen donor. *Carbon Resources Conversion*, *2*(2), 141–150. https://doi.org/10.1016/j.crcon.2019.06.004

Priyanto, S., Dasilva, T., Anggara, B. B., Triyahdiyani, N., Sudrajat, R. W., Kusworo, T. D., Pramudono, B., Untoro, E., & Ratu, P. (2021). Synthesis of Sodium Ligno Sulfonate (SLS) Surfactant from Black Liquor Waste and The Potential Test for EOR in Ledok Field Cepu. *IOP Conference Series: Materials Science and Engineering*, *1053*(1), 012075.

Priyanto, S., Pramudono, B., Kusworo, T. D., Suherman, Aji, H. A., Untoro, E., & Ratu, P. (2018). Synthesis Study of Surfactants Sodium Ligno Sulphonate (SLS) from Biomass Waste Using Fourier Transform Infra Red (FTIR). *MATEC Web of Conferences*, *156*, 2017–2019. https://doi.org/10.1051/matecconf/201815603030

Puziy, A. M., Poddubnaya, O. I., & Sevastyanova, O. (2018). Carbon Materials from Technical Lignins: Recent Advances. *Topics in Current Chemistry*, *376*(4).

Qiao, W., Li, S., Guo, G., Han, S., Ren, S., & Ma, Y. (2015). Synthesis and characterization of phenol-formaldehyde resin using enzymatic hydrolysis lignin. *Journal of Industrial and Engineering Chemistry*, *21*, 1417–1422. https://doi.org/10.1016/j.jiec.2014.06.016

Ragauskas, A. J., Beckham, G. T., Biddy, M. J., Chandra, R., Chen, F., Davis, M. F., Davison, B.

H., Dixon, R. A., Gilna, P., Keller, M., Langan, P., Naskar, A. K., Saddler, J. N., Tschaplinski, T. J., Tuskan, G. A., & Wyman, C. E. (2014). Lignin valorization: Improving lignin processing

in the biorefinery. *Science*, *344*(6185).

Rajan, M., Shahena, S., Chandran, V., & Mathew, L. (2021). Controlled release of fertilizers d concept , reality , and mechanism. In *Controlled Release Fertilizers for Sustainable Agriculture*. Elsevier Inc. https://doi.org/10.1016/B978-0-12-819555-0.00003-0

Rawat, J., Sanwal, P., & Saxena, J. (2016). *Potassium and Its Role in Sustainable Agriculture*. 235–253. https://doi.org/10.1007/978-81-322-2776-2

Riveiro, A., Maçon, A. L. B., del Val, J., Comesaña, R., & Pou, J. (2018). Laser surface texturing of polymers for biomedical applications. *Frontiers in Physics*, *5*(FEB).

Rodríguez-Félix, D. E., Pérez-Martínez, C. J., Castillo-Ortega, M. M., Pérez-Tello, M., Romero-García, J., Ledezma-Pérez, A. S., Del Castillo-Castro, T., & Rodríguez-Félix, F. (2012). PH- and temperature-sensitive semi-interpenetrating network hydrogels composed of poly(acrylamide) and poly(c-glutamic acid) as amoxicillin controlled-release system. *Polymer Bulletin*, *68*(1), 197–207. https://doi.org/10.1007/s00289-011-0549-1

Rodrı, D. E. (2018). *of urea from wheat-gluten membranes obtained by electrospinning*. 5305–5319. https://doi.org/10.1007/s00289-018-2327-9

Ross, K., & Mazza, G. (2010). Characteristics of lignin from flax shives as affected by extraction conditions. *International Journal of Molecular Sciences*, *11*(10), 4035–4050.

Ruser, R., & Schulz, R. (2015). *The effect of nitrification inhibitors on the nitrous oxide (N 2 O) release from agricultural soils — a review*. 171–188.

Ruwoldt, J. (2020). A Critical Review of the Physicochemical Properties of Lignosulfonates: Chemical Structure and Behavior in Aqueous Solution, at Surfaces and Interfaces. *Surfaces*, *3*(4), 622–648. https://doi.org/10.3390/surfaces3040042

Ruwoldt, J., Planque, J., & Øye, G. (2020). Lignosulfonate Salt Tolerance and the Effect on Emulsion Stability. *ACS Omega*, *5*(25), 15007–15015.

Sadeghi, N., Shayesteh, K., & Lotfiman, S. (2017). Effect of Modified Lignin Sulfonate on Controlled-Release Urea in Soil. *Journal of Polymers and the Environment*, *25*(3), 792–

799. https://doi.org/10.1007/s10924-016-0848-6

Saha, S. K., Rahman, S. M. A., Rahman, F. H., & Pramanik, S. (2021). *Nanofertlizers-A Potential Alternative to Chemical Fertilizers*. *2*(6), 32–37.

Sameni, J. K. (2015). *Physico-Chemical Characterization of Lignin Isolated from Industrial Sources for Advanced Applications*. 52–56. http://hdl.handle.net/1807/70871

Sameni, J., Krigstin, S., & Sain, M. (2017). Acetylation & lignin solubility. *BioResources*, *12*(1), 1548–1565.

Sarkar, A., Biswas, D. R., Datta, S. C., Dwivedi, B. S., Bhattacharyya, R., Kumar, R., Bandyopadhyay, K. K., Saha, M., Chawla, G., Saha, J. K., & Patra, A. K. (2021). Preparation of novel biodegradable starch/poly(vinyl alcohol)/bentonite grafted polymeric films for fertilizer encapsulation. *Carbohydrate Polymers*, *259*(January), 117679.

Seleiman, M. F., Almutairi, K. F., Alotaibi, M., Shami, A., Alhammad, B. A., & Battaglia, M. L. (2021). *Nano-Fertilization as an Emerging Fertilization Technique : Why Can Modern Agriculture Benefit from Its Use ? 2019*(Figure 1), 1–27.

Sen, S., Patil, S., & Argyropoulos, D. S. (2015). Thermal properties of lignin in copolymers, blends, and composites: a review. *Green Chemistry*, *17*(11), 4862–4887.

Shan, P., Liu, H., Li, D., Zhou, R., Huang, S., Cai, P., Wang, Z., Lu, Y., Li, Z., & Li, Z. (2021). Thiol-ene Click Chemistry Using Triethylamine Gas as a Promoter to Make Coated Slow-release Fertilizer. *Chemical Engineering Journal Advances*, *8*, 100189.

Shayesteh, K., Mohammadzadeh, ghasem, & Zamanloo, M. (2020). Study and optimization of parameters affecting the acetylation process of lignin sulfonate biopolymer. *International Journal of Biological Macromolecules*, *163*, 1810–1820.

Shen, X., Xin, Y., Liu, H., & Han, B. (2020). Product-oriented Direct Cleavage of Chemical Linkages in Lignin. *ChemSusChem*, *13*(17), 4367–4381.

Singh, R. P. (2012). Organic fertilizers: Types, production and environmental impact. In *Organic Fertilizers: Types, Production and Environmental Impact* (Issue May).

Sipponen, M. H., Rojas, O. J., Pihlajaniemi, V., Lintinen, K., & Österberg, M. (2017). Calcium Chelation of Lignin from Pulping Spent Liquor for Water-Resistant Slow-Release Urea Fertilizer Systems. *ACS Sustainable Chemistry and Engineering*, *5*(1), 1054–1061.

Sixta, H. (2008). Pulp Properties and Applications. In *Handbook of Pulp* (Vol. 2).

Skorupka, M., & Nosalewicz, A. (2021). Ammonia volatilization from fertilizer urea—A new challenge for agriculture and industry in view of growing global demand for food and energy crops. *Agriculture (Switzerland)*, *11*(9). https://doi.org/10.3390/agriculture11090822

Solt, P., Jääskeläinen, A. S., Lingenfelter, P., Konnerth, J., & Van Herwijnen, H. W. G. (2019). Impact of molecular weight of kraft lignin on adhesive performance of lignin-based phenol-formaldehyde resins. *Forest Products Journal*, *68*(4), 365–371.

Stenius, P. E. R. (n.d.). Aqueous m i x t u r e s o f l i g n i n s u l p h o n a t e a n d s o m e c a t i o n i c polymers. 2.

Taha, G., Farahat, S., Elnggar, E., & AL Molakab, M. (2016). Creation & Characterization of Different Coated Urea Materials & Their Impact as Controlled Release Fertilizers. *Journal of Soil Sciences and Agricultural Engineering*, *7*(10), 793–800.

Taleb, F., Ammar, M., Mosbah, M. ben, Salem, R. ben, & Moussaoui, Y. (2020). Chemical modification of lignin derived from spent coffee grounds for methylene blue adsorption. *Scientific Reports*, *10*(1), 1–13. https://doi.org/10.1038/s41598-020-68047-6

Thakur, V. K., & Thakur, M. K. (2015). Recent advances in green hydrogels from lignin: A review. *International Journal of Biological Macromolecules*, *72*, 834–847.

Thébault, M., Kutuzova, L., Jury, S., Eicher, I., Zikulnig-Rusch, E. M., & Kandelbauer, A. (2020). Effect of phenolation, lignin-type and degree of substitution on the properties of lignin-modified phenol-formaldehyde impregnation resins: Molecular weight distribution, wetting behavior, rheological properties and thermal curing profiles. *Journal of Renewable Materials*, *8*(6), 603–630. https://doi.org/10.32604/jrm.2020.09616

Torres-olivar, V., & Valdez-aguilar, L. A. (2014). *Role of Nitrogen and Nutrients in Crop Nutrition*. *January*.

Tripathi, N., & Katiyar, V. (2018). Lactic acid oligomer (OLLA) grafted gum arabic based green adhesive for structural applications. *International Journal of Biological Macromolecules*, *120*, 711–720. https://doi.org/10.1016/j.ijbiomac.2018.07.199

Umar, W., Czinkota, I., Gulyás, M., Aziz, T., & Hameed, M. K. (2022). Development and characterization of slow release N and Zn fertilizer by coating urea with Zn fortified nano-bentonite and ZnO NPs using various binders. *Environmental Technology and Innovation*, *26*, 102250. https://doi.org/10.1016/j.eti.2021.102250

Vainio, U., Lauten, R. A., Haas, S., Svedström, K., Veiga, L. S. I., Hoell, A., & Serimaa, R. (2012). Distribution of counterions around lignosulfonate macromolecules in different polar solvent mixtures. *Langmuir*, *28*(5), 2465–2475. https://doi.org/10.1021/la204479d

Vargas, Y., Díaz, A., & Viera, W. (2020). *Use of multivariate statistics to determine fertilization practices that affect fruit quality of naranjilla (Solanum quitoense Lam .). November*.

Vázquez, G., Antorrena, G., González, J., & Freire, S. (1997). The influence of pulping conditions on the structure of acetosolv eucalyptus lignins. *Journal of Wood Chemistry and Technology*, *17*(1–2), 147–162. https://doi.org/10.1080/02773819708003124

Version of Record: https://www.sciencedirect.com/science/article/pii/S0958166918300612. (n.d.).

Vishtal, A., & Kraslawski, A. (2011). Challenges in industrial applications of technical lignins. *BioResources*, *6*(3), 3547–3568. https://doi.org/10.15376/biores.6.3.vishtal

Wang, B., Chen, T. Y., Wang, H. M., Li, H. Y., Liu, C. F., & Wen, J. L. (2018). Amination of biorefinery technical lignins using Mannich reaction synergy with subcritical ethanol depolymerization. *International Journal of Biological Macromolecules*, *107*(PartA), 426–435. https://doi.org/10.1016/j.ijbiomac.2017.09.012

Wang, C., Kelley, S. S., & Venditti, R. A. (2016). Lignin-Based Thermoplastic Materials. *ChemSusChem*, *9*(8), 770–783. https://doi.org/10.1002/cssc.201501531

Wang, H., Pu, Y., Ragauskas, A., & Yang, B. (2019). From lignin to valuable products–strategies, challenges, and prospects. *Bioresource Technology*, *271*(September), 449–461.

Wang, H., Wang, B., Sun, D., Shi, Q., Zheng, L., Wang, S., Liu, S., Xia, R., & Sun, R. (2019). Unraveling the Fate of Lignin from Eucalyptus and Poplar during Integrated Delignification and Bleaching. *ChemSusChem*, *12*(5), 1059–1068. https://doi.org/10.1002/cssc.201802592

Wang, X., Zhang, Y., Hao, C., Dai, X., Zhou, Z., & Si, N. (2014). Ultrasonic-assisted synthesis of aminated lignin by a Mannich reaction and its decolorizing properties for anionic azo-dyes. *RSC Advances*, *4*(53), 28156–28164. https://doi.org/10.1039/c4ra03133d

Xia, H., Riaz, M., Zhang, M., Liu, B., Li, Y., El-Desouki, Z., & Jiang, C. (2022). Biochar-N fertilizer interaction increases N utilization efficiency by modifying soil C/N component under N fertilizer deep placement modes. *Chemosphere*, *286*(P1), 131594.

Xu, J., Zhu, S., Liu, P., Gao, W., Li, J., & Mo, L. (2017). Adsorption of Cu(II) ions in aqueous solution by aminated lignin from enzymatic hydrolysis residues. *RSC Advances*, *7*(71), 44751–44758. https://doi.org/10.1039/c7ra06693g

Yan, M., Yang, D., Deng, Y., Chen, P., Zhou, H., & Qiu, X. (2010). Influence of pH on the behavior of lignosulfonate macromolecules in aqueous solution. *Colloids and Surfaces A: Physicochemical and Engineering Aspects*,*371*(1–3), 50–58.

Yáñez-S, M., Matsuhiro, B., Nuñez, C., Pan, S., Hubbell, C. A., Sannigrahi, P., & Ragauskas, A. J. (2014). Physicochemical characterization of ethanol organosolv lignin (EOL) from Eucalyptus globulus: Effect of extraction conditions on the molecular structure. *Polymer Degradation and Stability*, *110*, 184–194.

Yetiş, F., Liu, X., Sampson, W. W., & Gong, R. H. (2020). Acetylation of lignin containing microfibrillated cellulose and its reinforcing effect for polylactic acid. *European Polymer Journal*, *134*, 109803. https://doi.org/10.1016/j.eurpolymj.2020.109803

Zhang, F., Jiang, X., Lin, J., Zhao, G., Chang, H. M., & Jameel, H. (2019). Reactivity improvement by phenolation of wheat straw lignin isolated from a biorefinery process. *New Journal of Chemistry*, *43*(5), 2238–2246. https://doi.org/10.1039/c8nj05016c

Zhang, L., & Huang, J. (2001). Effects of nitrolignin on mechanical properties of polyurethane-nitrolignin films. *Journal of Applied Polymer Science*, *80*(8), 1213–1219.

Zhang, M., & Ogale, A. A. (2014). Carbon fibers from dry-spinning of acetylated softwood kraft lignin. *Carbon*, *69*, 626–629. https://doi.org/10.1016/j.carbon.2013.12.015

Zhang, X., Davidson, E. A., Mauzerall, D. L., Searchinger, T. D., Dumas, P., & Shen, Y. (2015). Managing nitrogen for sustainable development. *Nature*, *528*(7580), 51–59.

Zonatto, F., Muniz, E. C., Tambourgi, E. B., & Paulino, A. T. (2017). Adsorption and controlled release of potassium, phosphate and ammonia from modified Arabic gum-based hydrogel. *International Journal of Biological Macromolecules*, *105*, 363–369.

Zulfiqar, F., Navarro, M., Ashraf, M., Akram, N. A., & Munné-Bosch, S. (2019). Nanofertilizer use for sustainable agriculture: Advantages and limitations. *Plant Science*, *289*(September).

APPENDICES

Appendix-1: Effects of Acetylation time and Temperature on the dissolution of U-e-Ac-Ls

A) Effects of Acetylation time on Total nitrogen release rate

Time(hrs)	6hrs	12hrs	24hrs
	N_{ave}	N_{ave}	N_{ave}
1	11.72	7.93	4.545
4	34.005	23.305	17.345
7	63.695	44.465	27.96
10	82.39	65.655	37.725
13	93.27	81.025	47.54
16	96.945	86.995	61.385
19	99.455	90.65	69.65
22		93.73	75.23
25		95.8	79.415

B) Effects of Acetylation temperature on total nitrogen release rate

Time(hrs)	60^oC	80^oC	100^oC
	N_{ave}	N_{ave}	N_{ave}
1	12.495	10.1	7.015
4	37.945	35.075	23.28
7	62.935	54.85	42.98
10	82.585	72.955	63.385
13	92.28	86.695	80.935
16	96.44	95.45	88.08
19	99.775	98.035	91.885
22		99.66	94.685

25	96.065

Nitrogen Release rate in Water

Appendix-2: Nitrogen Release Rate (%TN) for pure urea and U-e-Ac-Ls at pH 4

Time(hrs)	Pure urea	N_1	N_2	N_{ave}
1	99.11	12.03	11.95	11.99
4	100	37.15	36.22	36.685
7	100	62.21	61.72	61.965
10	100	75.31	76.06	75.685
13	100	87.17	87.43	87.3
16	100	94.72	95.15	94.935
19	100	99.93	99.71	99.82

Appendix-3: Nitrogen Release Rate (%TN) for pure urea and U-e-Ac-Ls at pH 7

Time(hrs)	Pure urea	N_1	N_2	N_{ave}
1	98.12	8.36	7.79	8.075
4	100	25.86	26.04	25.95
	100	45.22	44.86	45.04

7				
10	100	64.43	65.39	64.91
13	100	80.77	80.13	80.45
16	100	88.27	89.16	88.715
19	100	95.18	95.62	95.4
22	100	99.61	99.35	99.48

Appendix-4: Nitrogen Release Rate (%TN) for pure urea and U-e-Ac-Ls at pH10

Time(hrs)	Pure urea	N_1	N_2	N_{ave}
1	96.31	5.62	5.97	5.795
4	100	16.39	17.65	17.02
7	100	30.06	31.96	31.01
10	100	45.43	45.78	45.605
13	100	58.72	59.13	58.925
16	100	71.07	72.92	71.995
19	100	81.77	82.61	82.19
22	100	91.32	90.51	90.915

25	100	97.28	97.83	97.555

Appendix-5: Nitrogen Release Rate (%TN) for pure urea and U-e-Ac-Ls at 25^0C

Time(hrs)	Pure urea	N_1	N_2	N_{ave}
1	96.53	8.3	8.64	8.47
4	100	33.11	34.78	33.945
7	100	48.21	47.89	48.05
10	100	61.51	61.08	61.295
13	100	71.2	68.86	70.03
16	100	79.13	78.56	78.845
19	100	85.41	86.71	86.06
22	100	91.16	92.41	91.785
25	100	95.94	95.06	95.5

Appendix-6: Nitrogen Release Rate (%TN) for pure urea and U-e-Ac-Ls at 35^0C

Time(hrs)	Pure urea	N_1	N_2	N_{ave}
1	97.24	10.6	11.48	11.04
4	100	37.71	38.09	37.9
7	100	51.81	52.15	51.98
10	100	66.72	66.13	66.425
13	100	77.01	78.16	77.585
16	100	86.31	86.43	86.37
19	100	94.25	93.52	93.885
22	100	99.57	99.77	99.67

Appendix-7: Nitrogen Release Rate (%TN) for pure urea and U-e-Ac-Ls at 45^0C

Time(hrs)	Pure urea	N_1	N_2	N_{ave}
1	98.63	14.62	15.93	15.275
4	100	45.23	46.52	45.875
7	100	65.41	65.94	65.675
10	100	81.18	80.65	80.915
13	100	92.22	92.67	92.445
16	100	99.74	99.92	99.83

Appendix-8: Nitrogen Release Rate (%TN) of 60% urea Concentration

Time(hrs)	N_1	N_2	N_{ave}
1	8.43	7.87	8.15
4	25.27	26.51	25.89
7	40.1	39.89	39.995
10	52.4	53.03	52.715
13	62.61	61.75	62.18
16	70.21	70.61	70.41
19	77.32	78.73	78.025
22	83.59	84.67	84.13
25	87.37	88.58	87.975

Appendix-9: Nitrogen Release Rate (%TN) of 70% urea Concentration

Time (hrs)	N_1	N_2	N_{ave}
1	10.51	10.71	10.61
4	29.17	30.88	30.025
7	44.16	45.87	45.015
10	57.38	58.91	58.145
13	69.6	70.33	69.965

16	76.31	79.01	77.66
19	83.22	85.95	84.585
22	89.04	90.76	89.9
25	93.75	93.25	93.5

Appendix-10: Nitrogen Release Rate (%TN) of 80% urea concentration

Time(hrs)	N_1	N_2	N_{ave}
1	14.4	13.7	14.05
4	38.32	39.93	39.125
7	58.6	59.14	58.87
10	73.1	72.81	72.955
13	83.33	81.21	82.27
16	90.47	89.74	90.105
19	96.23	96.42	96.325
22	99.84	99.97	99.905

Weight loss percentage of synthesized U-e-Ac-Ls and pure urea

Appendix-11: Weight loss (%) for pure urea

Time(days)	1	4	7	10	13	16	19	22	25
Pure urea	71.83	100	100	100	100	100	100	100	100

Appendix-12: Weight loss (%) for U-e-Ac-Ls (60% urea concentration)

Time(days)	1	4	7	10	13	16	19	22	25
60% urea	16.08	35.19	49.17	59.31	67.07	74.29	81.64	87.53	92.92

Appendix-13: Weight loss (%) for U-e-Ac-Ls (70% urea concentration)

Time(days)	1	4	7	10	13	16	19	22	25
70% urea	19.59	40.17	54.23	64.74	73.63	81.06	87.27	91.61	94.86

Appendix-14: Weight loss (%) for U-e-Ac-Ls (80% urea concentration)

Time(days)	1	4	7	10	13	16	19	22	25
80% urea	21.10	43.02	57.04	67.15	76.72	84.76	89.24	93.91	96.82

Nitrogen Release Rate in the Soil

Appendix-15: Nitrogen Release Rate of U-e-Ac-Ls (70% urea) in soil

	%TN	
Incubation time (Days)	Pure urea	U-e-Ac-Ls
1	63.36	17.68
5	78.41	42.74
10	99.86	61.59
15	100	73.91
20	100	82.83
25	100	89.38
30	100	94.76

Appendix-16: Nitrogen Release Rate Calculation

Nitrogen Release Rate (%) $= \frac{C*V}{M} * 100$, Where C is the concentration of nitrogen in leachate (g/mL) obtained from Kjeldhal method, V is leachate volume in each sampling (mL) and M is total nitrogen present in a fertilizer (g). Accordingly, the total nitrogen in a sample which contains 7.0 g of urea was 3.22g. That was calculated as: M = 7*46% = 3.22 gram; leachate volume (V) is 100mL.

For instance, the total nitrogen release rate for the sample at pH-7 was calculated as follows:

Time (hrs)	C_1*V	N_1	C_2*V	N_2	N_{ave}	$(C*V)_{ave}$
1	0.269192	8.36	0.250838	7.79	8.075	0.260015
4	0.832692	25.86	0.838488	26.04	25.95	0.83559
7	1.456084	45.22	1.444492	44.86	45.04	1.450288
10	2.074646	64.43	2.105558	65.39	64.91	2.090102
13	2.600794	80.77	2.580186	80.13	80.45	2.59049
16	2.842294	88.27	2.870952	89.16	88.715	2.856623
19	3.064796	95.18	3.078964	95.62	95.4	3.07188
22	3.207442	99.61	3.19907	99.35	99.48	3.203256

Appendix-17: Natural logarithm (Ln) of Nitrogen release Fraction versus natural logarithm (Ln) of incubation time plot depicts Linear fit Model of Korsmeyer-Peppas

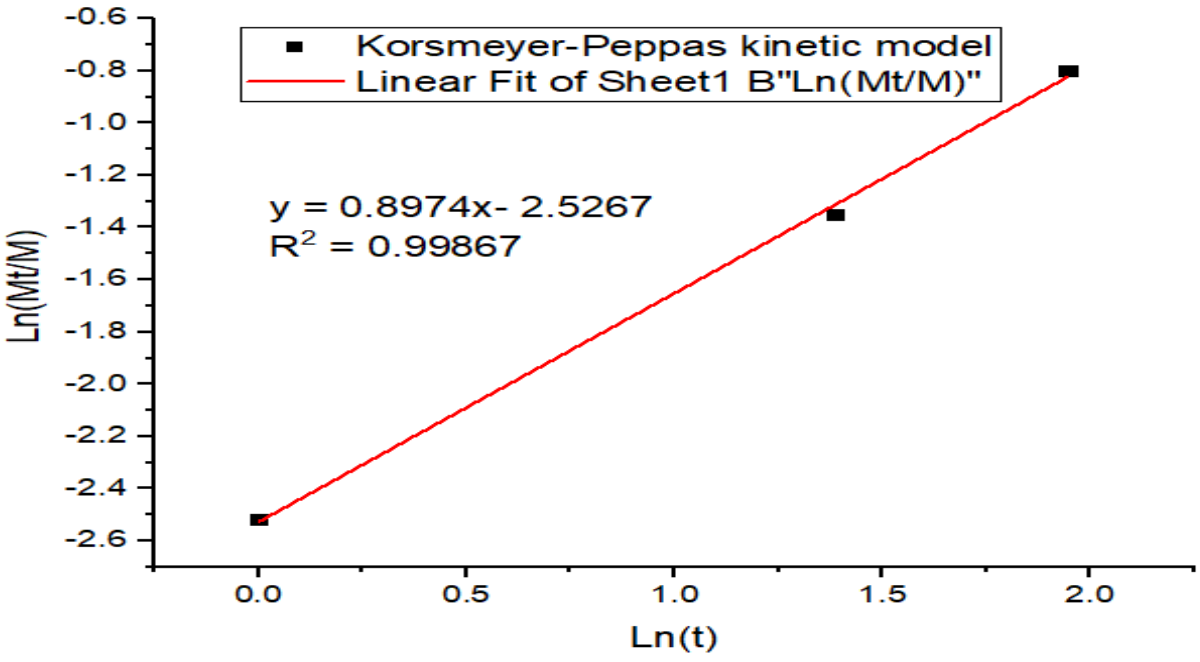

Appendix-18: Amount of Nitrogen released versus square root of incubation time plot depicting Linear fit Model of Higuchi

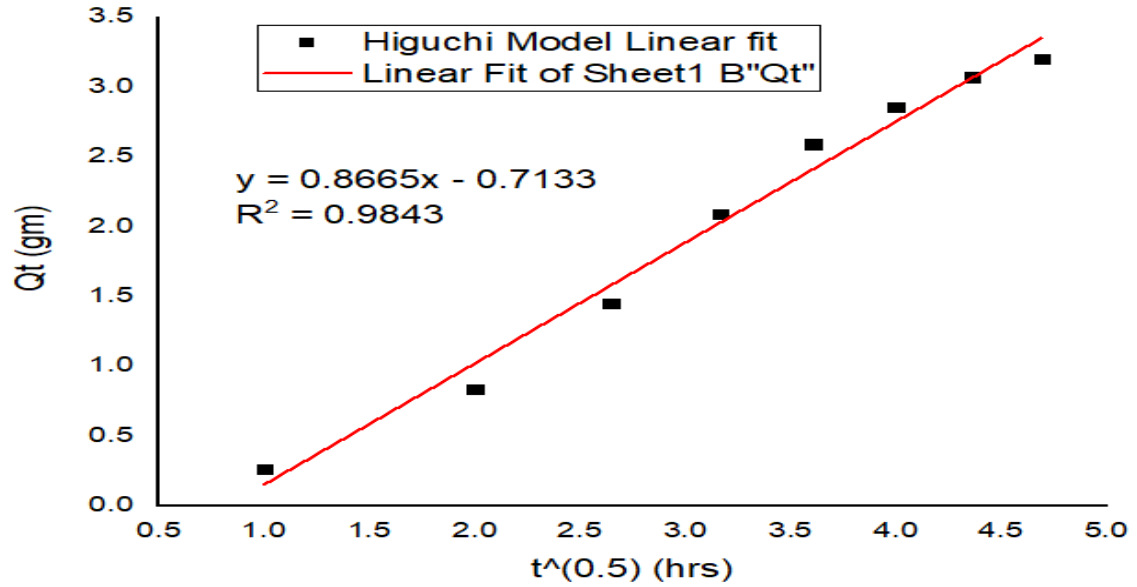

Appendix-19: Amount of Nitrogen released versus incubation time plot depicting Linear fit Model of Zero Order.

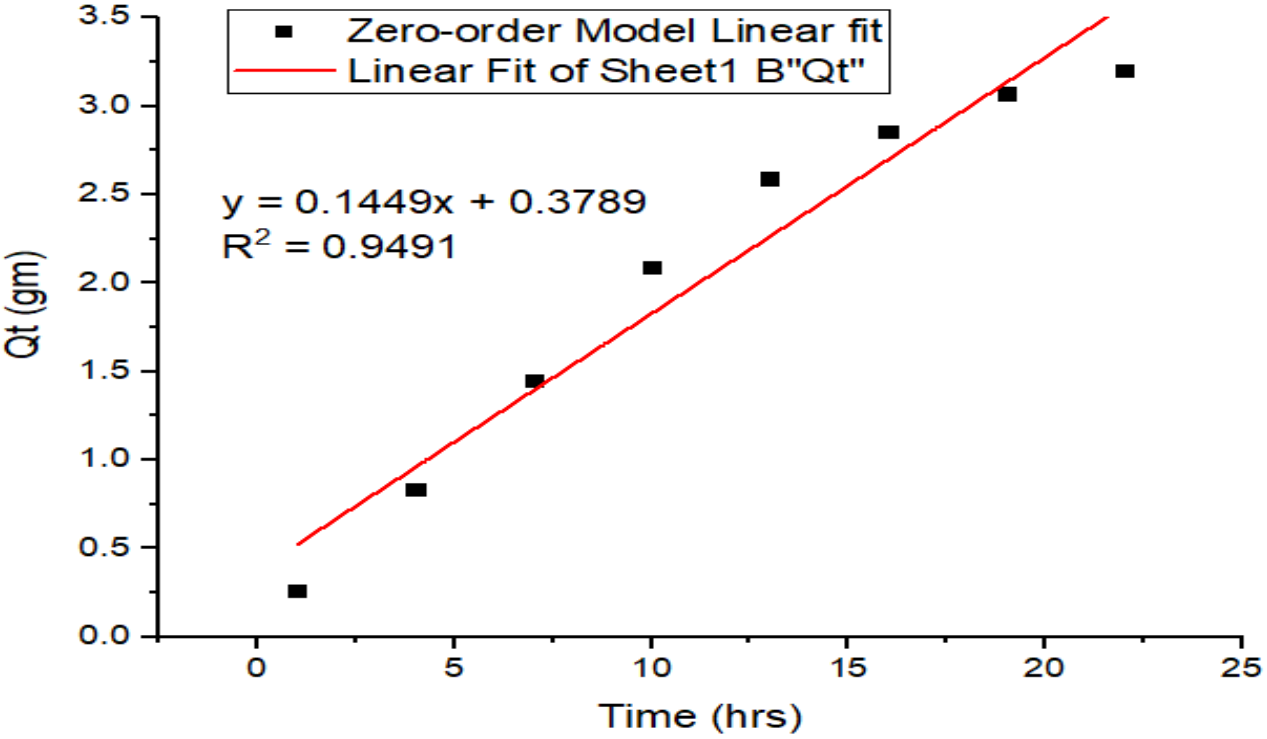

Appendix-20: Natural Logarithm (Ln) of amount of Nitrogen released versus incubation time plot depicting Linear fit Model of First Order

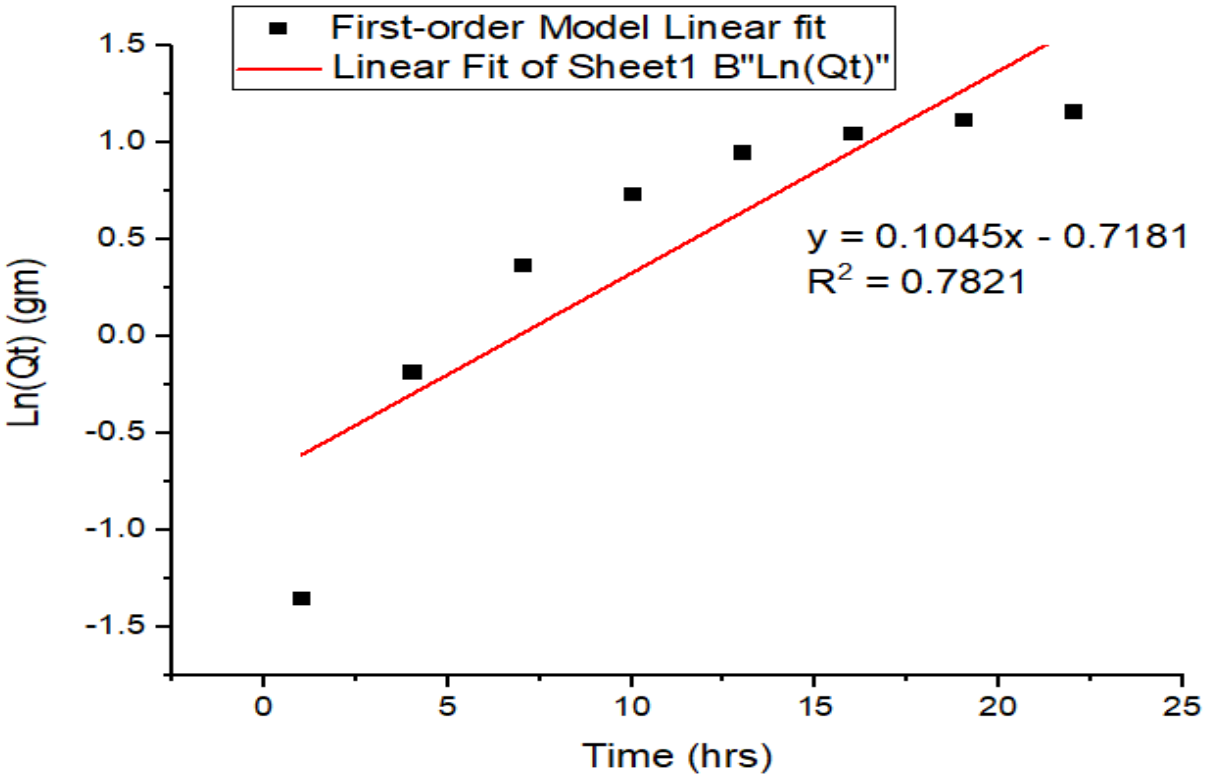

Appendix-21: Changes in pH during Nitrogen release rate test

Time(hrs)	0	1	4	7	10	13	16	19	22	25
Solution pH	6.98	7.34	7.27	7.16	7.10	7.03	6.69	6.95	6.89	6.78

Appendix-22: Recorded data for Contact angle measurement

A) N-Ls CA degree

```
#ImageJ 1.52a Preferences
#Thu May 25 15:45:44 BOT 2023
fps=3.0
new.slices=1
roicolor=\#FFFFFF
.ISP3D.windowWidth=720
div-by-zero=Infinity
new.height=512
.ISP3D.rotationZ=51.0
.ISP3D.rotationX=52.0
.ISP3D.xloc=100
raw.options=0
sample type: N-Ls
measured angle: 14 deg.
.import.sequence.dir=C\:\\Users\\Y COMP\\Desktop\\
fcolor=\#0000F
.ISP3D.yloc=10
raw.offset=0
.brush.loc=535,133
.arrow.style=0
noise.sd=25.0
raw.n=2
raw.type=0
ij.y=01
ij.x=112
jpeg=85
.ISP3D.min=0
pp.width=600
.log.width=400
raw.height=567
.results.loc=467,678
.log.height=200
.log.loc=111,761
showcolor=\#00FFFF
.cp.loc=615,88
.ISP3D.smooth=0.0
```

B) Ac-Ls CA degree

```
#ImageJ 1.53a Preferences
#Thu May 25 15:55:44 BOT 2023
fps=7.0
new.slices=1
roicolor=\#FFFFFF
.ISP3D.windowWidth=720
div-by-zero=Infinity
new.height=512
.ISP3D.rotationZ=39.0
.ISP3D.rotationX=65.0
.ISP3D.xloc=100
raw.options=0
sample type: Ac-Ls
measured angle: 74 deg.
.import.sequence.dir=C\:\\Users\\Y COMP\\Desktop\\
fcolor=\#0000FF
.ISP3D.yloc=50
raw.offset=0
.brush.loc=535,133
.arrow.style=0
noise.sd=25.0
raw.n=1
raw.type=0
ij.y=0
ij.x=629
jpeg=85
.ISP3D.min=0
pp.width=600
.log.width=400
raw.height=512
.results.loc=483,119
.log.height=250
.log.loc=483,119
showcolor=\#00FFFF
.cp.loc=615,88
.ISP3D.smooth=0.0
```